FUJIFILM
I&I – Imaging & Information

FCR (Fuji Computed Radiography)
General Description of Image Processing

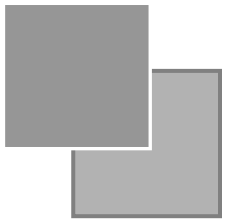

Fuji Photo Film Co., Ltd.

Contents

Chapter 1 Image Digitization 1
1.1 What Is Image Digitization 1
1.2 Relationship between Digitization Level and Image Reproducibility 1
1.3 FCR Image Digitization Level 2
1.4 Amount of Image Information 2
1.5 Amount of FCR Image Information 2
1.6 Objectives and Possibilities of Digitization 4

Chapter 2 Imaging Plate and FCR 5
2.1 What Is Photostimulable Phosphor 5
2.2 Luminescence Characteristics 7
2.3 IP System Noise Factors 10
2.4 Mechanism of FCR Image Formation 10
2.5 FCR History and Technological Targets 11
2.6 Dual-Light-Collection IP-Reading FCR System 11

Chapter 3 Automatic Sensitivity Correction Function (EDR) 15
3.1 Roles of EDR 15
3.2 Signal Conversion by Image Formation System 16
3.3 What Is EDR 17
3.4 Histogram 17
3.5 EDR Modes 19
3.6 AUTO Mode 19
3.6.1 Division exposure area recognition process 19
3.6.2 Irradiation field recognition process (PRIEF 4S) 21
3.6.3 PRIEF varieties 23
3.6.4 Methods of recognizing special ROIs (mammographic/cervical irradiation field recognition) 24
3.6.5 Histogram analysis types (Auto I to Auto VII) 25
3.6.6 Image recording area correction 28
3.7 SEMI AUTO Mode 29
3.8 FIX Mode 30
3.9 SEMI-X Mode 30
3.10 MANUAL Mode 30
3.11 S Value and Sensitivity 31

Chapter 4 Image Processing 33
4.1 Gradation Processing 33
4.2 Spatial Frequency Processing 36
4.3 Dynamic Range Control (DRC) 40
4.4 Tomographic Artifacts Suppression (TAS) 45
4.5 Multi-Objective Frequency Processing (MFP) 46
4.6 Energy Subtraction 57

Chapter 5 Image Display 60
5.1 FCR Image Display Formats 60
5.2 Image Enlargement/Reduction Process and Interpolation (Primarily for CT and MRI) 62
5.3 A-VRS (Advanced Variable Response Spline) 64
5.4 Dry Printer 66
5.5 CRT Display 67
5.5.1 Relationship between the image displayed on the CRT and the image of the film on a light box 66
5.5.2 CRT diagnostic capabilities 67
5.6 Relationship between Stationary Grid and Moire 70
5.6.1 Interference-induced moire patterns 69
5.6.2 Relationship between sampling interval and moire 69
5.6.3 Moire elimination/reduction method 71

Chapter 6 Image Electronic Archiving and Communication 73
6.1 Image Compression 73
6.1.1 Trends in image data compression technologies 72
6.1.2 Lossless JPEG 73
6.1.3 Lossy JPEG compression 74
6.1.4 Image compression by Wavelet transform coding 76
6.1.5 Compression algorithms for OD-F614/OD-F624 78

Appendix 1 Digital Image Evaluation Methods 79

Appendix 2 Fourier Transform (Real Space-to-Frequency Space Conversion) 82

Chapter 1 Image Digitization

1.1 What Is Image Digitization

Photographs, scenery, and all other images you see consist of analog data. As shown in Figure 1.1, the term "analog" refers to a series of spatially continuous data that expresses light intensity. When analog data is digitized, continuous data is spatially segmented, or **sampled**. The data values of all the segments, or **pixels**, are expressed by a series of discrete numerical values, or **quantized**, as indicated in Figure 1.2. Digitized data itself is not viewable, but can be viewed when it is converted to analog data.

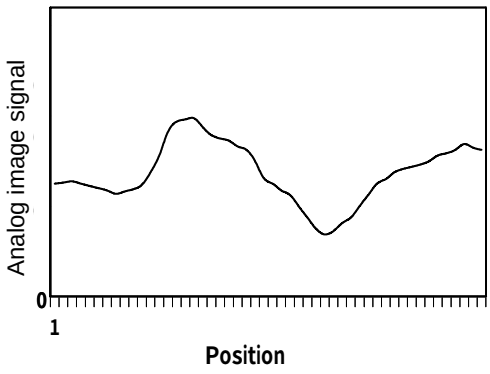

Figure 1.1 Analog data example

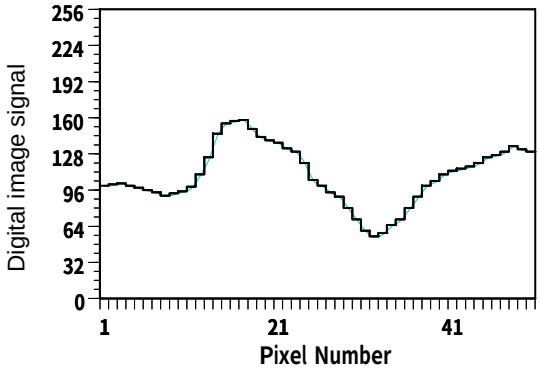

Figure 1.2 Digitized data example

1.2 Relationship between Digitization Level and Image Reproducibility

As is evident from the comparison between Figures 1.1 and 1.2, the similarity between the digitized image and original image can be enhanced by dividing the space into a larger number of segments (by reducing the pixel size) and by increasing the degree to which nearly equal data values of pixels can be discriminated. The **spatial resolution and density resolution** of digital data are determined in this manner.

If the digitization level is too low, or coarse, the resultant image becomes mosaicked or contains contours as shown in Figures 1.3 and 1.4. Conversely, because the resultant image is to be viewed by the human eye, the use of a resolution higher than the eye's is meaningless. An unnecessarily high resolution would not be efficient in terms of economy and operation because it would merely increase the amount of image data.

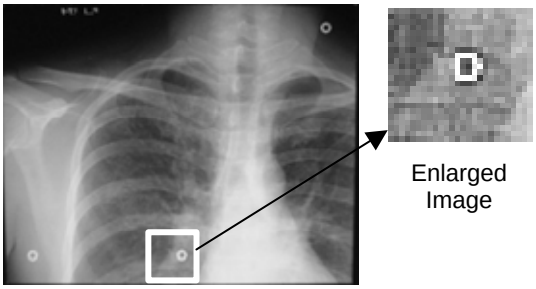

Figure 1.3 Digitally reproduced image

1.25 pixel/mm(800µm). 10bit

The image is mosaicked due to a large pixel size.

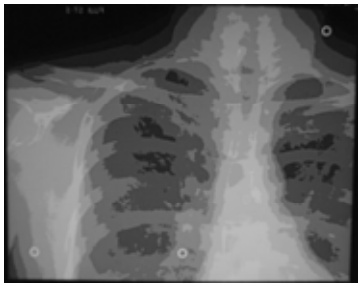

Figure 1.4 Digitally reproduced image

10 pixel/mm(100µm). 4bit

Contours are generated due to a low density resolution.

1.3 FCR Image Digitization Level

To determine the digitalization level for FCR image reading purposes, a high-resolution film digitizer was used to subject ordinary X-ray film to fine digitization (more specifically, 12 bit/pixel digitization at 50 μm/pixel [20 pixel/mm]). The digitization level was gradually lowered by a computerized process. Film output was generated with a laser printer. The resulting film output was evaluated subjectively and statistically from the viewpoint of X-ray diagnostics. The evaluation was conducted by a number of radiologists who compared the original radiograph and reproduced photographs. The results of an evaluation of a chest radiograph are summarized in Table 1.

It was assumed that no image deterioration occurred within the range marked by single- and double-circles. When the lower-limit quantization level was 200 μm (5 pixels/mm), 8 bits/pixel or 150 μm (6.7 pixels/mm), 7 bits/pixel, the results indicated that the diagnostic details of ordinary radiographs were adequately retained. Information about digitization levels adequate for FCR was obtained by repeating this evaluation procedure for all exposure targets and subject (or film) sizes.

Table 1 Chest image evaluation results

Sampling level \ Quantization level		Bits / pixel		
		8	7	6
Pixel size	50μm	◎	◎	◎
	100μm	◎	◎	××
	150μm	◎	○	××
	200μm	○	△	××
	400μm	×	×	××

Chest radiograph evaluation results

◎: No visible difference.

○: Virtually identical.

△: Slight image quality deterioration found.

×: Minor artifacts found.

××: Significant artifacts found.

1.4 Amount of Image Information

As shown in Figure 1.3, the amount of image information is the product of the pixel count and density resolution level (or pixel depth). If, for instance, there are 4096 pixels both horizontally and vertically and the density resolution level is 8 bits, the amount of information is (4096 × 4096) × 8 bits. The amount of information is usually expressed in megabytes.
Since 1M (mega) = 1024K (kilo), 1K = 1024, and 1 byte = 8 bits, the amount of information is 4 × 4 × 1 = 16 Mbytes.
Data processing by computers is done in units of 1024 instead of 1000. However, the conventional terminology of "kilo" and "mega" is retained.

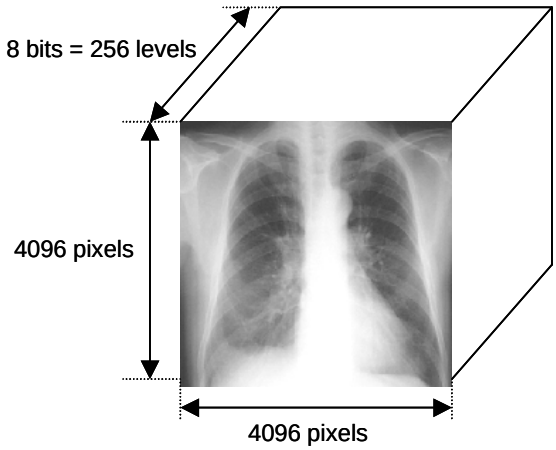

1.5 Amount of FCR Image Information

The digitization level for FCR images is determined in accordance with the results of experiments conducted as explained in Section 1.3. FCR offers two modes: standard mode (ST) and high quality mode (HQ). In the standard mode, the pixel size is varied according to the size of the Imaging Plate (hereinafter referred to the IP). In the high quality mode, the pixel size is fixed at 100 μm for all IP sizes.

Table 2 FCR reading pixel size and display reduction ratio

Reading mode	IP size	Pixel size	Density
ST	14" × 17" / 14" × 14"	200 μm	5 pix/mm
	10" × 12"	150 μm	6.7pix/mm
	8" × 10"	100 μm	10 pix/mm
HQ	All sizes	100 μm	10 pix/mm

Table 3 Amount of FCR information

Reading mode	IP size	Pixel count	Density resolution (bits)	Amount of Information (Mbytes)	Amount of information (DICOM) (Mbytes)
ST	14" × 17"	1760*2140	10	4.5	7.2
	14" × 14"	1760*1760	10	3.75	6
	10" × 12"	1670*2010	10	4	6.4
	8" × 10"	2510*2000	10	6	9.6
HQ	14" × 17"	3520*4280	10	18	28.8
	14" × 14"	3520*3520	10	15	24
	10" × 12"	2505*3015	10	9	14.4
	8" × 10"	2510*2000	10	6	9.6

Table 4 Amount of information generated at a model hospital having 1000 beds

Modality	Studies/day	Data (Mbytes/day)	Remarks
X-ray	1200	7200	1,760 × 1,760 × 2B (CR 14" × 14")
DSA	150	150	1,024 × 1,024 × 1B
CT	200	100	512 × 512 × 2B
RI	500	8	128 × 128 × 1B
MRI	300	150	512 × 512 × 2B
US	600	38	256 × 256 × 1B
Total	2950	8646	

Table 3 shows how the amount of information varies with the IP size and reading mode. Table 4 shows comparisons of the average amounts of information generated for various modalities. As implied in Table 4, the amount of digital information generated at hospitals mostly relates to radiography, necessitating proper management of the digital image files generated by FCR.

At hospitals, the radiographic data comprises the largest amount of data and cannot easily be handled. This is the reason why technologies for image compression and increased storage media density are important, details of which are discussed in a different section.

Supplementary Note: **Digitization units**

The digital image spatial resolution is usually expressed in pixels/mm. If, for instance, an area 1 mm square is divided into 5 × 5 blocks, the spatial resolution is 5 pixels/mm and the pixel size is 200 μm.

The density resolution is expressed in bits. This unit is used to indicate the number of binary digits. For example, 10 bits represents 2^{10}, indicating 1024 levels. When density values between 0.0 and 3.0 are uniformly assigned to a 10-bit range, the smallest discernible density change is 3/1024, or approximately 0.003.

Amount of information (Mbytes) = Number of images × Density resolution level (bits) / (1024 × 1024 × 8)

1M = 1024K, 1K = 1024, 1 byte = 8 bits

CAUTION

When an ordinary computer or DICOM format is used, due attention must be paid to the amount of information. For instance, if the density resolution level is 10 bits, it will be raised to an integer that is a multiple of 8 for format use, in this case 16 bits, thus providing 2 bytes per pixel.

1.6 Objectives and Possibilities of Digitization

Digital signals have the following advantages over analog signals:

1 Immune to noise.

Repeated recording and reproducing of data does not result in a deterioration of quality. In addition, when digital signals are transmitted, the degree of signal deterioration by extraneous noise is minimized.

2 A simple signal structure allows complex processing.

Since digital signals are highly conducive to arithmetic processing, image data conversion can be effected by image processing, thus offering easy-to-diagnose images. Image storage can be economically accomplished due to an image compression process. A complex network can be configured. Various other complicated processes can be performed.

In marked contrast from conventional screen/film system (hereinafter referred to as S/F system), digital signal use is characterized by film functionality that is divided into sensor, display, and storage functions. As a result, various devices having the separate functions are employed (Figure 1.5).

The biggest advantage of digital signal use is that you can increase work efficiency for various operations by establishing a network. Electronically stored images can be used in various situations to increase diagnostic accuracy and upgrade the quality of patient services. These purposes require the establishment of a system capable of handling high-quality images (large data files containing massive amounts of information) on demand.

Further, the linkage to text information (diagnostic information, medical charts, irradiation records, billing information, patient lists, etc.) can be defined to increase the efficiency of the execution of various tasks in hospitals.

At present, most institutions output diagnostic images on film. In the future, however, a changeover to software-based image diagnostics, or monitor diagnostics, will take place to realize economical value and increased speed.

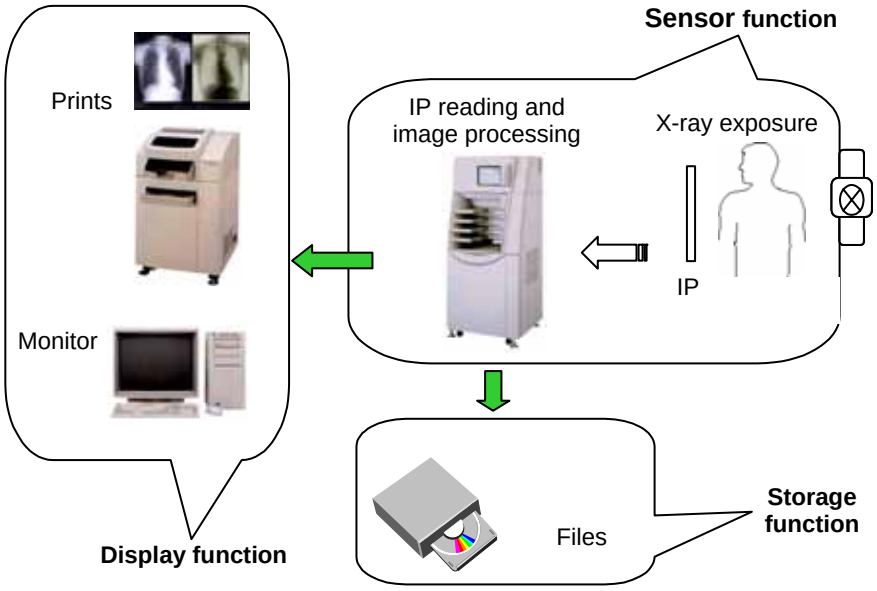

Figure 1.5 Functionality separation in digital image use

Chapter 2 Imaging Plate and FCR

2.1 What Is Photostimulable Phosphor

In China, around 1500 B.C, it was discovered that a certain substance emitted light when subjected to various external stimuli, a substance that is now called a fluorescent material or phosphor. However, this phenomenon does not seem to have been scientifically studied until a glowing stone called "Bologna stone" was discovered in Italy in 1603. In the latter half of 19th century, it was discovered that such a substance emitted light when stimulated by ultraviolet light, and glowed again later when exposed to infrared light. This phenomenon is called **"photostimulated luminescence" (PSL)**. Substances exhibiting PSL are called photostimulable phosphors. Well-known photostimulable phosphors include zinc sulfide, alkali halide, and oxide chemical compounds.

When PSL occurs, information about the first stimulus, or primary excitation, is recorded in the affected substance. Information about the first stimulus can be read by the second illumination, or secondary excitation. See Figure 2.1.

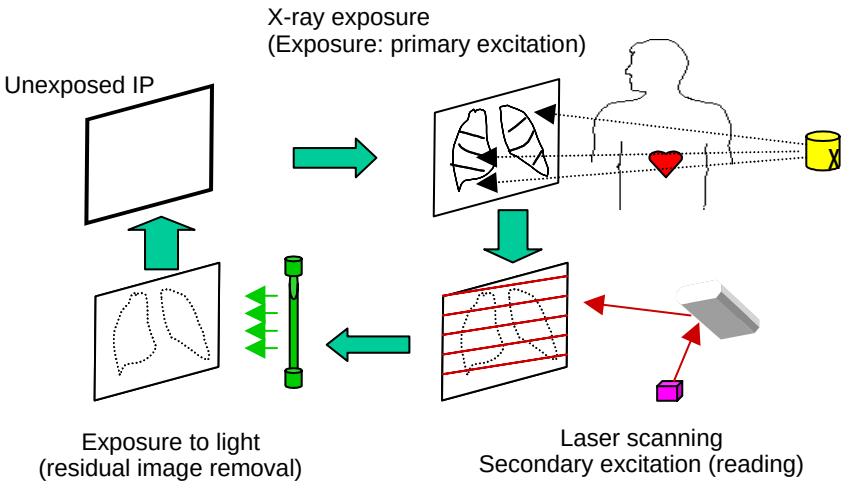

Figure 2.1 Imaging Plate operating principles
Recording → reading → erasure cycle

During IP development, various substances were synthesized and investigated, resulting in the adoption of barium fluorohalide compound (BaFX : Eu^{2+}, X = Cl, Br, I) crystal containing a trace amount of bivalent europium ions as the photostimulable phosphor for invoking PSL. This substance exhibits the highest degree of PSL among the known substances when the synthesis process is properly controlled.

It is known that this chemical compound stains when exposed for a prolonged period of time to X-rays, ultraviolet rays, or similar radiation. This phenomenon occurs when electrons are captured at a so-called color center, (also called an F center), a position without ions that absorbs light having a specific wavelength within the visible light range. This point is called an unoccupied lattice point. The trace amount of europium ion solid solution is called an activator. In the phosphor synthesis process, this activator replaces the barium ions in the BaFX crystal as a solid solution and forms the luminescence center. The color center and luminescence center are understood to play an important role in recording the X-ray information.

Figure 2.2 is an energy level diagram that shows the photostimulated luminescence mechanism of the BaFX:Eu phosphor (X = halogen). When this phosphor is used, an appropriate number of electrons is released to the conducting zone in accordance with the absorption energy prevailing at the time of primary excitation (exposure) by X-rays. These electrons are immediately separated into two groups. One electron group invokes luminescence (instantaneous light emission) in the excited state of Eu^{2+} (bivalent europium), which is the luminescence center. The other electron group becomes trapped at the halogen ion unoccupied lattice point initially formed within the phosphor, and forms a color center in the metastable state. (The latter group functions to record the radiographic information.)
When the phosphor is subsequently exposed to visible light (the secondary excitation light, or reading light) with a wavelength absorbed by the color center, the electrons trapped at the color center are released again to the conducting zone, causing photostimulated luminescence to occur in the excited state of Eu^{2+}. Radiographic information is read in this manner.

The description and diagram cover only the major aspects of the currently conceived photostimulated luminescence mechanism. Details have been avoided for brevity.

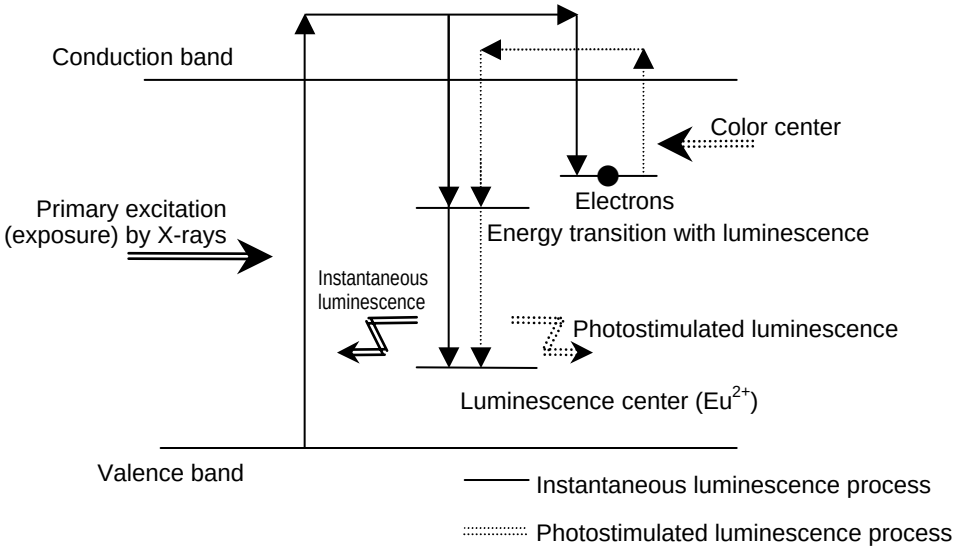

Figure 2.2 Mechanism of photostimulable phosphor PSL

2.2 Luminescence Characteristics

2.2.1 Luminescence spectrum and photostimulated excitation spectrum

As shown in Figure 2.3, the photostimulable phosphor employed by the IP emits bluish-purple light. This luminescence is invoked by the bivalent europium ions contained in a trace amount in the phosphor. The intensity of this luminescence varies with the wavelength of the light to which the IP is exposed after an X-ray exposure. This dependence of photostimulated luminescence on the wavelength is represented by a photostimulated excitation spectrum. Briefly, photostimulated luminescence is invoked most effectively by red light having a wavelength of about 600 nm. The photostimulated excitation spectrum is fairly consistent with the light absorption spectrum of the color center formed within the phosphor upon exposure to X-rays. This is one of the main reasons for stating that photostimulated luminescence is caused by the color center.

To enhance the image S/N ratio in the IP-based FCR system, it is necessary that the wavelength of photostimulated luminescence that has X-ray information be sufficiently different and optically separable from the wavelength of the photostimulated excitation light, and that the peak of the photostimulated luminescence spectrum be close to the 400 nm point, at which the photomultiplier (hereinafter referred to as the PMT) detects luminescence with high efficiency. The two spectra shown in Figure 2.3 have desirable characteristics that meet the above conditions.

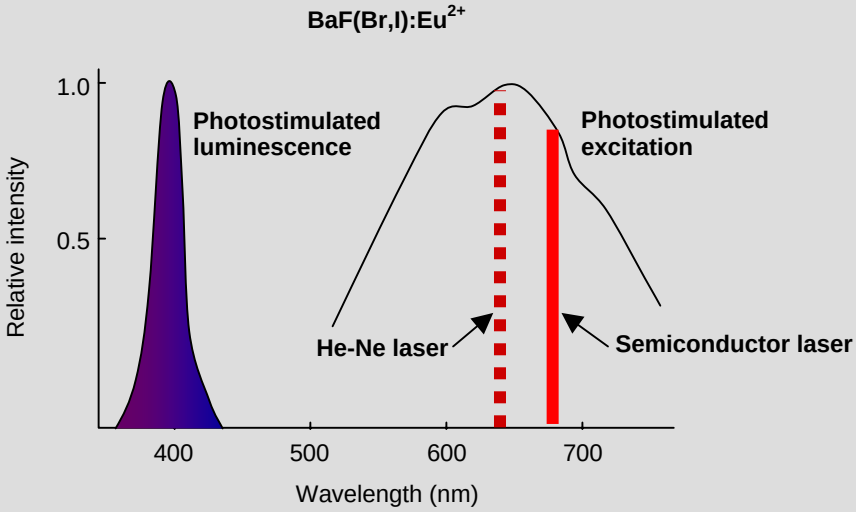

Figure 2.3 Spectra of IP photostimulated luminescence and photostimulated excitation

2.2.2 Luminescence response time

When photostimulated excitation light from an He-Ne laser or similar light source falls on an IP that has been exposed to X-rays, photostimulated luminescence occurs immediately. When light emission to the IP is stopped, luminescence stops accordingly. However, luminescence does not immediately decrease to zero. It gradually decreases until it reaches zero while exhibiting the luminescence attenuation characteristic specific to the luminescence process of the photostimulable phosphor. This attenuation characteristic is an important factor for the FCR system, which attempts to rapidly read radiographic information from the IP. If the attenuation rate is low when laser light falls on a certain pixel portion during scanning, the FCR system detects not only the luminescence, or radiographic information, of that pixel portion but also the residual luminescence, or noise, of the preceding pixel portion, which is still glowing, resulting in image quality deterioration. To achieve speedy high-resolution radiographic information-reading, the duration of attenuation needs to be less than a microsecond.

2.2.3 Dynamic range

Figure 2.4 shows how the amount of luminescence from the IP depends on the X-ray dose when the IP is exposed to X-rays. The figure shows that excellent linearity is exhibited over a 4-digit or wider X-ray dose range. This dynamic range, unobtainable on conventional S/F system, is a major feature that can be offered by the IP-based FCR system.

The FCR system uses a PMT to convert the IP's photostimulated luminescence to electrical signals, allowing the use of the IP's entire 4-digit wide dynamic range as valid diagnostic information.

This wide dynamic range not only enables the correct detection of slight differences in X-ray absorption characteristics among the various tissues of the subject, but also permits the use of a fully-automatic image processing system called EDR, details of which are discussed in a separate section. This system can constantly generate consistent digital radiographs under any X-ray exposure conditions. It also enables the enlargement of the visibility range for the dynamic range control process, as explained in a separate section.

2.2.4 Fading

The term "fading" refers to a phenomenon in which the radiographic information recorded in the IP upon exposure to X-rays decreases with the elapsed time until it is read. This occurs when photoelectrons generated by primary excitation of X-rays within a photostimulable phosphor crystal are thermally released with time while being trapped at the color center inside the crystal, and therefore rendered unable to contribute to photostimulated luminescence. Figure 2.5 shows how the photostimulated luminescence intensity attenuates with time during the interval between X-ray exposure and radiographic image reading. If, for instance, the elapsed time before image reading is eight hours, the amount of luminescence decreases by about 25%. The longer the elapsed time and the higher the storage temperature, the higher the degree of fading. While fading is an unavoidable aspect of photostimulated luminescence, it can be reduced. Reduction of fading is therefore an important point in the improvement of photostimulable phosphors.

The FCR system is devised so that the EDR function prevents any fading-induced decrease in the amount of luminescence from causing a diagnostic problem. However, if the IP is exposed to a lower than normal radiation dose and then left standing for a long period of time before being read, it will suffer from graininess deterioration and natural-radiation-induced graininess degradation (to be discussed later). To avoid such problems, the image reproduction process should be completed within eight hours after IP exposure.

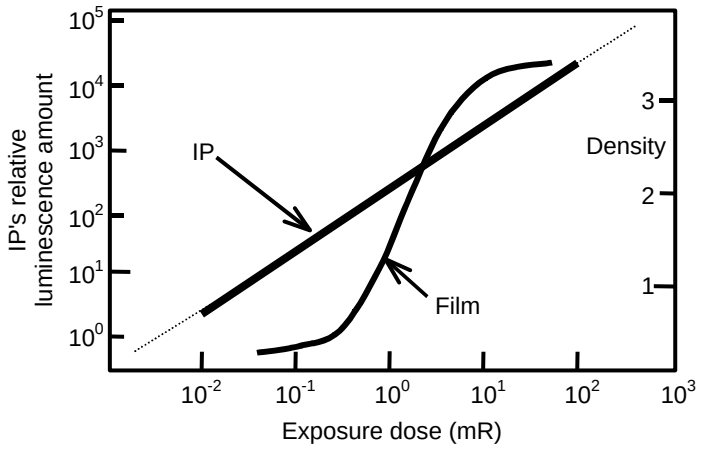

Figure 2.4 IP dynamic range

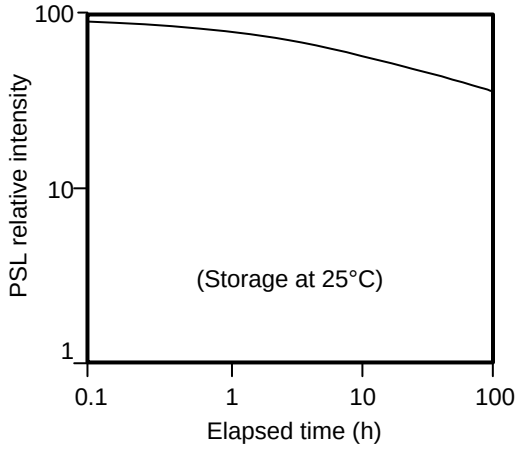

Figure 2.5 Fading characteristic

2.2.5 Influence of natural radiation

The IP is sensitive not only to X-rays but also to electromagnetic radiation such as ultraviolet rays and γ rays and particle radiation such as α rays, β rays, and electron rays. It acts as a highly sensitive sensor capable of storing absorbed radiation energy and detecting it as an image. These characteristics also make the IP susceptible to the influence of natural radioactive elements contained in walls, and objects within the building where the IP is placed or in the earth crust of the local area, and to the influence of cosmic rays and other radiation irradiating the Earth. If a thoroughly erased IP is allowed to stand for a long period of time and then used in the FCR system to achieve image reproduction under high-sensitivity conditions, slight black spots will appear in random locations. The number of such black spots varies depending on the length of time since erasure. Some black spots are attributable to the IP itself, i.e., the IP records the radiation from trace amounts of radioactive isotopes contained in the phosphor. Others are attributable to the natural radiation discussed above. The influence of the IP itself can be practically eliminated through control of the raw material for the IP.

When reading an image from an IP under high-sensitivity conditions, the IP must not be allowed to stand for a long period of time. If the IP has stood for a long period of time, you must radiate it with light before radiographic exposure to avoid the influence of the natural radiation discussed above. You should keep in mind that the bedrock in some districts contains a large number of radioactive isotopes and that natural radiation is constantly emitted from concrete, marble, potassium-containing wall materials, and various other substances.

NOTE

Before using an IP that has been stored for a long period of time without being used, it is recommended that you subject the IP to erasure for reasons said above.

2.3 IP System Noise Factors

The noise affecting the IP image quality can be divided into three types: fixed noise, X-ray quantum noise, and light quantum noise.

(1) Fixed noise

Fixed noise is generated when luminescence amount planar nonuniformity is caused by phosphor spatial distribution nonuniformity within the phosphor layer.

This noise largely depends on the phosphor grain size distribution (statistical variance relative to grain size). It can be effectively reduced by making the phosphor grains finer. Note that each stage of IP improvement, beginning with the improvement over Type I, has seen a finer rendering of the phosphor grains.

(2) X-ray quantum noise and light quantum noise

Fixed noise can be reduced by making the phosphor grains finer. However, merely rendering them finer results in a decrease in the amount of luminescence from the phosphor, or luminescence brightness, and the phosphor filling density in the phosphor layer. A decrease in the luminescence brightness causes the light quantum noise to increase, while a decrease in the phosphor filling density causes the X-ray quantum noise to increase. The most important task for IP improvement has been to make the grains finer while preventing these decreases.

For Type VN and VI IPs, the grain shape was modified to reduce X-ray quantum noise. Since the conventional BaFX phosphor was amorphous and planar, planar parallel orientation readily occurred within the phosphor layer at the time of IP production. In such a situation, both the excitation light and luminescence light easily disperse in the direction of the phosphor layer plane. However, they do not easily propagate in the direction of the thickness. If a phosphor having grains are shaped like a sphere could be created, the light scattered within the IP phosphor layer would be rendered isotropic for improved image quality. An appropriate phosphor production method was therefore devised to develop an isotropic phosphor that is mainly a polyhedron having fourteen faces similar to a sphere. The use of this newly developed phosphor resulted in an X-ray quantum noise level lower than that of its predecessor, as expected.

2.4 Mechanism of FCR Image Formation

The excitation light from the semiconductor laser radiates an IP that has been exposed to X-rays to invoke photostimulated luminescence. A drive motor precisely conveys the IP. A polygon mirror uses the laser light to conduct a scan. During this operation, luminescence concerning the IP coordinates is collected via the light-collecting guide and converted to an electrical signal by the PMT. The resultant signal is converted to a digital equivalent when it passes through the AD converter. The digital signal is sent to the CPU section, where it is converted to the final signal by EDR and image processing (Figure 2.6).

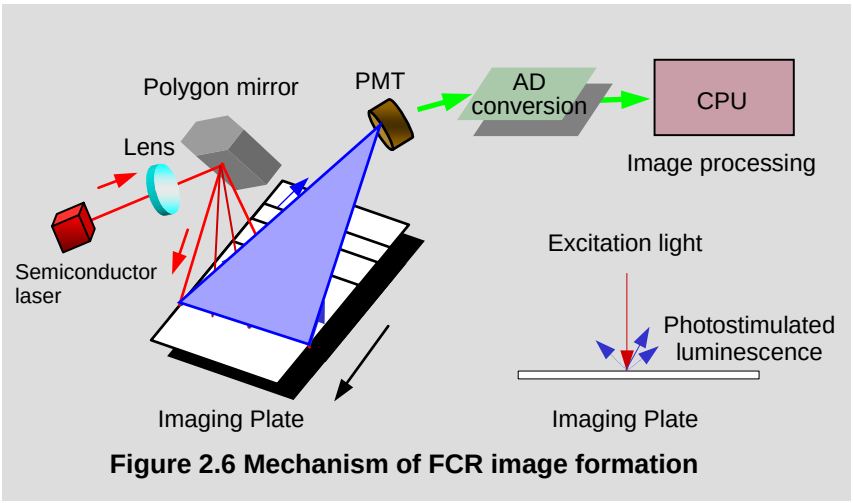

Figure 2.6 Mechanism of FCR image formation

2.5 FCR History and Technological Targets

The technological targets for FCR have been offering higher quality images, reducing the equipment size, and improving the image reproduction performance. The following improvements have been made since the release of the FCR101 in 1983:

1983: FCR101 released..... (first generation)
1985: FCR201 released, built-in type 501 released ..... (second generation)
1988: FCR7000 Series and AC-1 released ..... (third generation)
1993: FCR9000 Series and AC-3 released ..... (fourth generation)
1998: FCR5000 Series released ..... (fifth generation)
2000: Dual-light-collection IP-reading type FCR released

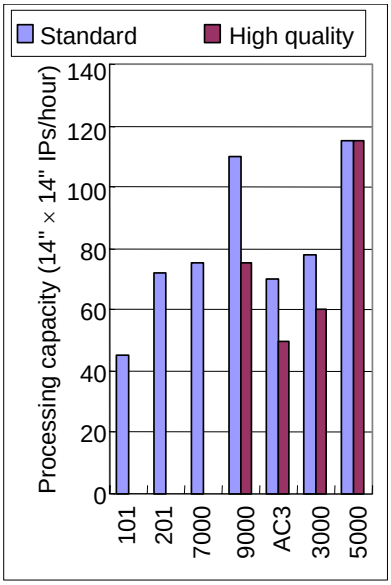

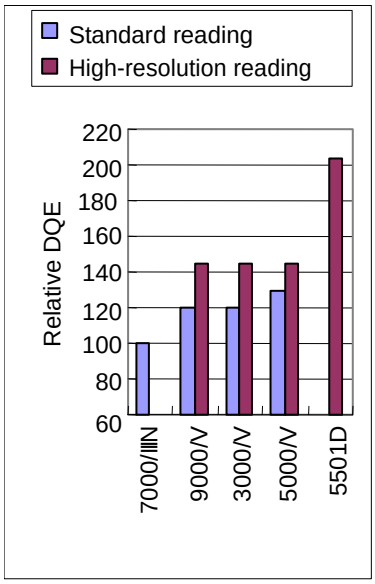

1985 - FCR201

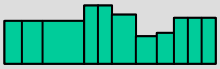

Width: Approx. 8 m
Processing capacity:
72 IPs /hour
(14" × 14" size)

1998 - FCR5000

Width: Approx. 1.7 m
Processing capacity:
120 IPs /hour
(14" x 14" size)

2.6 Dual-Light-Collection IP-Reading FCR System

2.6.1 Introduction

The most important objective of radiography is to offer an accurate image of the internal human body structure. This objective can be achieved by improving physical image quality factors such as the S/N ratio and dynamic range and by enhancing the diagnostic imaging quality through processing that converts it into an easily interpretable image. For image processing purposes, technologies such as gradation processing and spatial frequency processing were developed. In 1999, a new image processing technology called Multi-Objective Frequency Processing (MFP) was developed and has been favored since then. This section describes dual-light-collection IP-reading technology, newly developed to greatly increase the image S/N ratio, and the high-quality FCR system that incorporates it.

2.6.2 Principle of the dual-light-collection IP-reading system

To reduce X-ray quantum noise, which exerts the most significant influence upon image quality, it is necessary to substantially increase the amount of X-ray absorption. This increase can be achieved by converting the absorbed X-ray energy into detectable IP photostimulated luminescence. However, simply increasing the IP phosphor layer thickness to increase X-ray absorption will not significantly increase practical X-ray use efficiency for the currently employed single-sided IP reading system shown in Figure 2.7. The reason is that the luminescence inside the photostimulable phosphor layer, which is separated by a distance from the laser excitation section, needs to reach the surface detector through the phosphor layer, which acts as a scatterer, resulting in a low probability of detection by the detector.

Therefore, a new IP reading system was devised as shown in Figure 2.8. This system uses a transparent IP support that is also equipped with a detector for detecting the fluorescence from the support. The image data detected by the respective detectors is added at the optimum ratio (discussed in a separate section), and then used as the final image data. With this method, the detector on the back surface of the support can effectively detect the luminescence corresponding to the X-ray information absorbed inside the phosphor located at a distance from the laser excitation section. Using the detected luminescence in conjunction with the information provided by the detector on the front surface increases the amount of available information. As a result, any significant amount of X-ray signals absorbed in the thick phosphor layer can be obtained as an image signal.

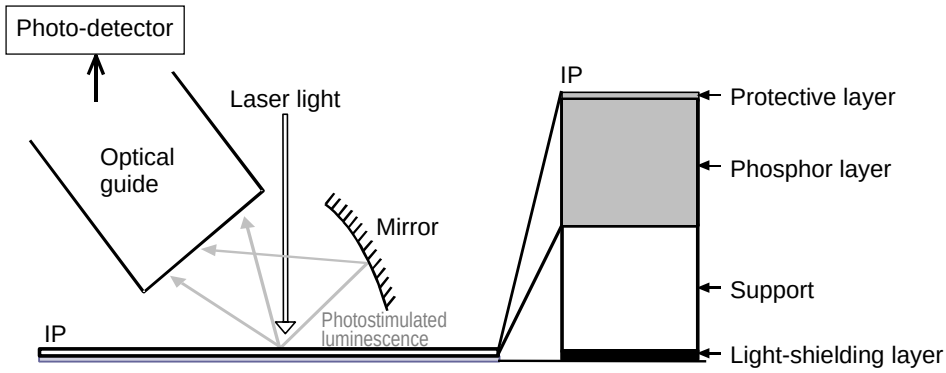

Figure 2.7 Single-side light collection IP reading system

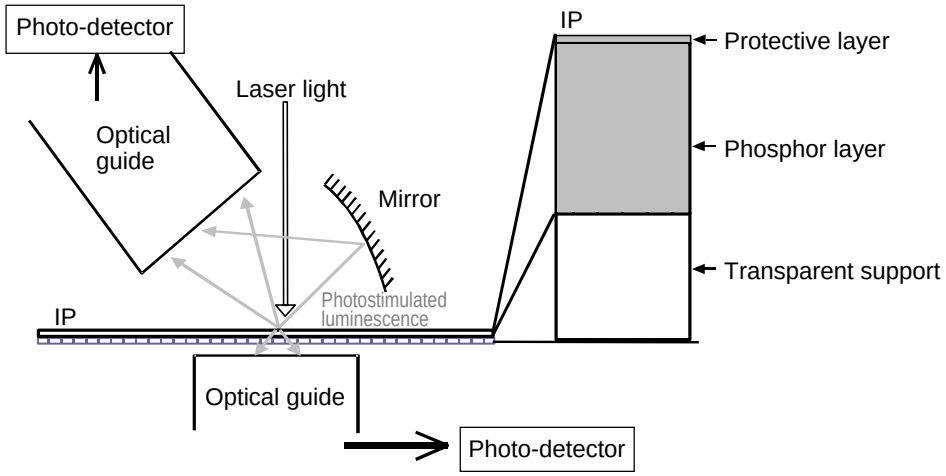

Figure 2.8 Dual-light-collection IP-reading system

2.6.3 Image quality improvement by unique image addition

Figure 2.9 shows the NEQ (noise equivalent quanta) values of the IP front-surface image (X-ray incidence side) and back-surface image (support side). The surface image NEQ value exhibits virtually the same dependence on the spatial frequency as that described for the current IP reading system. In addition, while the NEQ value of the back-surface image is virtually the same as that of the front-surface image in the low spatial frequency region, it sharply decreases in the high spatial frequency region. This leads to the expectation that using the back-surface image information will contribute to image quality improvement particularly in the low spatial frequency region. However, simple addition will not produce satisfactory results in all the spatial frequency regions.

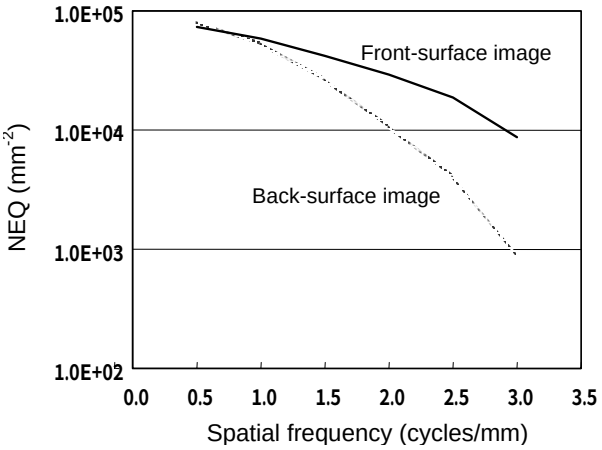

Figure 2.9 NEQ of front- and back-surface images (0.5 mR)

The effects of addition were examined by changing the addition ratio for each frequency component. The results are shown in Figure 2.10. As expected, it was found that optimum image quality (NEQ) improvements were obtained when addition was performed with the back-surface signal proportion increased for low frequency regions and decreased for the high frequency regions.

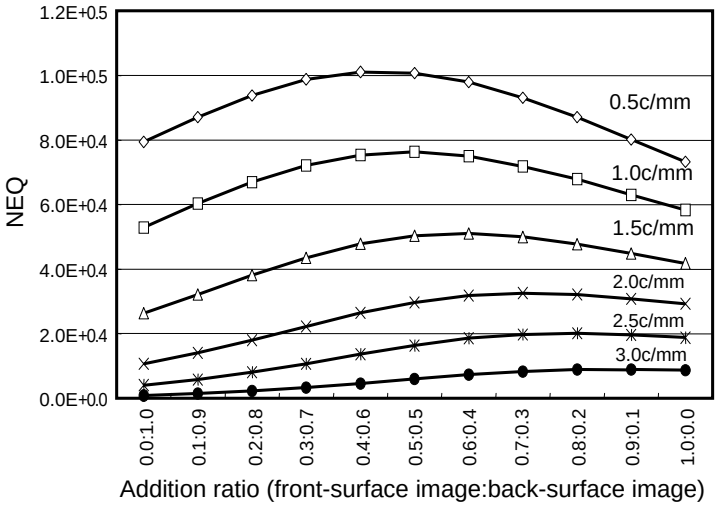

Figure 2.10 Dependence of NEQ on addition ratios at various spatial frequencies (0.5 mR)

Using the Fourier transform method made it possible to perform the addition at varying ratios for the spatial frequencies. However, because this method was not practical in terms of computation speed and memory capacity, a method based on spatial filter use was developed. Figure 2.11 shows the NEQ values of images obtained when this method was used, and the simple additions that were performed to maximize the NEQ values at 0.5 c/mm and at 3 c/mm. The figure indicates that the NEQ values are maximized at almost all frequencies, resulting in considerably higher image quality than when used in the conventional single-light-collection IP-reading system.

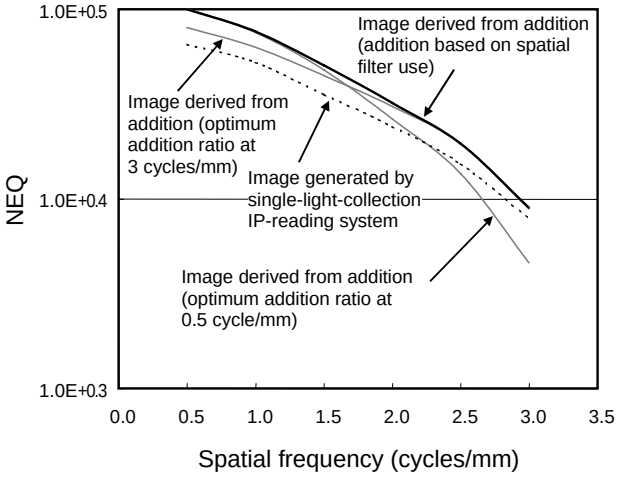

Figure 2.11 NEQ values after addition

2.6.4 Built-in type FCR development based on dual-light-collection IP-reading technology

The FCR5501D (standing type) and FCR5502D (bed type) were developed using dual-light-collection IP-reading technology. Figure 2.12 shows the relationship between image quality and processing capacity. The figure indicates that the FCR5501D has the same processing capacity as the FCR5501H but exhibits a substantial image quality improvement over the FCR5501H. Further, the internal equipment layout was made more compact so that the required installation space would be equal to that of the FCR5501H. In addition, an IP with a maximum image recording area of 17" × 17" is built in to handle patients of large build, a highly evaluated feature of the FCR5501H. The renowned multi-objective frequency process of course incorporated as a standard feature

The bed type FCR5502D also has substantial performance improvements over its predecessor. Compared to the preceding FCR9502HQ model, the FCR5502D has nearly twice the processing capacity and 1.3 to 1.4 times better image quality. In addition, the FCR5502D is patient-friendly with its mechanism for varying the bed height between about 485 mm and 820 mm. It is also designed to support the 17" × 14" landscape, 12" ×10" landscape, and 10" × 8" landscape sizes, enabling it to handle all types of lying position exposures.

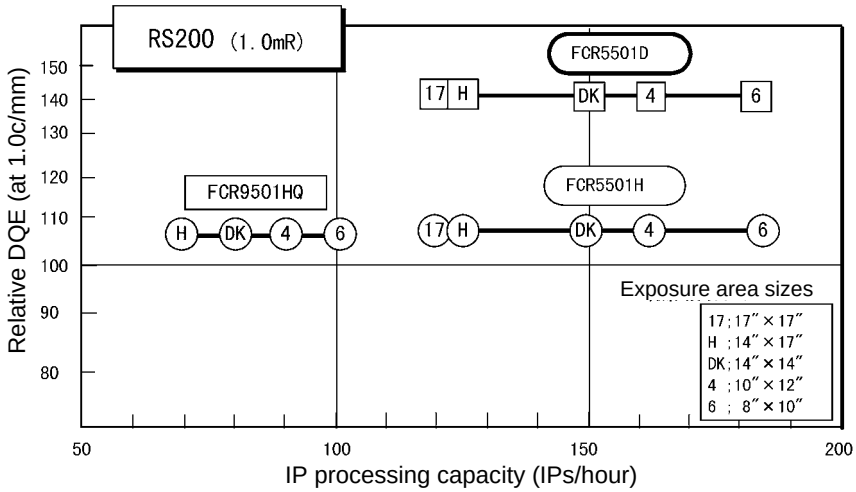

Figure 2.12 FCR5501D IP processing capacity and image quality

FCR5501D

FCR5502D

Chapter 3 Automatic Sensitivity Correction Function (EDR)

3.1 Roles of EDR

In order to provide high diagnostic value, radiographs need to have suitable density and contrast. When the S/F system is used, the exposure conditions need to be carefully set up to obtain density and contrast suitable for the subject thickness and position.

EDR (Exposure Data Recognizer) is an automatic image adjustment function that provides suitable density and contrast even when the exposure conditions slightly vary.

The following skull images were obtained by exposing them at 3 mAs and 30 mAs and then reading them in the FCR's AUTO mode. The two images have exactly equal density. However, they completely differ in image noise, indicating the difference in quantum noise.

When the conventional S/F system is used, the 3 mAs image would be entirely transparent if the finished 30 mAs image had normal density.

When varying the exposure voltage for the same subject, decreasing the voltage increases the contrast

3 mAs 30 mAs

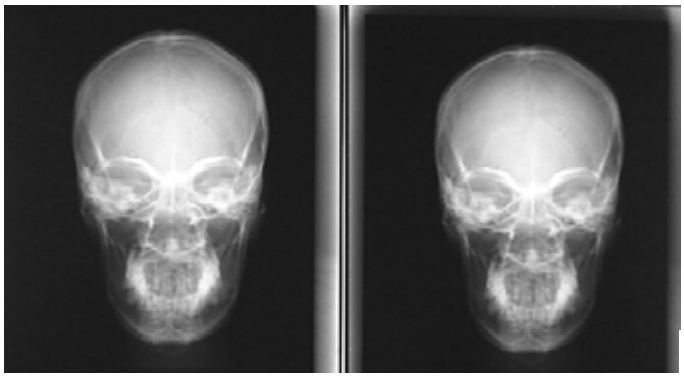

and narrows the visibility range. This frequently occurs when the S/F system is used. Since the EDR automatically adjusts the acquisition range in accordance with the image signal width, it provides constant contrast and visibility area. For comparison, chest rediatrams obtained at 60 kVp and 120 kVp are shown below:

60 Kvp 60 Kvp

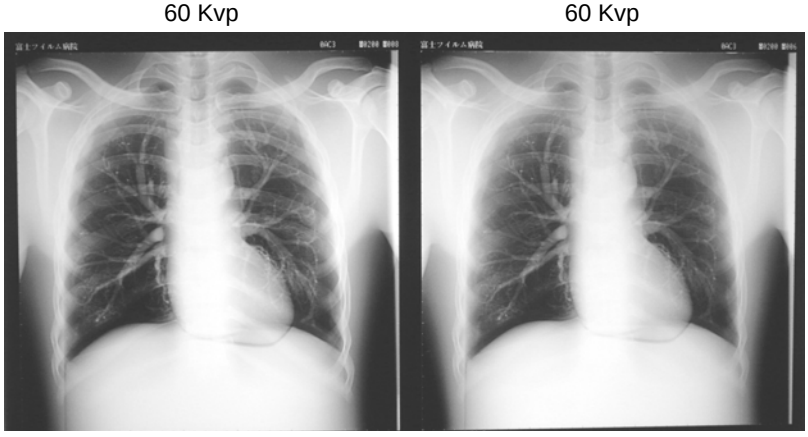

CAUTION

This does not mean that images can be exposed at any arbitrary exposure conditions. Since images are derived from X-ray transmission signals, it is necessary to establish proper exposure conditions for acquiring appropriate X-ray signals. The same exposure conditions as used for the S/F system are recommended.

The FCR system is serviceable when the proper exposure conditions are difficult to determine. This is because, for example, if the deviation from the correct conditions setup is as great as 20%, the S/F system usually produces unacceptable results while the FCR system frequently yields acceptable results. The use of the FCR system will be useful, for instance, in taking bedside shots with a portable device and taking images of a critical surgical operation that has no margin for error.

3.2 Signal Conversion by Image Formation System

First conversion: Converting X-rays to light

The figure below shows the relationship between the amount of photostimulated luminescence caused by laser excitation and the IP's unique property of X-ray absorption amount. The relationship is linear over a 4-digit or wider range, thereby contributing to the enhancement of FCR system sensitivity and dynamic range.

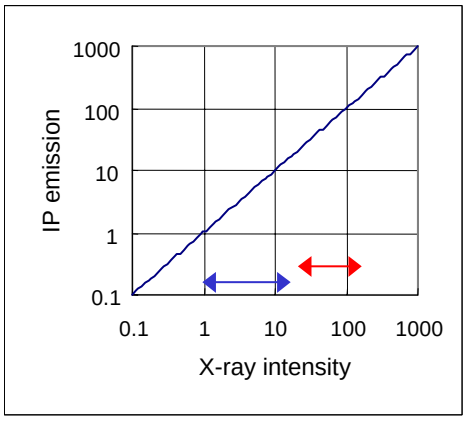

Second conversion: Converting light to a digital value

The amount of luminescence from the IP is converted to a digital value. In this phase, quantization is not effected over the entire luminescence range. The range of imaging is predefined, after which quantization is performed over the predefined range. This function (EDR mechanism) enables the density and constant to be maintained constant.

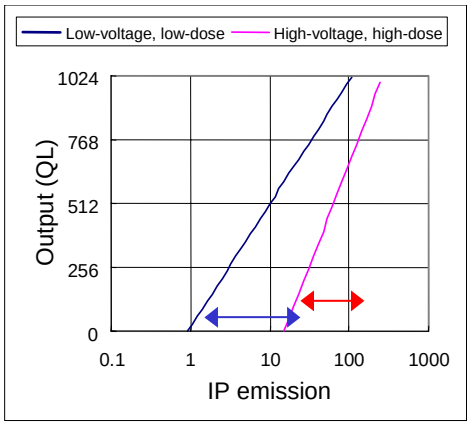

Third conversion: Digital value conversion by image processing

The image processing function is incorporated. Various image processes are performed as needed to display images suitable for diagnostics. The image processes performed include gradation processing and spatial frequency processing operations.

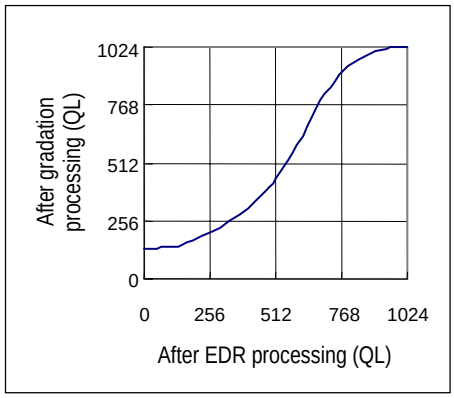

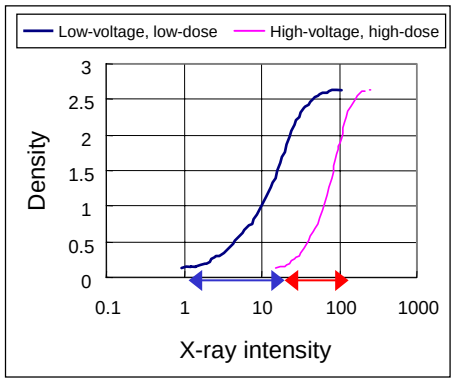

Fourth conversion: Converting the FCR output value to film density

The image signal fed to the image recording unit is converted again to an optical signal to produce a radiograph. Automatic corrections are made to ensure that the resulting film characteristic curve is linear.

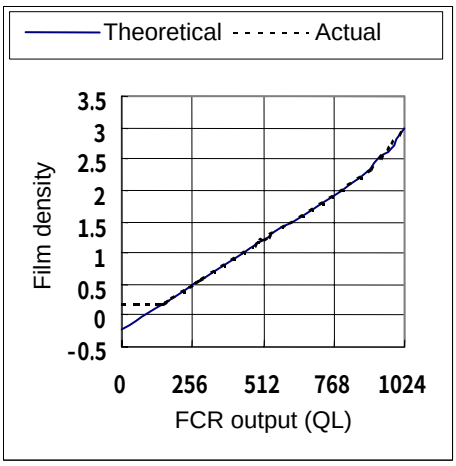

Final characteristic curves

The figure shows the characteristic curves of radiographs generated by the FCR system. Unlike the characteristic curves of conventional radiographs, those of the FCR system vary with the X-ray dose and image range to form images having uniform density and contrast.

NOTE:
The arrows in the figures indicate imaging ranges.

3.3 What Is EDR

The IP's sensor function is characterized by a wide X-ray exposure range (4-digit or wider) and linear response over the entire exposure range. However, if this wide exposure range is directly digitized, a low density resolution results. Therefore, the FCR system digitizes only the necessary information within read 4-digit data.

More specifically, the whole 4-digit range is finely digitized. Low resolution data is then derived from the digitized data to generate a histogram. After the image properties are analyzed with the generated histogram and registered menus, the optimum image display range is determined to perform 10-bit quantization. The mechanism for performing this processing operation is called the **EDR** (Exposure Data Recognizer).

3.4 Histogram

The histogram shows a distribution of pixel values. When the pixel values are as indicated in the lower left table, the number of pixels of a specific pixel value is counted (no pixels have the value 0, four pixels have the value 1, eight pixels have the value 2, etc.). The data obtained in this manner is graphed to show the distribution in the form of a histogram.

Image pixel values

1	4	4	4	1
4	2	2	2	4
4	2	3	2	4
4	2	2	2	4
1	4	4	4	1

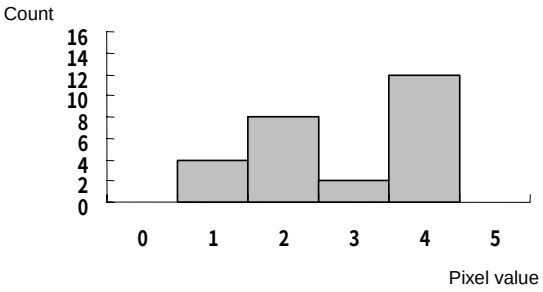

3.4.1 Histogram analysis

Image stability is achieved by keeping constant the image density of the points of interest. The histogram shown in Figure 3.1 is used for explanation purposes. In the chest region, for instance, the lung field and heart densities are generally regarded as needing to be close to 1.6 and 0.5, respectively. Therefore, when you find the histogram points that correspond to the lung field and heart, you can assign such points (Smax, Smin) to digital values (Qmax, Qmin) that correspond to the density values 1.6 and 0.5. According to the available information about exposure regions and orientations (that is, exposure menus), nearly the same histogram shape results, allowing analyses to be empirically made.

The X-ray dose range assigned to the digital values between 0 and 1023 with the intersection of Smax and Qmax joined with the intersection of Smin and Qmin is expressed as the image. When the width of the range is **the L value (logarithm)** and the central point of the range is Sk, the **S value** is defined by the equation $S = 4 \times 10^{(4-Sk)}$ (the relationship to the normally used specific sensitivity is explained in a separate section).

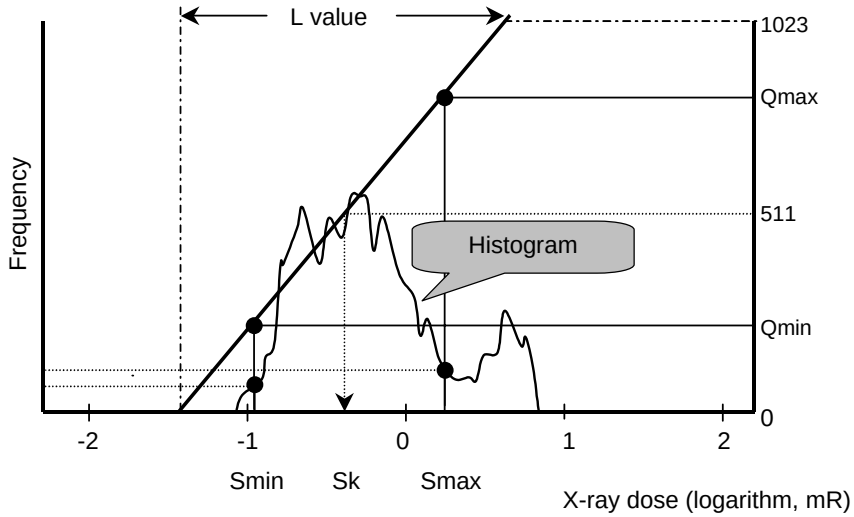

Histogram, AUTO mode FCR image (when a gradation close to film gradation is obtained by gradation processing), S value, and L value changes with the exposure conditions and subject

Relationship between film/screen system X-ray dose and density
Relationship between FCR X-ray dose and density under the original conditions
Relationship between FCR X-ray dose and density under the varied conditions

Image shot with the exposure amount doubled

FCR:
The histogram is translated toward the high X-ray dose side. The X-ray dose-density curve is translated by the same amount. As a result, the image density and contrast remain unchanged. The S value is reduced to half. The L value remains unchanged.

Film/screen:
The density is greatly raised.

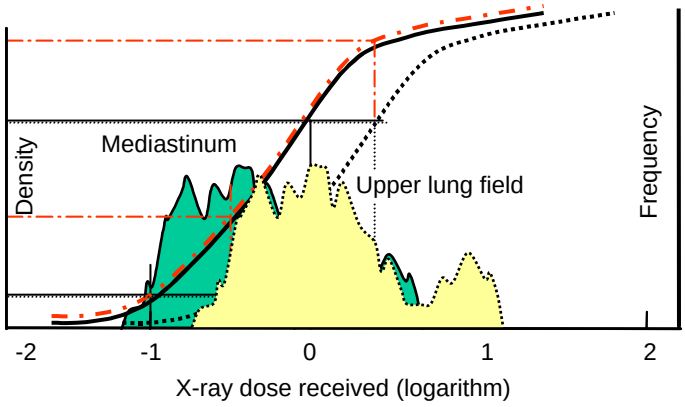

Image shot with the exposure voltage raised and the phototimer setting left unchanged

FCR:
The histogram width is decreased. The X-ray dose-density curve is shifted toward the higher γ region accordingly. As a result, there is no significant change in the image density or contrast. The S value remains almost the same. The L value is decreased.

Film/screen:
The image contrast is low.

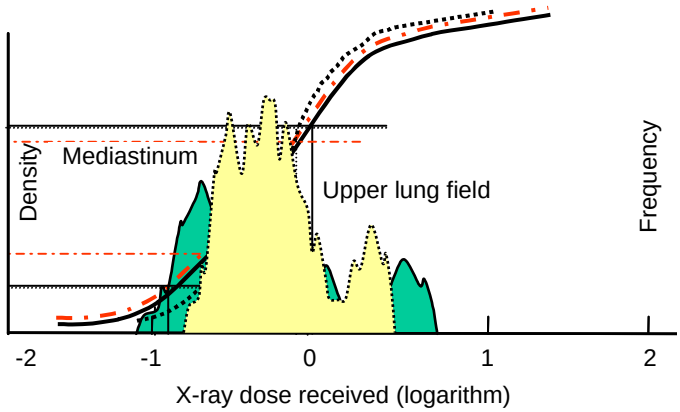

Heavy-set person is radiographed without changing the exposure voltage or phototimer setting

FCR:
The histogram width is increased. The X-ray dose-density curve is shifted toward the lower γ region accordingly. As a result, the image contrast is slightly lowered and the entire area depicted. The S value remains almost the same. The L value is increased.

Film/screen:
While image contrast remains unchanged, the mediastinum is not readily depicted. The exposure voltage should normally be raised. A radiograph obtained with raised exposure voltage would be similar to the FCR image.

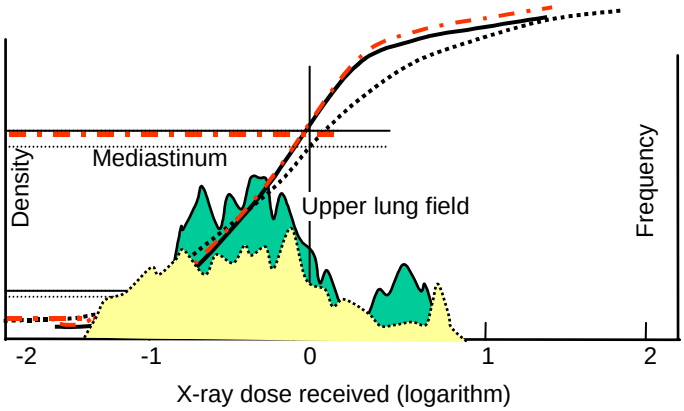

3.5 EDR Modes

The EDR offers the following five modes:

(1) AUTO mode: The reading latitude and sensitivity are automatically adjusted. This mode is activated for most menus.

(2) SEMI AUTO mode: The reading latitude is fixed. Only the sensitivity is automatically adjusted.

(3) FIX mode: The dose needs to be controlled as is the case with the S/F system.

(4) SEMI-X mode: The reading latitude is fixed. Only the sensitivity is automatically adjusted.

(5) MANUAL mode: The image recording range is to be manually determined while viewing the image on the monitor.

3.6 AUTO Mode

In the AUTO mode, the image recording range is automatically determined. When the AUTO mode is selected, you must determine before histogram analysis whether the target image is divided and what IP area is to be subjected to histogram analysis. The reason is that the area to be subjected to histogram analysis needs to be free of portions irrelevant to the image when a radiograph is shot with the area divided and an aperture diaphragm inserted.
In FCR, the above function is generally referred to as the PRIEF (Pattern Recognizer for Irradiation of Irradiation Field).

The EDR process flowchart is shown in Figure 3.2.

1 First, the EDR determines whether the image is divided (division recognition).

2 Next, the irradiation field is determined (irradiation determination).

3 Finally, the image recording range is determined according to histogram analysis (S value/L value determination).

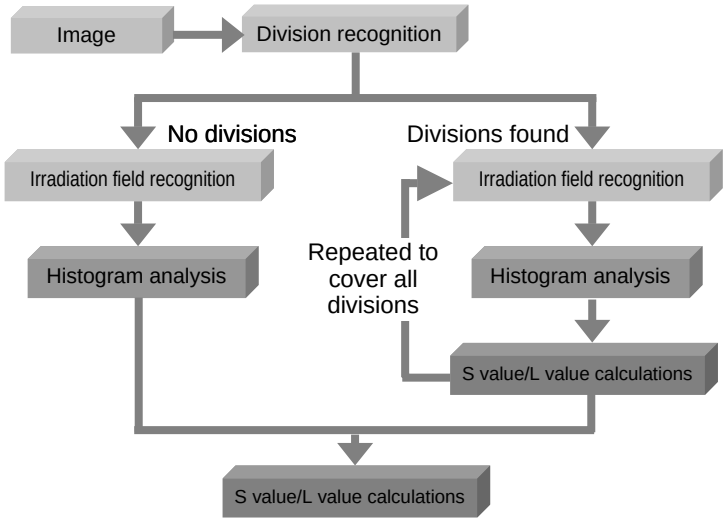

Figure 3.2 EDR process flowchart

3.6.1 Division exposure area recognition process

The division exposure process determines that the image area is not divided, divided into the upper and lower halves, divided into the right- and left-hand halves, or divided into four sections. The division patterns are automatically recognized.

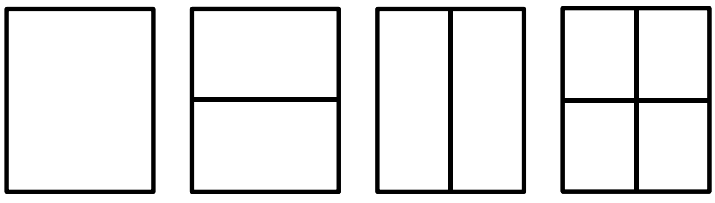

Division recognition algorithm

The following two methods are combined to achieve final division recognition.

(1) In the cross region consisting of vertical and horizontal lines extending from the image center, a differentiation process is performed independently for the vertical and horizontal directions to detect division edges.

(2) Division recognition is achieved by means of pattern matching.

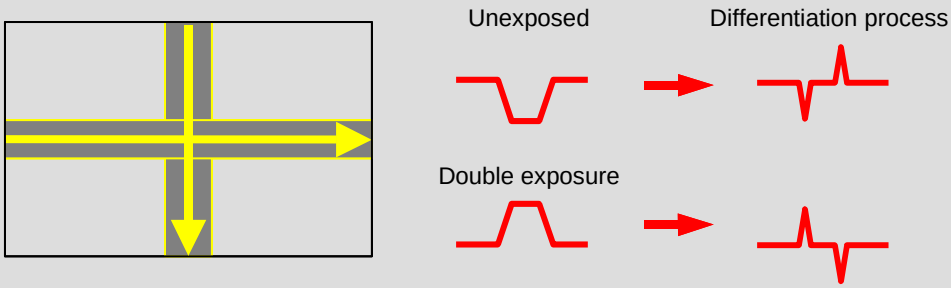

Figure 3.3 Division line recognition method

The differentiation process is performed independently for the main scanning and subscanning directions so that any gaps between image divisions are detected in accordance with the threshold value (th).

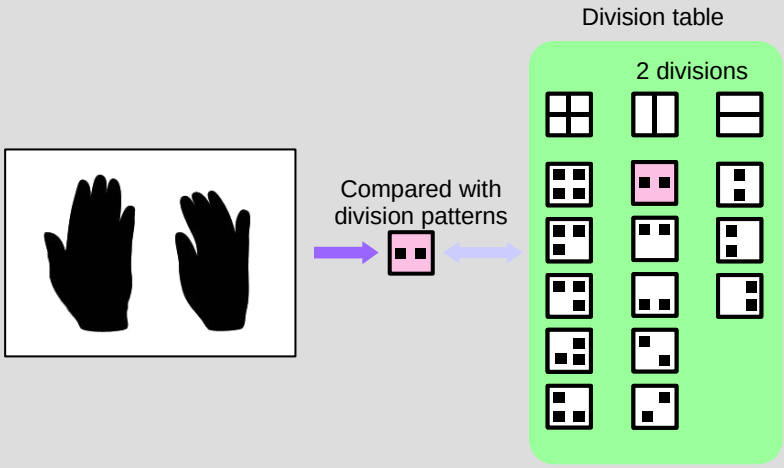

Figure 3.4 Recognition method based on pattern matching

The image histogram is used to perform a binarization process so that image data greater than a digital threshold value is set to "1", and image data smaller than the threshold value set to "0". Binarization is performed so that the image data within the division aperture is mostly set to "1" and the data outside the aperture set to "0". Next, the degree of binarized pattern matching is calculated with reference to previously prepared four-division, upper/lower two-division, and left/right two-division patterns. The pattern with the greatest match is then selected. If the degree of matching is found lower than the threshold value with respect to all the above three division patterns, the system concludes that no division pattern exists.

3.6.2 Irradiation field recognition process (PRIEF 4S)

Importance of irradiation field recognition

If the histogram is derived from the entire IP surface and used for analysis in situations where a radiograph is made with an irradiation field aperture diaphragm inserted, an attempt is made to radiograph a wide area as shown in Figure 3.5, resulting in an increase in the density of the region of interest (ROI). The optimum density is obtained if the irradiation field shape is recognized and the data within the irradiation field is used for histogram creation and analysis.

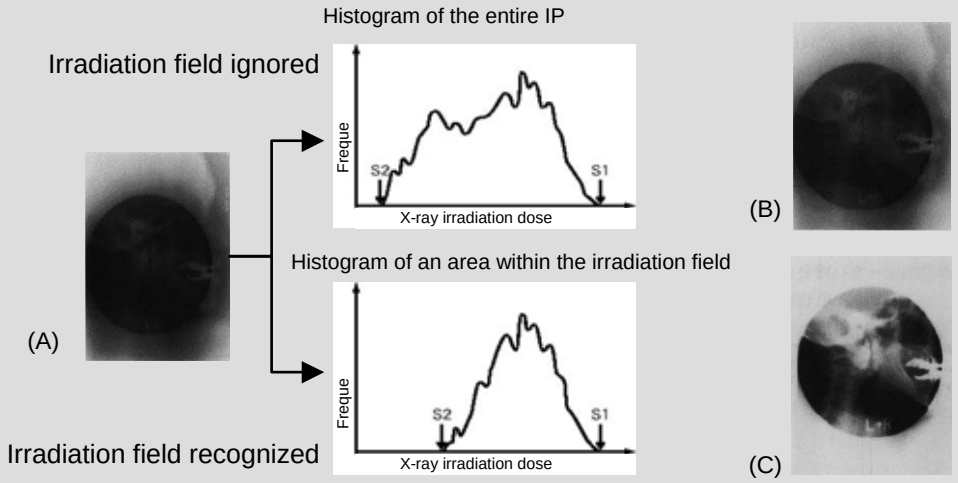

Figure 3.5 Difference in histograms derived from the entire IP surface and irradiation field internal area

Flow of irradiation field recognition

1 The start point for locating the irradiation field is determined. The center of gravity of the differential density value should normally be determined as shown in Figure 3.6, and then used as the start point.

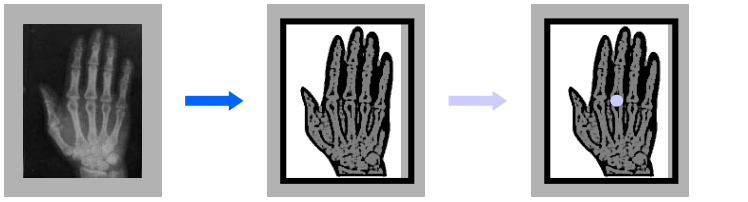

Figure 3.6 Central point determination

2 A differentiation process is performed in one radial direction from the determined irradiation field center to locate the positions at which the differential exceeds a predetermined threshold value. The located positions are regarded as candidate irradiation field edge points. The candidate edge points are then checked to locate actual irradiation field edges. Eventually, eight irradiation field edge points are sequentially joined to form a polygon, which is recognized as the irradiation field. If any concave area (G) is encountered, it is corrected. The resultant polygon is converted to a rectangle depending on the conditions.

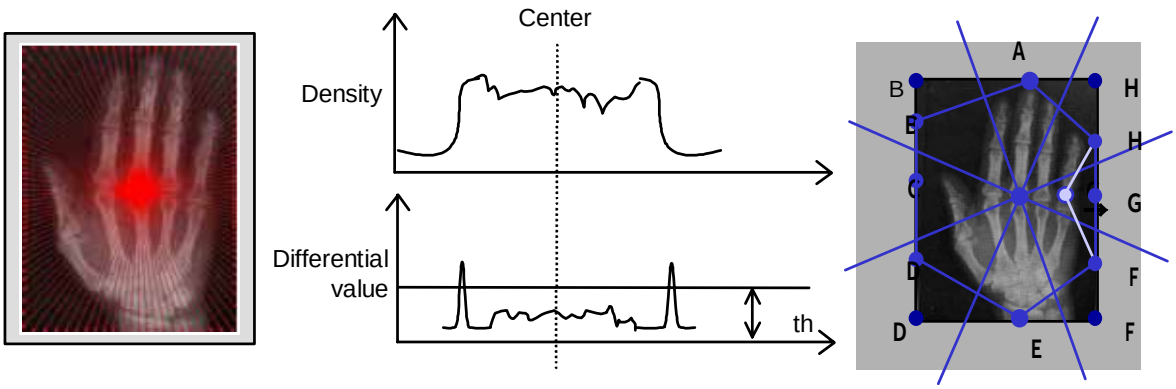

3.6.3 PRIEF varieties

The commonly used PRIEF (PRIEF 4S) performs division recognition and then recognizes an arbitrary convex irradiation field. In tomography, however, blurred images might increase the probability of error in division recognition/irradiation field recognition. To avoid such an increase, limitations are imposed so that a rectangle parallel to the IP sides is recognized. Since the PRIEF 1 does not make division radiographs, do not insert the aperture diaphragm to make division radiographs. The PRIEF 1 exposes the entire IP surface to radiation. It also uses special algorithms depending on the exposure region.

PRIEF 1: Used for tomography (chest, abdomen, pelvis, upper extremity, and lower extremity) and esophagus contrast radiography.
A rectangular aperture diaphragm parallel to all IP sides is detected. The division recognition function is not incorporated.

PRIEF 1S: Used for cervical tomography and intestine contrast radiography.
A rectangular aperture diaphragm parallel to all IP sides is detected.

PRIEF 2: Used with the breast menu.
A semicircular or rectangular aperture diaphragm tangent to IP sides is detected.

PRIEF 4: Used for adult chest and pediatric chest radiography.
A convex polygon is detected without division recognition.

PRIEF 4S: Used for general plain radiography and some contrast tomography.
The aperture position and convex polygon are both detected.

AUTO NECK: The main cervical section position is detected. Shoulder and chin projections are eliminated from radiographs.

NOTE
The letter "S" in the PRIEF names indicates that division recognition is automatically performed. The PRIEF 1 and PRIEF 4 perform irradiation field recognition and do not provide division recognition.

	Plain	Contrast	Tomography
Head	4S	4S	4S (1 for pantomography)
Neck	4 S AUTO NECK	4S	1S
Chest	4S/4	4S (1 for esophagus)	1
Breast	2	2	
Abdomen	4S	4S (1S for stomach and intestines)	1
Pelvis	4S	4S	1
Upper extremity	4S	4S	1
Lower extremity	4S	4S	1

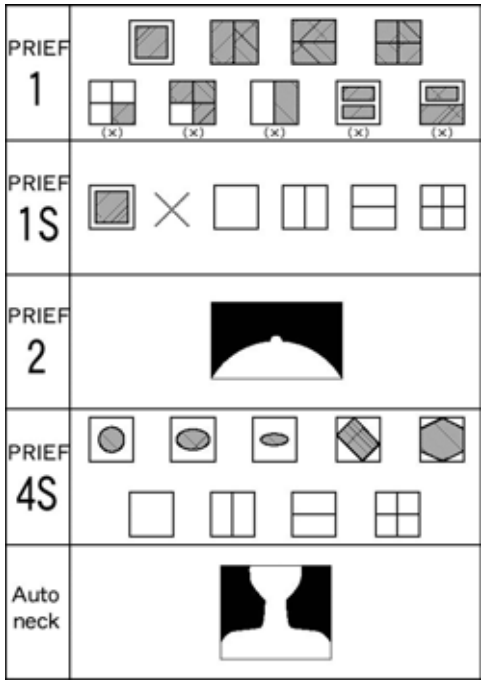

NOTE
PRIEF 1/PRIEF 1S: Ensure that the employed aperture is rectangular and parallel to the IP sides.
PRIEF 1: Do not insert an aperture diaphragm to make a division exposure. The entire IP surface is exposed to radiation.
PRIEF 4S: Do not use a concave aperture except for the hip joint.
AUTO NECK: Direct radiation must be provided on the right- and left-hand sides of the neck.

3.6.4 Methods of recognizing special ROIs (mammographic/cervical irradiation field recognition)

1 Mammographical irradiation field recognition - PRIEF 2

Mammography differs from general radiography. In mammography, a special irradiation field recognition process is needed with the image being exposed in close contact with a side of the IP. Further, the direct X-ray section density is not uniform because of the short distance to the X-ray source.

The entire histogram needs to be made within the breast area, which is the ROI (region of interest). It is therefore necessary to locate the ROI. The ROI can be located by the following sequence:

(1) Binarize the image
(2) Detect the side of the IP on which the subject exists.
Conduct a 3-point scan and then determine the IP's side in accordance with 0/1 transition and roundness. After the IP's side is determined, the ROI can be determined by performing Steps (3) through (5) below
(3) Detect points A, B, C, D, and D'.
(4) Detect points E, F, and F'.
(5) Detect points G, G', H, and H'.
(6) Create a histogram within ten points designated A, H, F, D, G, B, G', D', F', and H'.

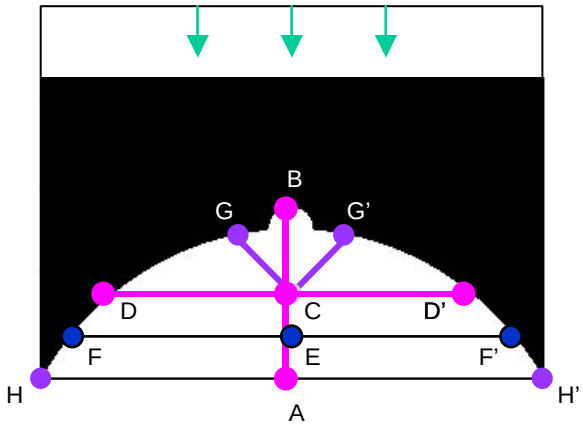

2 Cervical irradiation field recognition

In cervical radiography, the proper minimum value of the neck cannot be determined because of the influence of the shoulder and chin. Therefore, a special algorithm called "Auto Neck" is used so as to detect the position of the neck from the image and remove the shoulder and chin portions.

This is accomplished by varying the binarization threshold value to determine the digital value that blackens the entire neck (when the right- and left-hand direct radiation sections join). The portion greater than the determined digital value is then used for histogram analysis. The region without the shoulder and chin can be specified in this manner.

CAUTION

For normal functioning of this algorithm, it is necessary that separate direct radiation sections exist on the right- and left-hand sides of the neck portion (Figure 3.6).

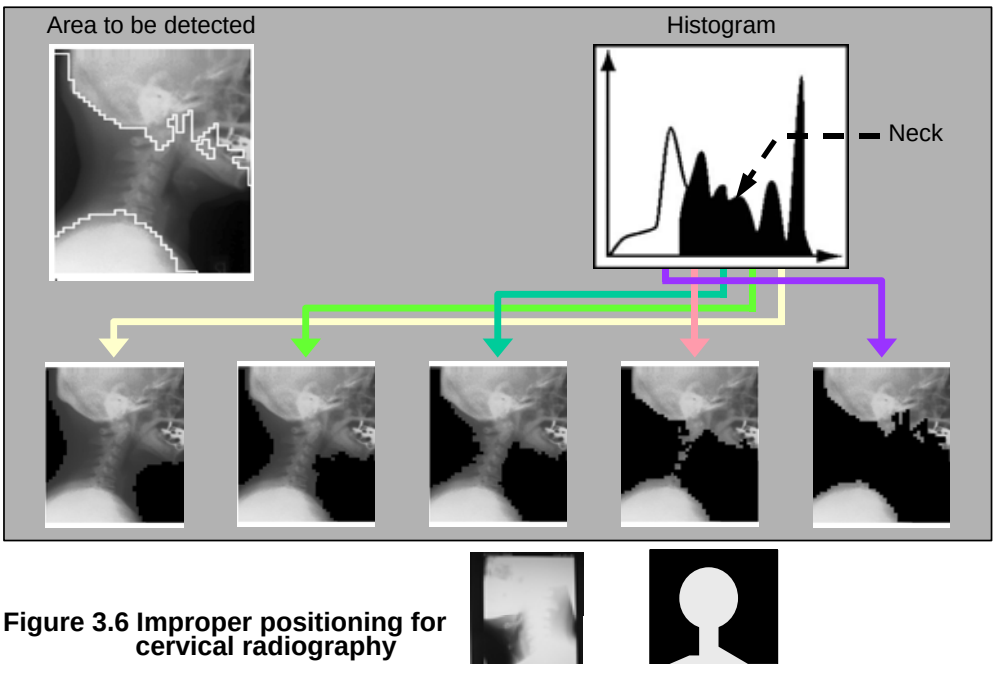

Figure 3.6 Improper positioning for cervical radiography

3.6.5 Histogram analysis types (Auto I to Auto VII)

In the AUTO mode, either Auto I to Auto V histogram analyses or Auto VI and Auto VII neuro-analyses are made. The Auto I to Auto VII analyses are described below:

AUTO I: The direct radiation section's lower slope is suppressed.

Target regions: Almost all extremity bones

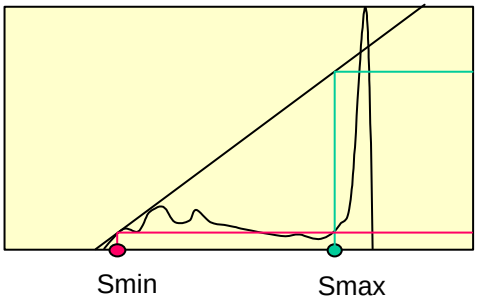

Example: Upper arm

The direct radiation section is essential. The suppression points are determined so as to include soft tissues and bones.

AUTO II: Only the main histogram is used for analysis.

Target regions: Head, chest, abdomen, and bones

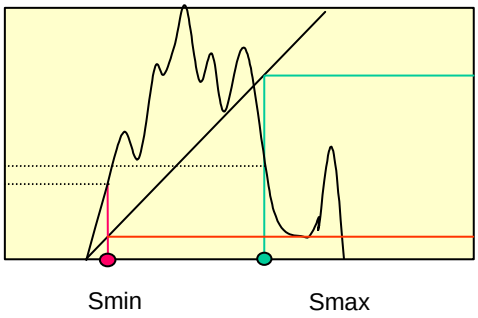

Example: Chest

The suppression points are determined in accordance with the main histogram of regions from the lung field to the mediastinum, excluding the direct X-ray section. The lack of the direct X-ray section presents no problems.

AUTO III: The mountain-shaped low-luminescence region corresponding to the area filled with contrast medium is cut off.

Target regions: Stomach and intestines

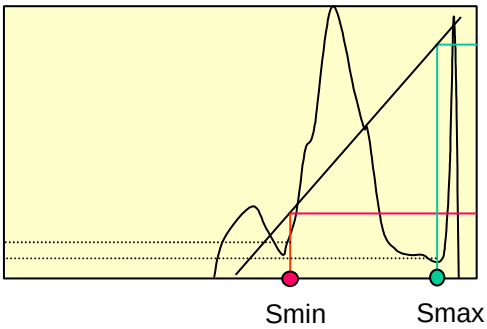

The mountain-shaped main histogram portion is used, excluding the barium's mountain-shaped low-luminescence portion.

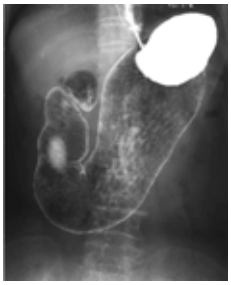

AUTO IV: A predetermined region is recorded, beginning with the maximum value.

Target regions: Axial menu and soft tissue menu

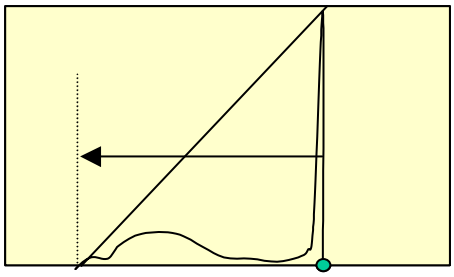

Smax

Example: Patella, axial

The direct radiation section outside the subject must always be present.

Since a predetermined region is recorded beginning with the maximum brightness point, the exposure tube voltage must be controlled carefully.

AUTO V: A predetermined region is recorded with the histogram minimum value suppressed.

Target regions: Hip joint axial 2 menu

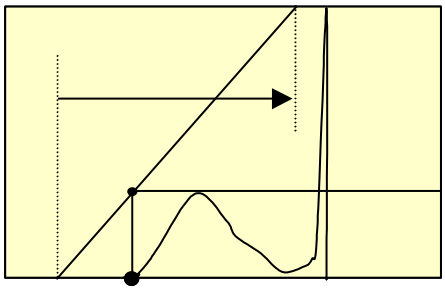

Smin

Example: Hip joint, axial 2

A predetermined range is recorded, beginning with the minimum value of a limited range of a thigh bone.

AUTO VI: (Neuro-analysis)

Target regions: Pediatric chest and feet

When, for instance, a pediatric chest is radiographed, the following patterns of histogram shapes result depending on positioning and the presence of foreign matter or irregularities.

Various images are subjected to neuro-analysis with the results of learning being memorized in the FCR system. The acquisition range is defined by determining which histogram pattern is closest to the histogram of the obtained radiograph.

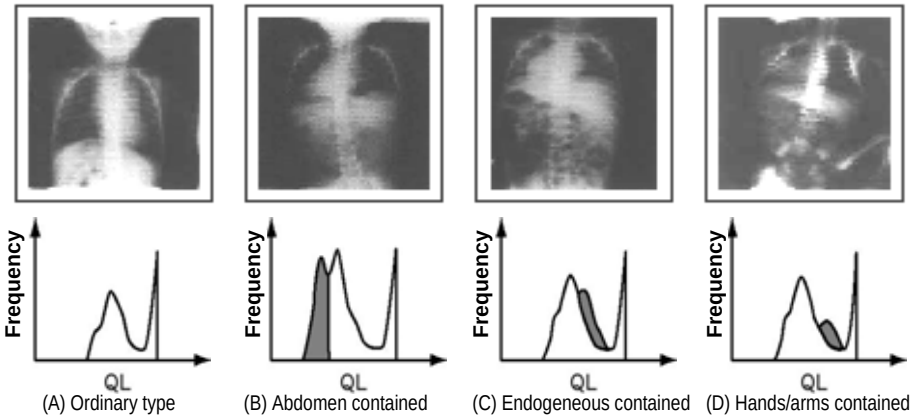

Pediatric chest histogram patterns

AUTO VII: Neuro-analysis

Target region: Shoulder

When, for instance, a shoulder joint is radiographed, the joint position within the histogram varies, as shown below, depending on how positioning is achieved. The overall histogram shape itself does not vary. It is therefore difficult to ensure the consistent output required for histogram analysis when ROI (region of interest) changes are caused by differences in positioning.

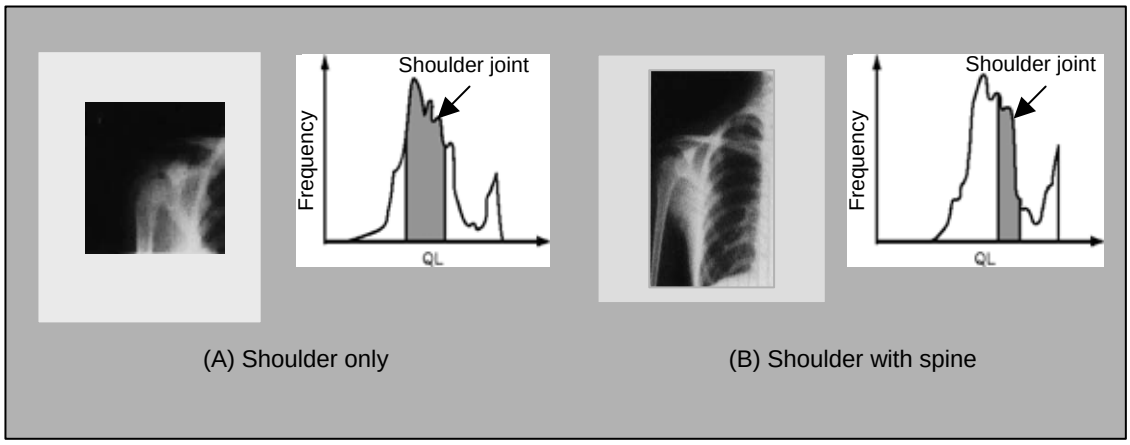

Shoulder joint front histogram pattern

If the irradiation field is variously narrowed, the ROI in the histogram, in this case the shoulder joint position, greatly varies although the histogram shape itself does not significantly change.

In Figure (A), the irradiation field is adequately narrowed, and the ROI is located at the center of a mountain of the main histogram (valid image signal region).

When the irradiation field is large, as indicated in Figure (B), the ROI is positioned toward the maximum value of the mountain of the main histogram. The reason is that a larger histogram mountain is formed in the low-luminescence region than in the ROI because the mediastinum signal is lower in luminescence and larger in area than in the ROI.

As long as the ordinary method is used, it is theoretically impossible to specify the normalization conditions from the shoulder joint menu in such a way as to maintain constant the density of the ROI.

Therefore, the neuro-analysis method is employed to have the system "memorize" various image patterns and learn the suppression points of respective histograms. The results obtained in such a manner are memorized in the FCR system. The FCR system then specifies the manner of histogram suppression by determining which image pattern is close to the obtained radiograph.

3.6.6 Image recording area correction

1 Correcting an abnormal EDR recording range

If, for some reason (positioning, influence of scattered radiation, background irregularities), the imaging range (EDR recording range) is found to be abnormal, the FCR system can automatically correct the recording range.

In ordinary radiography, the X-ray absorption difference is not great, although it varies with the exposure region and orientation. (The approximate logarithm is 2 in chest radiography.) Therefore, the upper and lower limits of the recording range are predetermined for each menu. Any portions exceeding the upper or lower limits are eliminated.

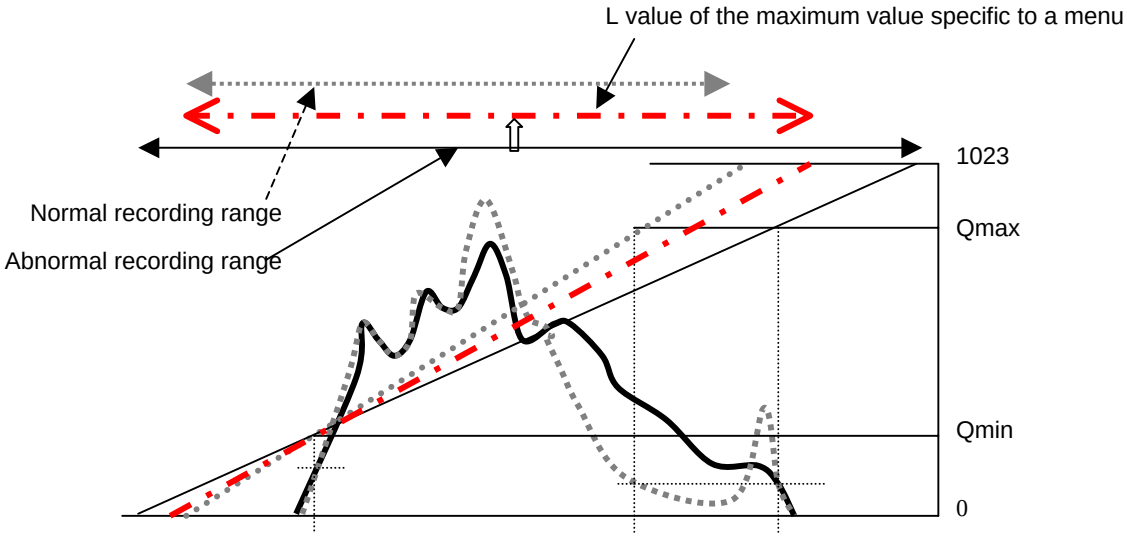

2 Correcting a biased histogram

If the histogram is significantly biased for some reason, the FCR system uses a scheme to shift the range that is determined according to a regular procedure. The shifting procedure will not be discussed in detail here. Note, however, that the histogram is integrated. If the resultant intermediate value (Sm) greatly deviates from the midpoint between the original Smin and Smax values, the correction scheme works to eliminate the deviation. If, for instance, a metal is included, biasing toward the high luminescence side results. Since the metal portion is expected to appear whitish, the analysis results are corrected so as to decrease the density.

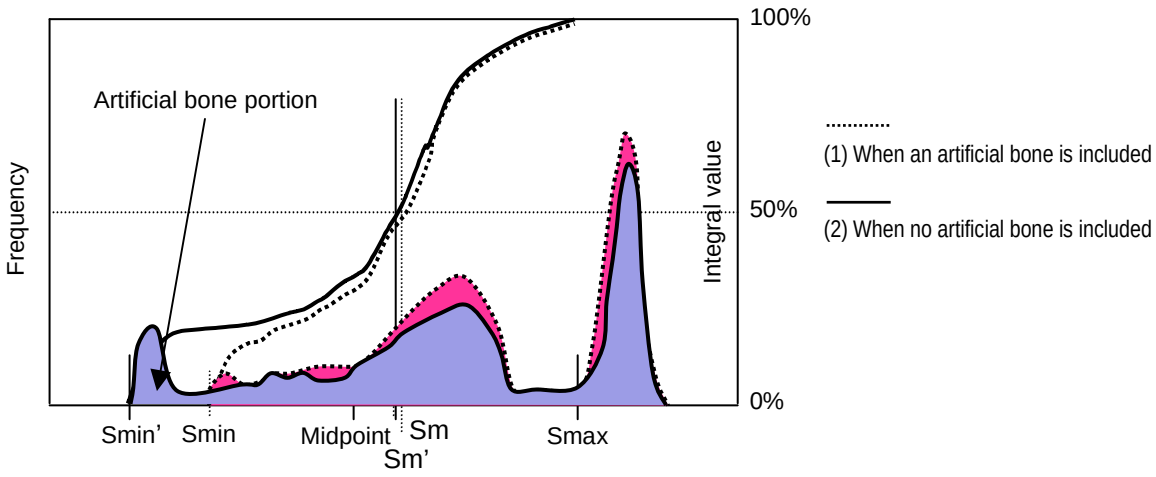

→ Smin' is shifted toward higher X-ray dosage in accordance with the deviation of the Sm' value from the midpoint between Smax and Smin'.

3.7 SEMI AUTO Mode

■ Function for assigning the average luminescence (Save) of a photometry area to a certain digital value (Qave). Division recognition and irradiation field recognition are not performed. This function is similar to that of a phototimer. It provides an effective method for situations where the employed radiography properly accomplishes positioning (by using jigs and other such tools).

The photometry area size, the digital value representing the average luminescence, and the L value vary with the exposure region and method. They are predefined variously for all menus.

■ The ROI needs to be positioned within the IP's photometry area. Therefore, positioning must be properly accomplished. Further, careful attention must be paid to the exposure tube voltage because, as with the S/F system, the recording width (L value) is constant.

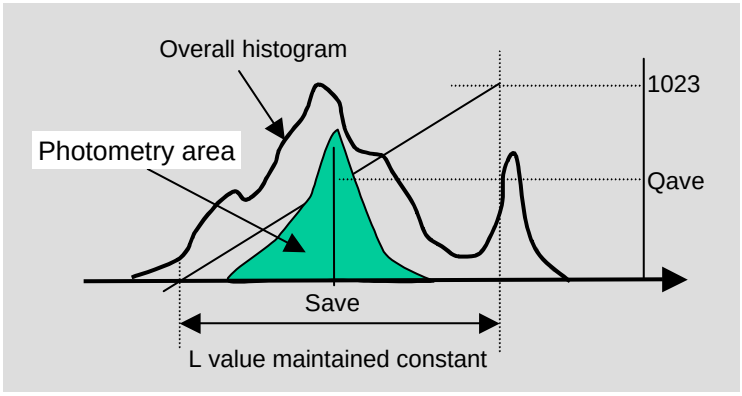

Photometry area varieties

The predefined photometry areas are shown below. The "Operation Manual" shows the relationship between exposure menus and SEMI AUTO mode types.

<SEMI I>
[Photometry area]
10 cm × 10 cm square at the IP center.

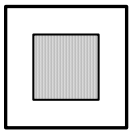

<SEMI II>
[Photometry area]
7 cm × 7 cm square at the IP center.

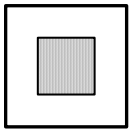

<SEMI III>
[Photometry area]
5 cm × 5 cm square roughly positioned at the IP center when the IP image area is divided into the upper and lower halves, divided into the right- and left-hand halves, divided into four sections, or not divided.

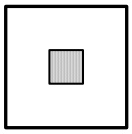

<SEMI IV>
[Photometry area]
Five areas (the values of the areas are determined and the resultant maximum value is used). "Semi" for chest.

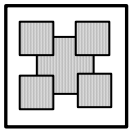

3.8 FIX Mode

In the FIX mode, because the reading sensitivity (S value) and latitude (L value) are constant, the exposure conditions need to be controlled in a conventional manner.

When the S/F system is used, the exposure conditions are determined by the film and screen to be used. **In CR, however, the FCR conditions can be defined according to predetermined exposure conditions**. For example, the radiation dose can be reduced to half with the S value setting increased by two.

A setting of 200 (or 50 for mammography) is used a s the preset value for the reading sensitivity (S value). However, in consideration of the fact that that the S value differs from the relative sensitivity (RS value) for the S/F system, you should empirically determine the S value setting. You can also use the average S value that is used in the AUTO mode.

The S value can be entered from the ID-T (ID terminal). The L value is variously predetermined for all menus.

3.9 SEMI-X Mode

The user selects from the nine areas shown at right. The SEMI AUTO mode works for the selected areas. The precautions to observe are the same as discussed for SEMI AUTO mode use.

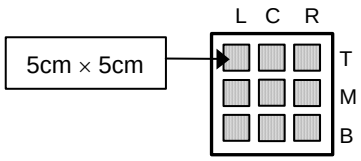

3.10 MANUAL Mode

In the MANUAL mode, the S and L values are manually determined. The image recording area is determined according to the manually determined S and L values. You should determine the S and L values so as to obtain the proper density and contrast while observing the image on the FCR system monitor.

You should use the MANUAL mode only when the density and contrast cannot be stabilized in either the AUTO mode, SEMI AUTO mode, or FIX mode.

3.11 S Value and Sensitivity

3.11.1 What is S value

The S value is defined by the equation $S = 4 \times 10^{(4 - Sk)}$, which is derived from the Sk value determined by the EDR. (Sk: Central value of logarithmic expression of the X-ray dose range read as digital image data, that is, the value correlating to the logarithmic dose to which the digital value 511 is assigned in 10-bit quantization. See Section 3.4.1.)

Therefore, the meaning of the S value differs from that of relative sensitivity used in the case of the F/S system. However, the S value can be used as the guide that roughly represents relative sensitivity. Note, however, that the S value varies if the positioning setup changes even if the X-ray dose and tube voltage remain unchanged. If the exposure voltage changes, the histogram changes, varying the S value. Further, if the X-ray apparatus changes, the S value changes even if the same exposure conditions are used. If the exposure menu is changed, the EDR conditions change so S value comparisons would be invalid. Even when exactly the same conditions are employed, the S value changes if the time interval between IP exposure and IP insertion changes. However, if the X-ray generator, tube voltage, patient, menu, positioning setup, and elapsed time from exposure remain unchanged, the S value is a relative representation of the X-ray dose. For example, the S value is approximately doubled when the dose is reduced by half.

This Sk value (or S value) is set as explained below for the ST and HR type IPs. Strictly speaking, the S value is set while using the reference radiographic device and reference IP with the elapsed time from exposure predefined.

(1) ST type

When the IP is uniformly exposed to 1.0 mR of radiation at 80 kVp (Al 3.0 mm or equivalent filter) with a W X-ray tube radiographic device and then processed with the TEST SENSITIVITY menu (gradation A of SEMI AUTO mode), the S value is 200 (Sk = 2.30).

If the X-ray dose is changed while employing the same reading method, the S value is adjusted as indicated below so that the digital value for the image acquisition center is 511:

80 kVp (Al 3.0 mm or equivalent filter), 10 mR $\rightarrow$ S value: About 20
80 kVp (Al 3.0 mm or equivalent filter), 0.1 mR $\rightarrow$ S value: About 2000

Because the X-ray spectrum may vary with the X-ray source type and other factors, the correspondence between the radiation dose and S value should be used as a guide only. For increased accuracy, the radiation dose needs to be measured whenever the X-ray source is changed.

For invariance testing and other management tasks, it is also necessary to pay attention to X-ray source tube voltage changes with time, dosimeter accuracy, Imaging Plate individual specificity, and other related factors.

(2) HR type

When the IP is uniformly exposed to 20 mR of radiation at 25 kVp (Mo 0.03 mm or equivalent filter) with an Mo X-ray tube radiographic device and then processed with the TEST SENSITIVITY menu (gradation A of SEMI AUTO mode), the S value is 120 (Sk = 2.52).

If the X-ray dose is changed while employing the same reading method, the S value is adjusted as indicated below so that the digital value for the image acquisition center is 511:

25 kVp (Mo 0.03 mm or equivalent filter), 200 mR $\rightarrow$ S value : About 12
25 kVp (Mo 0.03 mm or equivalent filter), 2 mR $\rightarrow$ S value : About 1200

Because the X-ray spectrum may vary with the X-ray source type and other factors, the correspondence between the radiation dose and S value should be used as a guide only. For increased accuracy, the radiation dose needs to be measured whenever the X-ray source is changed.

For invariance testing and other management tasks, it is also necessary to pay attention to X-ray source tube voltage changes with time, dosimeter accuracy, Imaging Plate individual specificity, and other related factors.

3.11.2 Relationship between S value and relative sensitivity (RS value)

The RS value is intrinsically constant without regard to the exposure conditions and exposure region. In contrast, the S value is not constant because it is initially defined as the factor that determines the optimum sensitivity for the employed exposure conditions and exposure region. Therefore, although they may seem similar, the S value will differ from the RS value.

Their differences are outlined below in relation to various exposure regions:

(1) Chest

When an FCR exposure process is performed under optimum exposure conditions for the S/F system, slightly raise the sensitivity for the FCR system in order to properly read the mediastinum and abdomen as well as the lung field. In subsequent image processing, slightly lower the density for the FCR system to generate a film output with optimum density. This yields an S value that is slightly greater than the RS value.

(2) Pediatric chest

When an FCR exposure process is performed under optimum exposure conditions for the S/F system, slightly raise the sensitivity for the FCR system in order to properly read the mediastinum and abdomen as well as the lung field. In subsequent image processing, slightly lower the density for the FCR system to generate a film output with optimum density. This yields an S value that is slightly greater than the RS value. (Since the abdomen area is relatively large, the S value is slightly greater than in the FCR exposure process for the adult chest.)

(3) Extremity bones

When an FCR exposure process is performed under optimum exposure conditions for the S/F system, slightly raise the sensitivity for the FCR system in order to properly read the soft tissue and skin as well as the bones. In subsequent image processing, slightly raise the density for he FCR system to generate a film output with optimum density. This yields an S value that is slightly smaller than the RS value.

Chapter 4 Image Processing (Gradation Processing)

The image recording range determined by the EDR is converted to 10-bit digital data. The data is then subjected to various image processes and converted to an image that can readily be used for diagnostics when printed out on film.

The usual image processes that the FCR equipment performs are **gradation processing (G), spatial frequency processing (R), dynamic range control (DR), and tomographic artifacts suppression (OR).** As a special process, the subtraction process may also be performed.

4.1 Gradation Processing

Gradation processing is described with reference to Figure 4.1. The horizontal axis represents the digital value defined by the EDR. **Gradation processing** is performed to convert the digital input data to an image with appropriate **density** and **contrast**. (In actuality, 10-bit-to-10-bit digital data conversion is effected.)

The gradation process is controlled by the following four parameters:

GT (gradation type) : Table for providing gradation → Nonlinear curve

GA (rotation amount) : Parameter for varying the contrast
$\gamma = \gamma(GT) \times GA$ The γ value determined by GT is multiplied by GA to obtain the final γ value.

GC (rotation center) : Density center for rotation → The density at the rotation center remains unchanged even when the GA changes.

GS (density shift) : Parameter for changing the density → Density change amount when GA = 1.0 for linear gradation

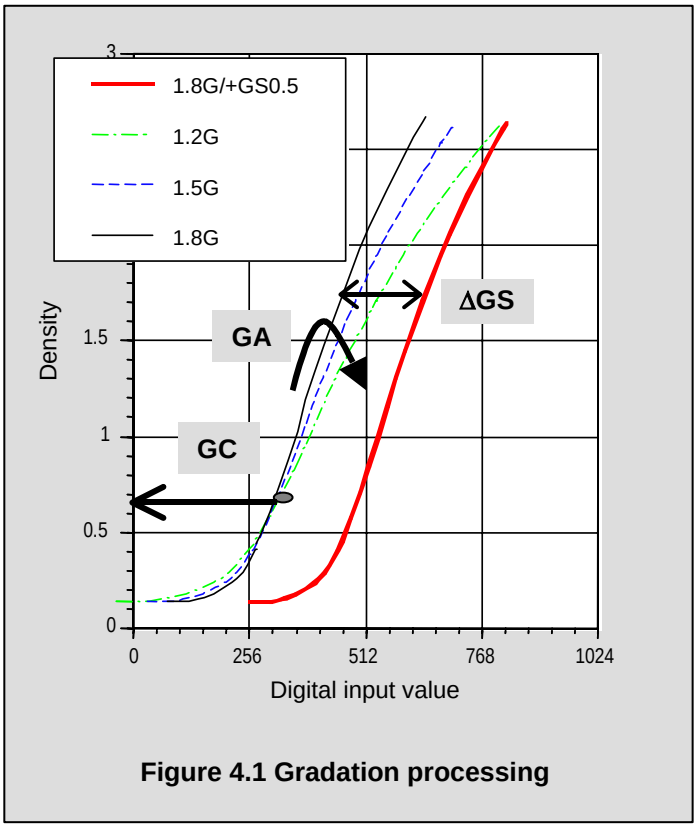

Figure 4.1 Gradation processing

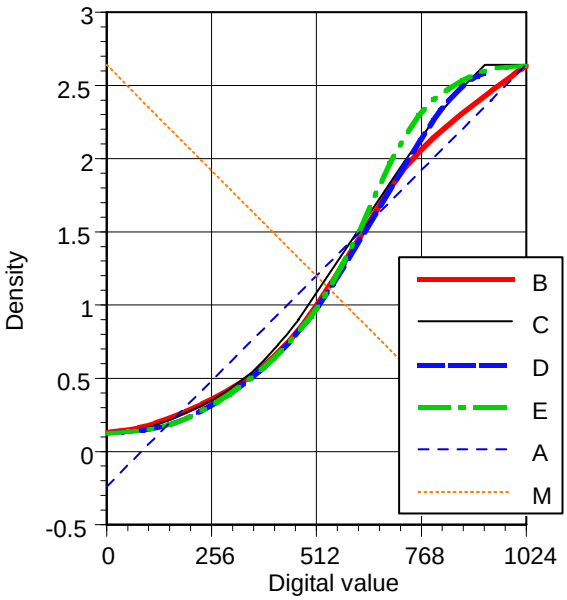

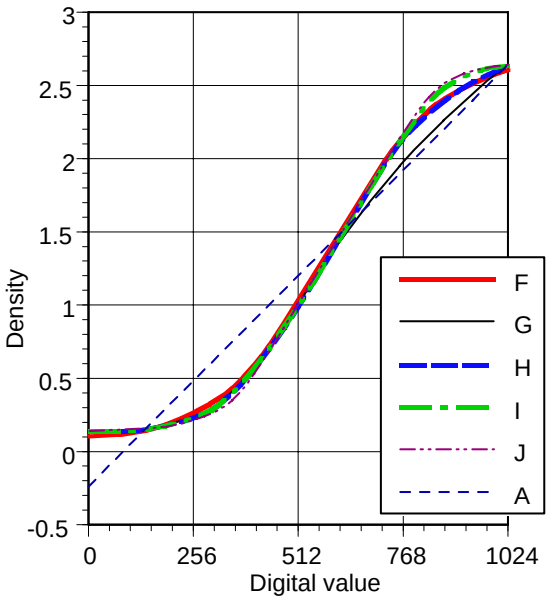

GT varieties

A: No conversion. Linear gradation providing a wide latitude. Used for the right-hand image in the two-image output mode.

M: Reversed gradation. Images are displayed with black and white reversed.

B - J: Nonlinear gradation created by systematically varying the shoulder (high-density) and foot (low-density) portions. Used for almost all menus for head, neck, chest, breast, abdomen, and pelvis.

K and L: Nonlinear gradation with the contrast specially raised for subtraction images.

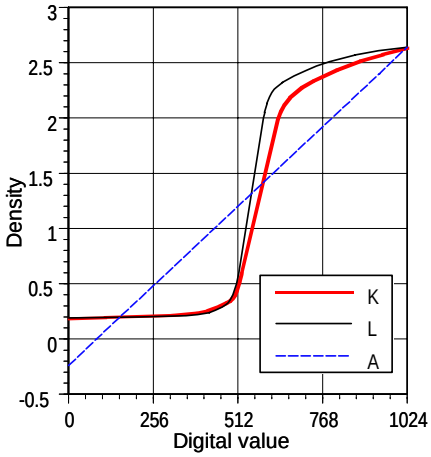

NOTE

The graph's vertical axis represents the density. In actuality, it is derived from digital (10-bit)-to-digital (10-bit) conversion.

The equation below shows the relationship between the density generated by the imager and the output digital value:

D = 0.00281 × QL - 0.237

The vertical axis shows density values that are calculated using the above equation, the reason why minus density values are indicated.

Frequently used type

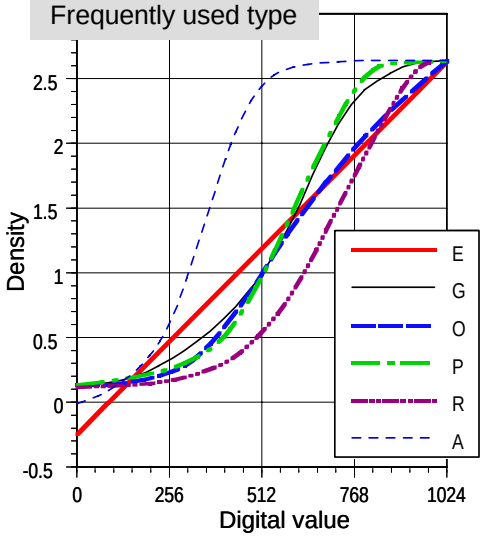

E: For chest
G: Latitude type
O: For orthopedics
P: General HR-S gradation
R: Mammographic high-contrast gradation

GA changes (E gradation, GC = 1.6)

GA = 0.7 GA = 1.0 GA = 1.3

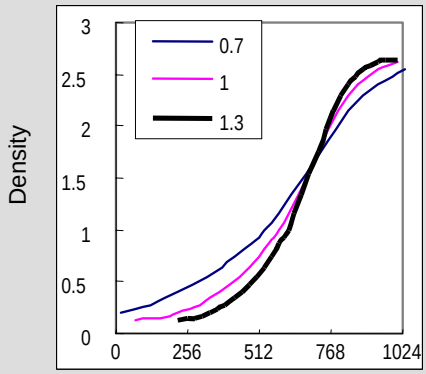

GS changes (E gradation)

GS=-0.5 GS=-0.2 GS=0.1

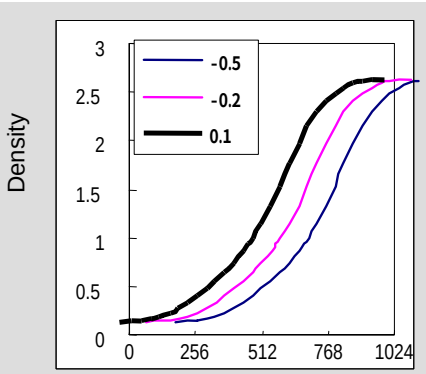

Gradation process adjustment procedure

Most adjustments can be made by varying the GA and GS parameters. If such adjustments do not help, you should reassess the GT parameter.(There is no need to vary the GC parameter.)

1 **First, vary the GS parameter so as to obtain the proper density.**

(If ΔGS is changed by 0.1 when GA = 1.0 for gradation A, the density changes by 0.1. A greater density change will occur under normal conditions [e.g., GA = 1.0 for O].)

2 **Next, vary the GA parameter so as to obtain the proper contrast.**

If, for instance, GA = 1.2, the resulting contrast is 1.2 times higher than exhibited when GA = 1.0.

4.2 Spatial Frequency Processing

Sharpness control is referred to as spatial frequency processing. When the S/F system is used, the higher the frequency, the lower the frequency response. However, the FCR system is capable of controlling the response as required. To enhance the image with spatial frequency processing, the FCR system uses an unsharp masking process. This process is simpler and faster than a process based on the Fourier transform.

4.2.1 Unsharp masking

The unsharp masking process is performed as follows:

1 In the unsharp masking process, the FCR system performs averaging on neighboring pixels to create an unsharp image (the degree of unsharp masking is determined by the parameter RN).

2 The original image is subtracted from unsharp image.

3 The difference signal thus obtained is multiplied by the coefficient RE and density-dependent coefficient RT. The resultant value is added to the original image.

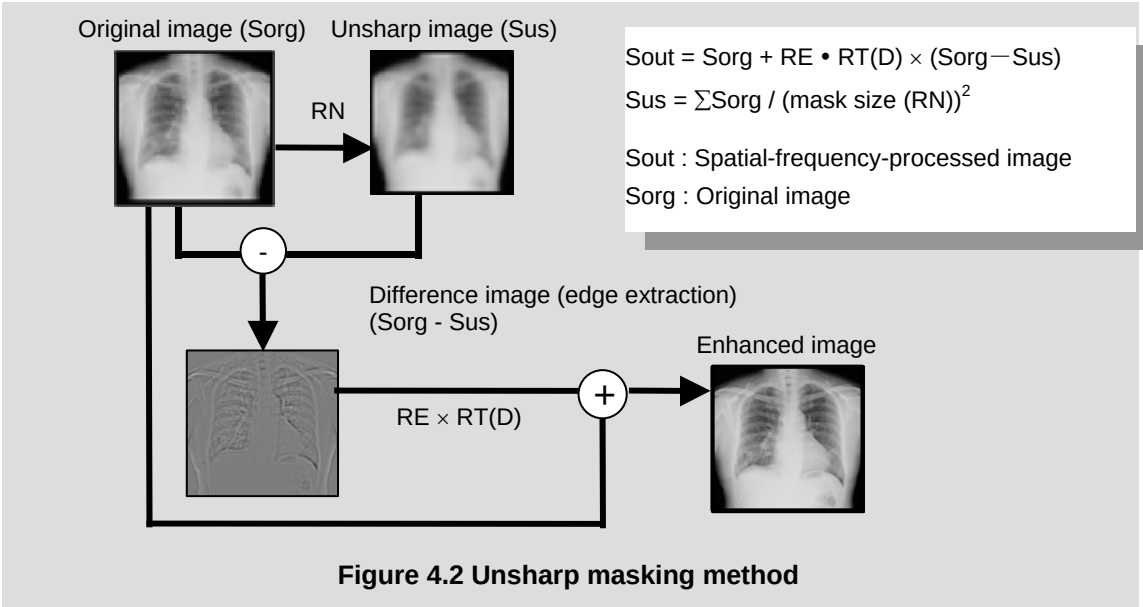

Figure 4.2 Unsharp masking method

4.2.2 Response characteristic of the enhanced image

A normal signal transmission system is characterized by a lower response to higher frequencies. As an example of FCR enhancement processing, Figure 4.3 shows the characteristics of high-frequency and intermediate-frequency enhancement.

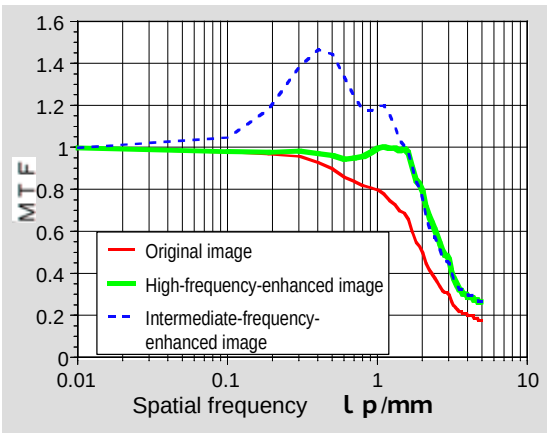

Figure 4.3

4.2.3 Meanings of frequency enhancement process parameters

Three parameters are used: (1) frequency rank (RN), (2) degree of frequency enhancement (RE), and (3) enhancement type (RT).

(1) Frequency rank (RN)

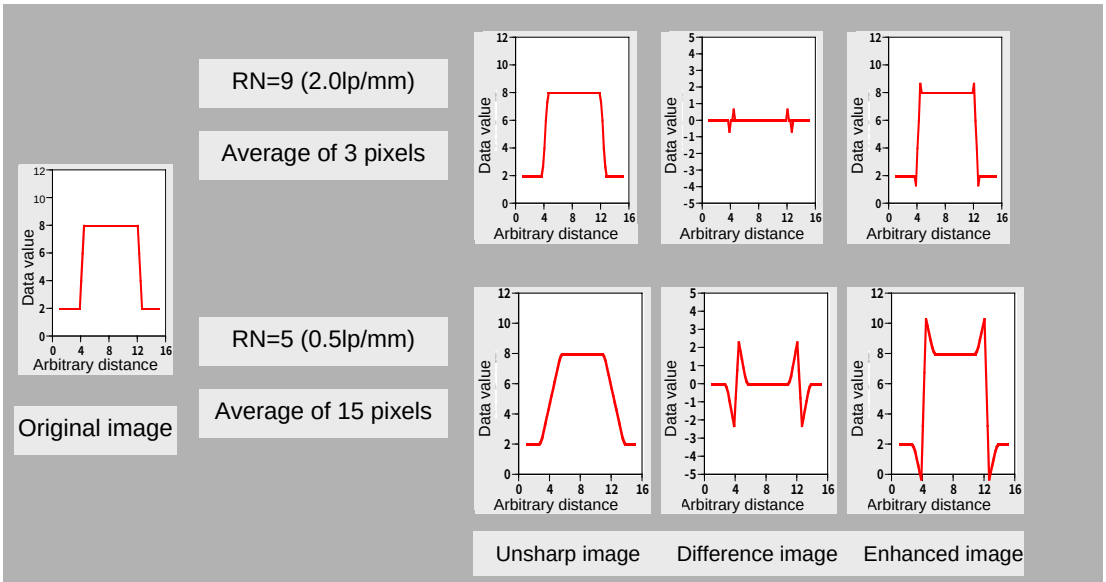

Figure 4.4 Explanation of simple-signal processing

The above enhanced images were obtained by enhancing a simple rectangular signal with the RN parameter values 9 and 5. When RN = 9 and the neighboring two pixels are involved in averaging, the degree of unsharp masking is insignificant and the resulting difference image is sharp and small. However, when RN = 5 and seven nearby pixels each on the right and left sides are involved in averaging, the degree of unsharp masking is significant so that the resulting difference image is thick and large. The enhanced image is obtained by adding the difference image to the original image. Therefore, the image generated when RN = 9 may look as if it is obtained by tracing the edge with a thin pencil, and the image generated when RN = 5 may look as if it is obtained by tracing the edge with a relatively thick pencil.

Table 5 shows the relationship between parameter RN, the number of averaging masks, and the central enhancement frequency. The greater the RN value, the higher the frequencies of enhanced components.

The parameter RN should be determined in accordance with the target of diagnosis as suggested below:

Low-frequency ranks (0 to 3)	:	Enhancement of large structures such as soft tissues and the outlines of kidneys and other internal organs
Intermediate-frequency ranks (4 and 5)	:	General structures such as lung field blood vessels and bone outlines
High-frequency ranks (6 to 9)	:	Small structures such as minute bone tissues and gastric areas

Table 5 Relationship between RN (frequency rank), the mask count, and the central enhancement frequency

RN		0	1	2	3	4	5	6	7	8	9
Spatial frequency enhanced (lp/mm)		0.09	0.13	0.18	0.25	0.35	0.50	0.71	1.00	1.40	2.00
Mask size	0.2 mm/pixel	81	57	41	29	21	15	11	7	5	3
	0.15 mm/pixel	109	77	55	39	27	19	13	9	7	5
	0.1 mm/pixel	127	115	81	57	41	29	21	15	11	7

(2) Degree of frequency enhancement (RE)/(3) Enhancement type (RT)

Before determining the degree of frequency enhancement, it is necessary to determine the degree of difference image (the edge extraction image) addition. The degree of such addition is determined by the parameter RE. However, if enhancement is provided indiscriminately, the resulting image will appear coarse because of the tendency of the low-density portion to be noisy.

The parameter RT is a table that uses image signal digital values (virtually proportional to density) to determine the degree of enhancement. The data in this table can be used to control the degree of enhancement variously for all densities. Under normal conditions, tables are selectively used so that the degree of enhancement is low for the low-density portion and high for high-density portion.

RT = F provides uniform enhancement. RT = V, on the other hand, does not enhance the low-density portion. If the exposure X-ray dose is extremely low and noise likely to be intrusive, the parameter RT should be set to X or W to generate blurred images.

Sharpness-oriented type : F>P>T>U Graininess-oriented type : W>X>V>S>R>Q

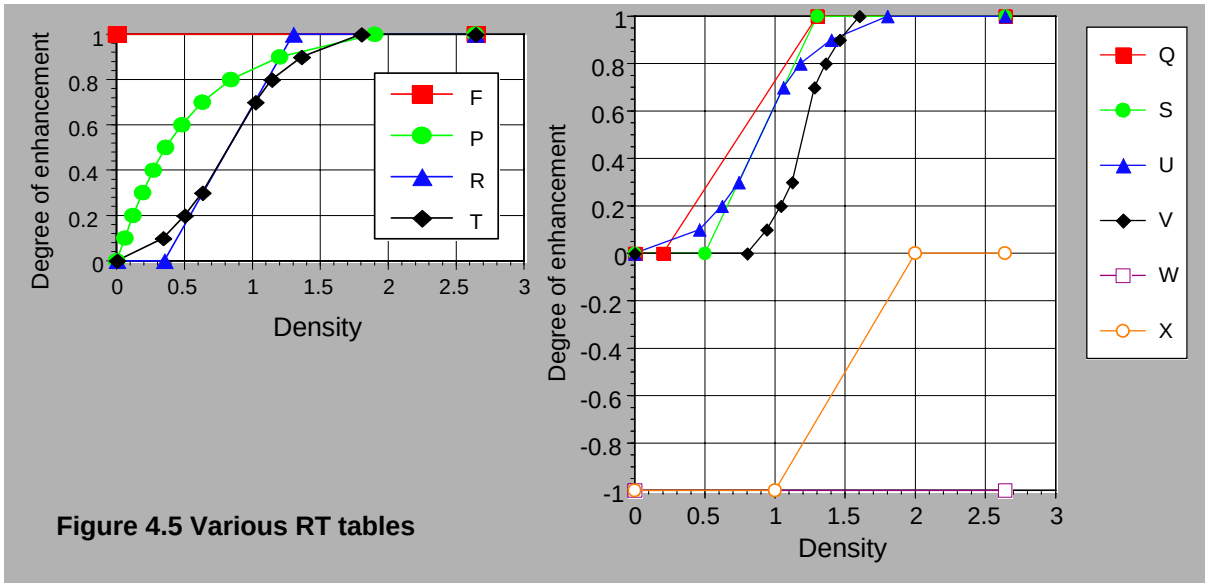

Figure 4.5 Various RT tables

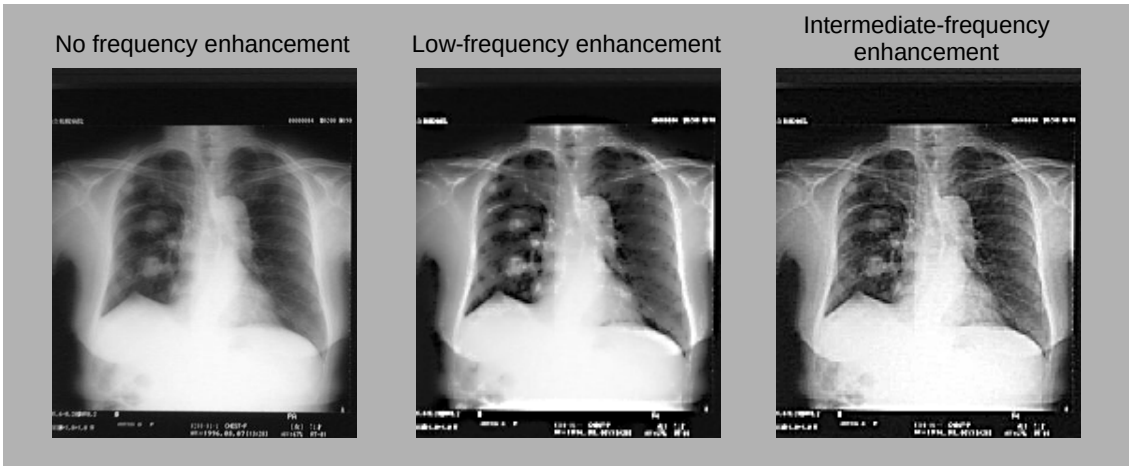

Supplementary Note

Response function for situations where the unsharp masking process is performed with mask size a (mm). When the original response is MTFo and the frequency is X (cycles/mm), the following equation results:

$MTF(X) = MTF_O(X) \times \{1+RE \times RT(1-\mathrm{Sin}\,\pi aX / \pi aX)\}$

The value within braces ({ }) is maximized when X = 1.4/a. The resultant maximum value is the enhancement central frequency. If, for instance, a = 0.7 mm (mask count: 7; pixel size: 0.1 mm → RN = 9), X = 2.0 cycles/mm..

4.3 Dynamic Range Control (DRC)

4.3.1 Two-image display format and objective of DR control

The history of FCR began with a two-image display format.

The left-hand image was similar to those derived from the conventional S/F system based on gray-scale display allowing diagnoses to be made in a conventional manner.

The right-hand image was generated by making full use of image processing features. It had a wide visibility range, depicted various objects ranging from bones to soft tissues, and enhanced the visibility of dot and line shadows. These two images were generated to offer increased diagnostic ease.

However, the two images displayed on a 26 × 36 cm size film were so small that they could not easily be interpreted. Studies were therefore conducted to determine whether it was possible to make use of the above-mentioned features displaying only one image.

When a one-image display format is used, some portions of the image may be excessively whitened or blackened or otherwise rendered invisible. To deal with this, the DR control process is performed so as to depict such invisible portions without changing the density or contrast of the most important ROI (region of interest).

Two-image display format

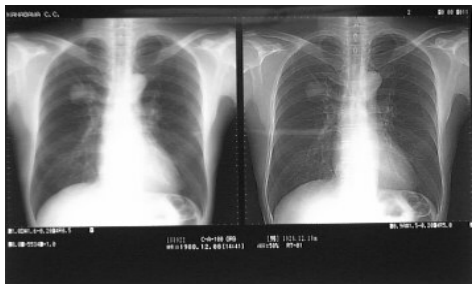

The DR control process enables the same size as for the S/F system to be used for observation (when HQ model is used) with properly adjusted contrast and increased visibility range. The DR control process is particularly effective for regions where the X-ray absorption difference is great.

Output format	Two-image output		One-image output		One-image output	
FCR model	Standard model/HQ model		Standard model		HQ model	
IP size	Reduction ratio	Film size	Reduction ratio	Film size	Reduction ratio	Film size
14" × 17"/14" × 14"	50%	26 × 36 cm	67%	26 × 36 cm	100%	14" × 17"
10" × 12"	67%	26 × 36 cm	100%	26 × 36 cm	100%	26 × 36 cm
8" × 10"	87%	26 × 36 cm	100%	26 × 36 cm	100%	26 × 36 cm

4.3.2 Principles of dynamic range control (DR control)

A considerably unsharp image is derived from the original image. A control (image data compression) table is created using unsharp image data coordinates to prepare a level increase or level decrease signal. The resulting signal is added to the original image. When this process is performed, the ROI can be depicted without any change to its signal while at the same time preventing underexposed areas from being excessively whitened, overexposed areas from being excessively blackened, and retaining the normal frequency component signals. This method is based on the "chest self-compensating digital filter", which was developed by Anami, et al at National Cancer Center.

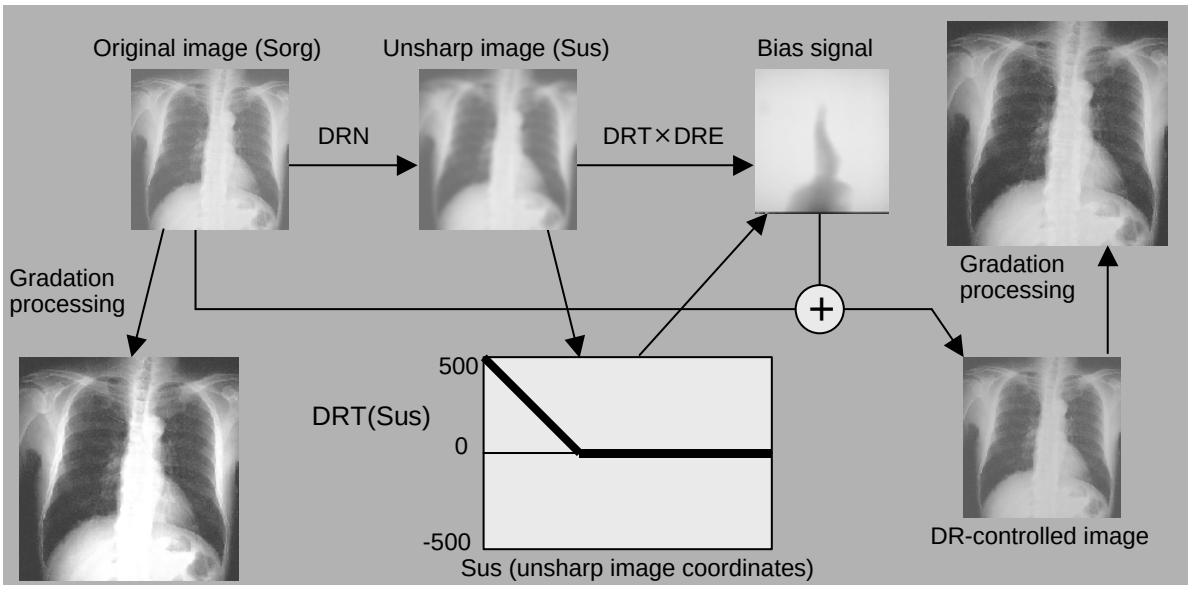

The significance of unsharp image use in the DR control process is explained below.

Consider a compensating filter that is used for chest radiography. Both underexposed and overexposed areas contain signals that are not properly depicted. When a level increase signal (DC component) is added to such an underexposed/overexposed area signal, the resultant signal can be used to express densities visible to the human eye.

Let us use Figure 4.6 for explanation. Imagine that minute signals are on aluminum steps. Now suppose that an underexposed area cannot be expressed (in terms of density) when a radiograph is normally displayed (a). The horizontal axis represents position coordinates and the vertical axis indicates pixel values of coordinate points. When the unsharp masking process is performed, minute signal changes are smoothed out and lost; however, the large aluminum step signals are retained. When the signals are converted with the functions indicated in graphs (b) and (c) below, and the converted signals are added to the original image signals, the signals indicated in graph (d) are obtained. The density of a low-density area signal is increased and the image's dynamic range is narrowed. The signals above a certain density level remain unchanged. Meanwhile, the original image signal's minute changes over the steps are retained over the entire density range. The use of this process does not lower the signal contrast. This is how this process differs from the conventional gradation process.

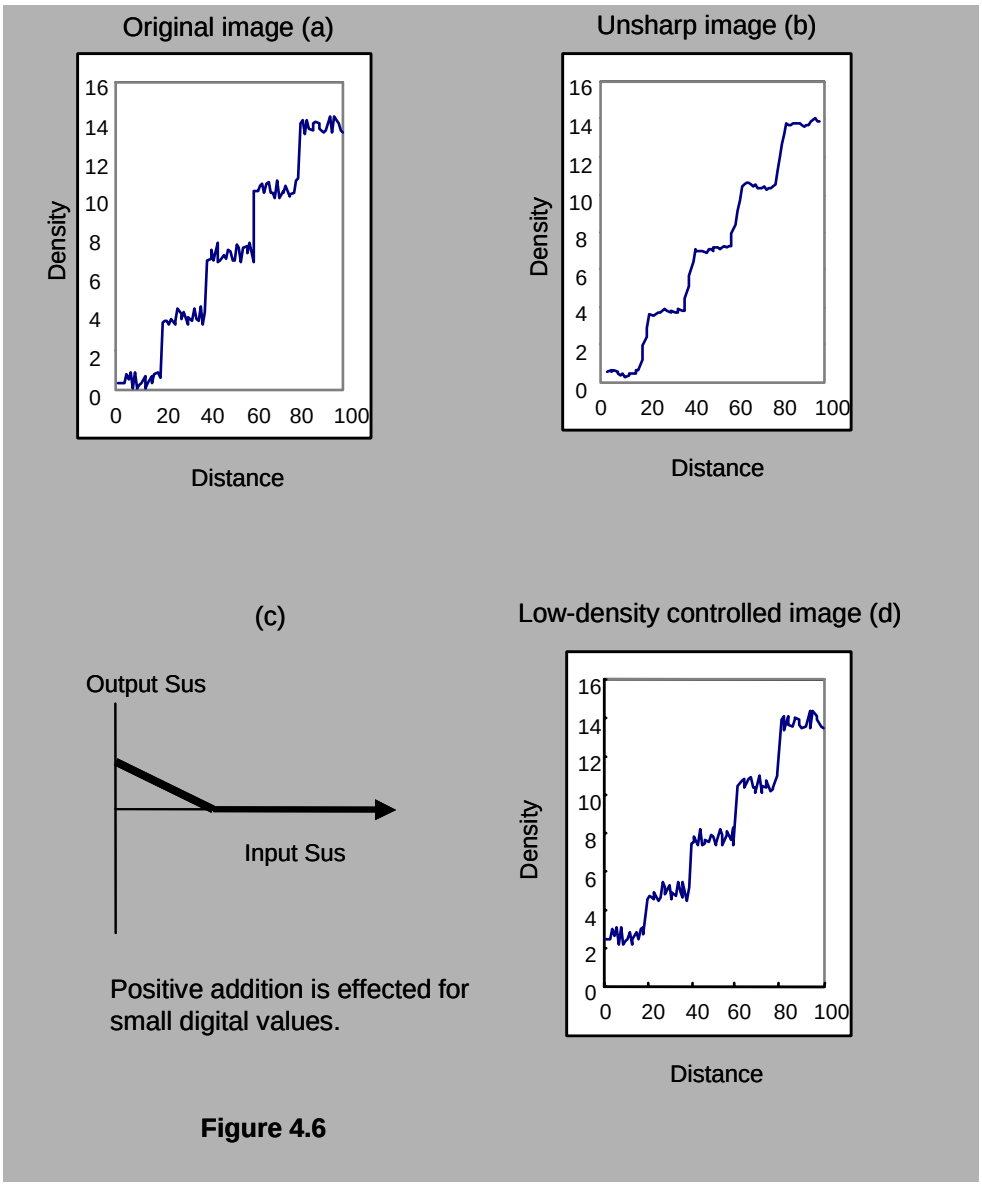

Figure 4.6

4.3.3 DR control process parameters

The following three parameters are available for the DR control process:

Abbreviation	Name	Setting range
DRN	DR control rank	0 to 9
DRT	DR control type	8 types (A to H)
DRE	DR control enhancement level	0.0 to 2.0

DRN

This parameter determines the number of pixels for unsharp image generation. It serves as a factor for determining the degree of unsharp masking. In general, a large mask should be created. Under normal conditions, you should use a DRN setting of 2.

DRN and averaging pixel count

Rank	**0**	**1**	**2**	**3**	**4**	**5**	**6**	**7**	**8**	**9**
5 pixels/mm	229	161	115	81	57	41	29	21	15	11
6.7 pixels/mm	255	215	153	109	77	55	39	27	19	13
10 pixels/mm	147	147	147	147	115	81	57	41	29	21

DRT

This parameter determines the density range over which DR control is to be exercised. The parameter values A through D are for low-density control. The parameter value B or C should normally be used. The parameter values E through H are for high-density control. The parameter value E or F should normally be used.

Low-density control

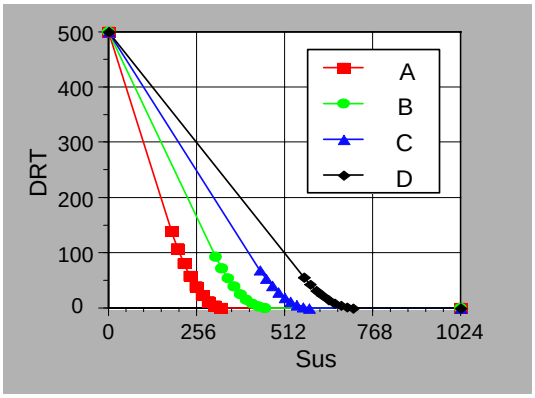

High-density control

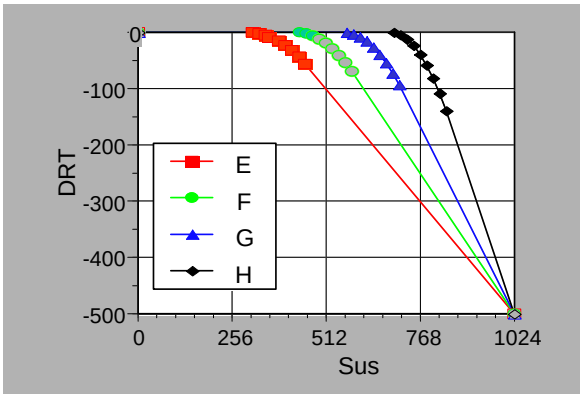

DRE

This parameter determines the degree of control. An excessively high setting may cause white/black image reversal, fog significantly the image of a low-density controlled area, or lower the highest density of a high-density controlled area. A setting of 0.6 or lower should normally be used.

4.3.4 Effects of DR control

Cervical spine (when high-density control used)

The conditions of the respiratory tract and soft tissues are properly depicted. There is no change in the visibility of the cervical spine.

DR control not applied

DR control applied

Ribs (when high-density control used)

Noteworthy improvements are effected despite excessive blackening of the upper ribs over the lung field that made them nearly invisible.

DR control not applied

DR control applied

Thoracic spine/lumbar spine (when low-density control used)

Improvements are effected despite an excessive whitening of the lower portion of the spine that makes it nearly invisible.

DR control not applied

DR control applied

Lumbar spine (when high-density control used)

Spinous processes are rendered visible by improving the high-density area, which was darkened, without changing the appearance of the vertebrate body.

DR control not applied

DR control applied

4.4 Tomographic Artifacts Suppression (TAS)

Although CT (computed tomography) is now widely used in the field of clinical medicine, X-ray tomography remains as an important radiographic method. In X-ray tomograms, however, artifacts can theoretically be generated, as shown in Figure 4.7, under the influence of a certain substance positioned away from the tomographic cross section.

The tomographic artifacts suppression (TAS) process was developed by making use of the fact that the orientation of artifact generation is fixed. Easy-to-interpret diagnostic images can be generated by performing an image process that lowers the contrast of artifacts generated in linear tomography.

A new image processing algorithm, called the one-dimensional unsharp masking process (hereinafter referred to as the one-dimensional USM process) is used for achieving this task.

Artifacts consist of low-frequency components only. Consequently, the y-direction frequency components of a linear tomogram are mostly low-frequency ones. Components of higher frequencies are enhanced to reduce the relative amount of artifact information to practically zero levels. This is the basic principle behind the new image processing algorithm. This idea of artifact suppression was proposed in 1985 by Asada, et al. The one-dimensional USM process was developed by implementing this idea of artifact suppression with the aim of enabling the FCR system to perform real-time processing.

Although the one-dimensional USM process is similar to the conventional frequency enhancement process (unsharp masking process), they differ in that the former only averages the unsharp mask image (Sus) with a 1 x m, thin, long area stretched in the y-direction, the direction in which the artifacts are generated. In other words, the one-dimensional USM process performs frequency processing in one direction only.

The one-dimensional USM process reduces the relative amount of artifact information. It does not accurately extract and eliminate only the artifact information. It is therefore essential that you carefully select a mask size and degree of enhancement in accordance with the exposure region and exposure conditions.

Figure 4.8 presents an image derived from a normal two-dimensional frequency process (a) and the other image derived from the one-dimensional USM process (b). A comparison of these images clearly shows the one-dimensional USM process provides an enhanced image with artifacts suppressed.

Not processed Enhanced normally Enhanced one-dimensionally

Figure 4.7 X-ray tomogram

Figure 4.8 (a)
Image derived from the two-dimensional frequency process

Figure 4.8 (b)
Image derived from the one-dimensional USM process

4.4.1 Parameters and their meanings

ORN (same as DRN) : 0 through 9. Corresponds to a mask size for unsharp image creation.
ORT : Vertical direction (0) or horizontal direction (1) relative to the direction of laser scanning (FCR reading direction).
ORE : 0.0 through 9.9 and 10 through 16. Degree of one-dimensional enhancement.

CAUTION

Special attention should be given to the parameter ORT. If the ORT setting is reversed when the selection of the vertical direction is correct, the resulting image quality will be extremely impaired by artifacts. (When you use the 8" × 10" size, you should pay particular attention to the ORT setting because the vertical/horizontal orientation is reversed.)

4.5 Multi-Objective Frequency Processing (MFP)

4.5.1 Overview

The multi-objective frequency process (hereinafter referred to as the MFP) was developed intended to improve the diagnostic image quality provided by image processing. This new process depicts gray-scale shadows and shape shadows while providing natural appearing enhancements and offering a wide visibility range suitable to the diagnostic purpose. Moreover, this process makes well-balanced enhancements to all spatial frequency components and suppresses overshoots that might be caused by strong signals. Further considerations are also given to this process to avoid unnaturalness.

The MFP was developed by upgrading the spatial frequency and DR control processes that are based on the previously developed unsharp masking method. The development of the MFP was also accompanied by due consideration to future CRT-based diagnostics.

4.5.2 Radiograph features

The MFP can make well-balanced enhancements to various structures, from large to small ones. When used in conjunction with a gradation process, the MFP also offers the following features:

(1) Gray-scale shadows and shape shadows can be enhanced in a well-balanced manner without sacrificing the graininess.

(2) Invisible areas can be depicted with an increased degree of naturalness (the DR control process is improved).

(3) The degree of enhancement is suppressed for metals and other structures extraneous to the human body.

4.5.3 Principles

1 Process overview

The MFP has two functions: frequency enhancement for enhancing dot and line shadows and DR control for controlling the image dynamic range. In the basic MFP, smoothed images are first generated, after which the difference between each smoothed image is determined. The resulting difference-images are subjected to nonlinear conversion, and then the sum of the converted difference-images is used to perform frequency enhancement and DR control processes. Figure 4.9 shows the algorithm block diagram of the MFP's frequency enhancement function (MFP-USM). The MFP's DR control process is detailed in a separate section.

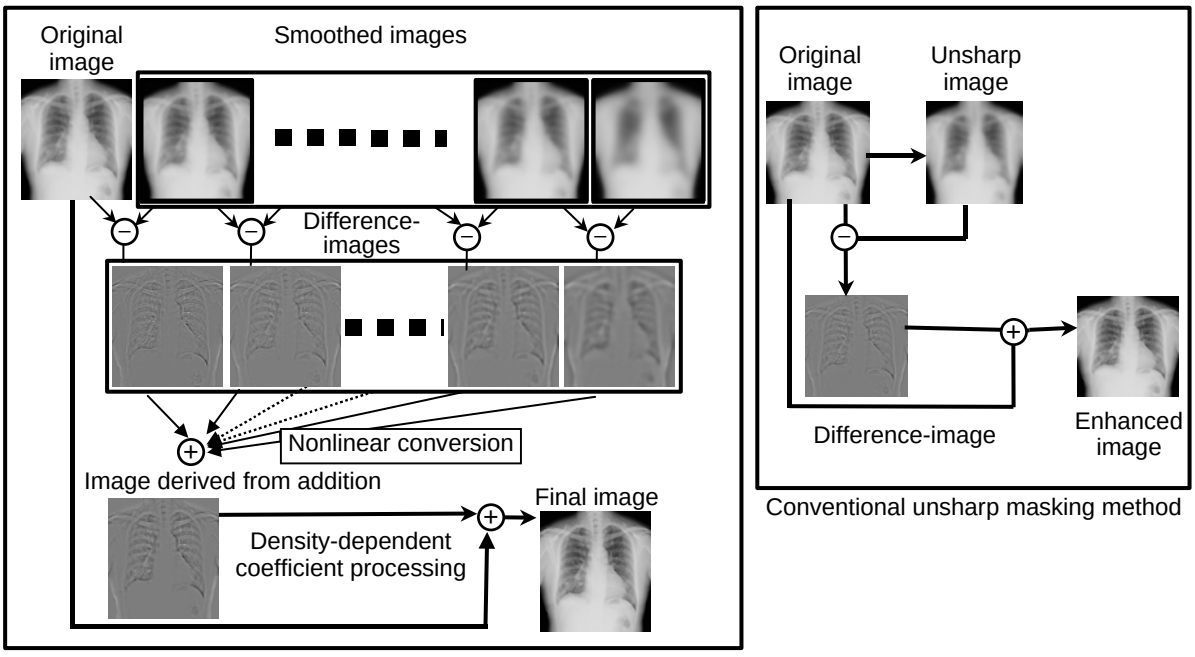

Figure 4.9 MFP block diagram

2 Smoothing process and subtraction process

In the MFP's smoothing process, because weighting is conducted prior to smoothing, the resulting smoothed images are more natural than those derived from simple averaging. (See Figure 4.10.) The frequency response shown in Figure 4.11 indicates that the response characteristic is smooth.

The signal differentials between neighboring smoothed image signals have a response characteristic shown in Figure 4.12, representing a so-called bandpass signal consisting of specific frequency components.

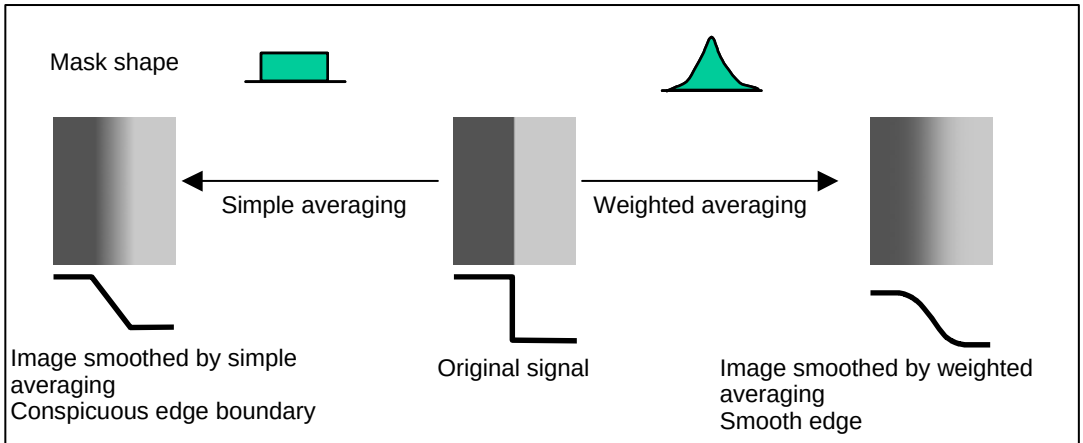

Figure 4.10 Difference in smoothing

3 Enhancement signal components

All bandpass signals (signal differentials between smoothed signals) are subjected to nonlinear conversion, which is detailed later. Further, they are added with their sizes adjusted to create basic enhancement signal components. A typical example is shown in Figure 4.13.

The enhancement frequency response can be controlled as desired for enhancement signal components.

Unlike the conventional frequency process, a smooth response characteristic is obtained, minimizing the degree of unnaturalness inherent in processing.

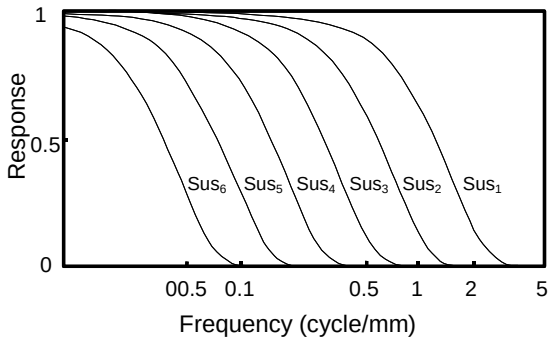

Figure 4.11 Smoothing signal response

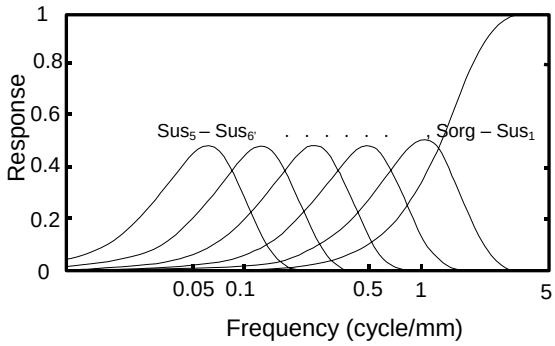

Figure 4.12 Response of signal differentials between neighboring smoothing signals

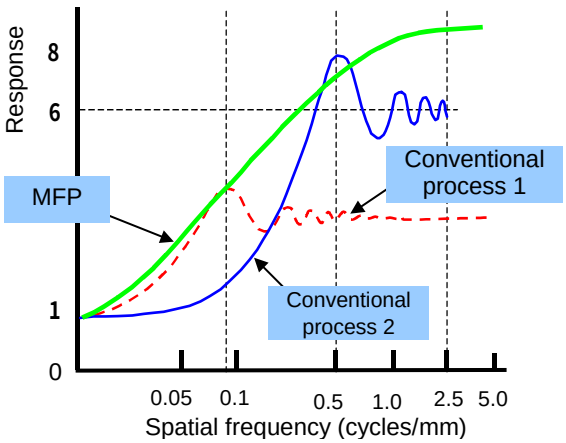

Figure 4.13 Frequency response of MFP

4 Contrast-dependent nonlinear function conversion

If an image containing a metal or other strong signals is enhanced by the conventional process, artifacts may be generated around the signal. The MFP suppresses such strong signals, providing the enhanced image a natural look. With reference to Figure 4.14, if, for instance, a bandpass signal (difference-image signal) having a relatively low contrast (as indicated by ① in the figure) is entered in relation to the indicated nonlinear function, the resulting output signal ①' has the same contrast as the input signal. However, if a high-contrast signal is entered (as indicated by ②, it is converted to generate an output signal having a lower contrast (②').

When the nonlinear function is used in the frequency enhancement process, the very small signals with low contrast are enhanced normally while the degree of enhancement is suppressed for metal portions and other high-contrast edges.

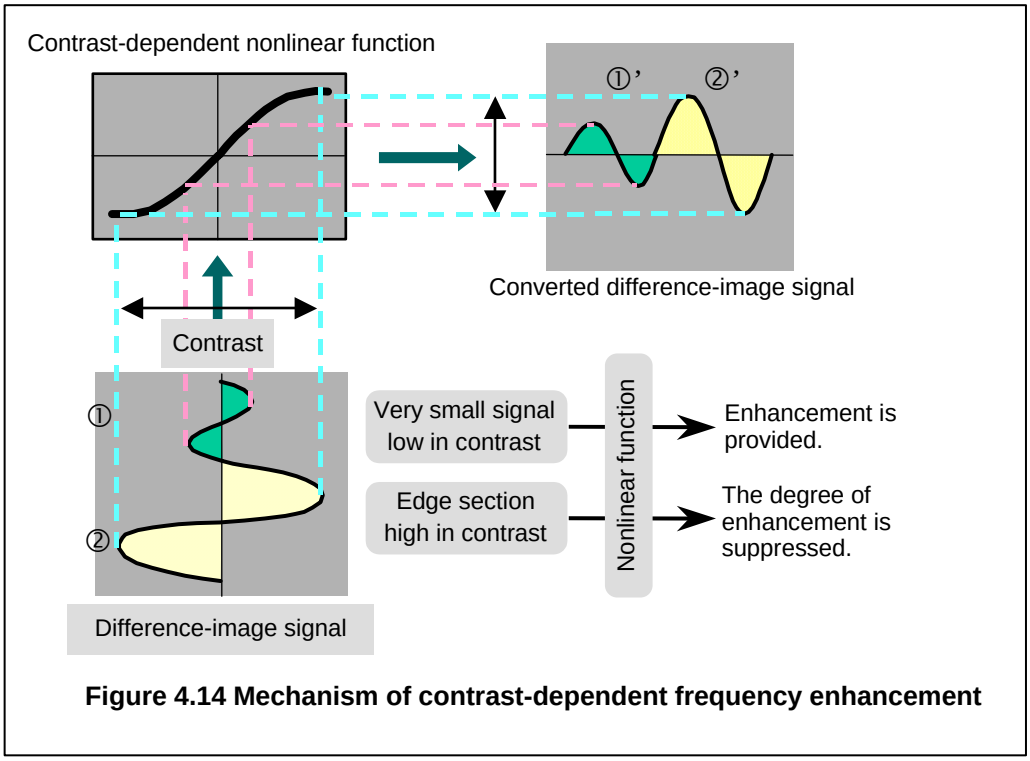

Figure 4.14 Mechanism of contrast-dependent frequency enhancement

Contrast-dependent nonlinear function

$$fm(Sm) = |Sm| \times \frac{\exp(Xm/Sm) - 1}{(\exp(Xm/Sm) + 1) \times Ym}$$

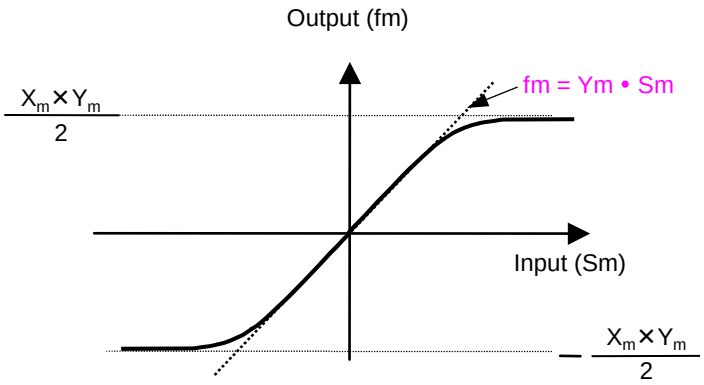

Xm : Parameter that varies the degree of contrast dependence

Ym : Parameter that varies the addition ratio

Sm : Difference-signal strength

5 Actual enhancement characteristic

The MFP's frequency enhancement function offers various parameters that enable you to freely control enhancement frequency characteristics. A typical response function for normal expression is shown in Figure 4.13. In actuality, the response characteristic has the frequency response and contrast characteristic variables shown in Figure 4.15. While these let you adjust various frequency components and the degree of contrast dependence, sophisticated knowledge of adjustments is also required.

To avoid this expertise issue, various parameters are predefined for implementing standard frequency responses so that you can perform frequency enhancement processes having various frequency responses simply by choosing a frequency balance type.

The FCR system has six different response characteristics, or balance type parameters. To facilitate the comparison of the frequency responses, Figure 4.16 shows the frequency responses in the low-contrast region when the degree of enhancement (MRE) is 1.0.

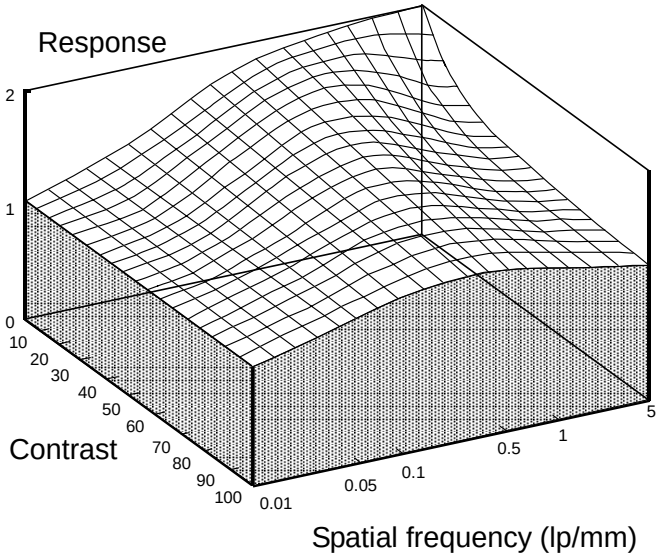

Figure 4.15 Frequency response (MRT = F, MRE = 1.0) dependent on input signal contrast

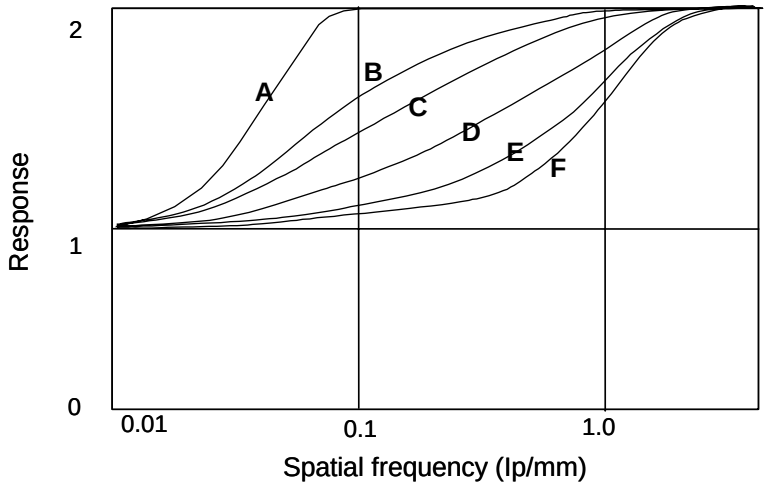

Figure 4.16 Frequency enhancement characteristics in the low-contrast region when the degree of enhancement (MRE) is 1.0

4.5.4 CR control process based on edge-retention smoothing signal components

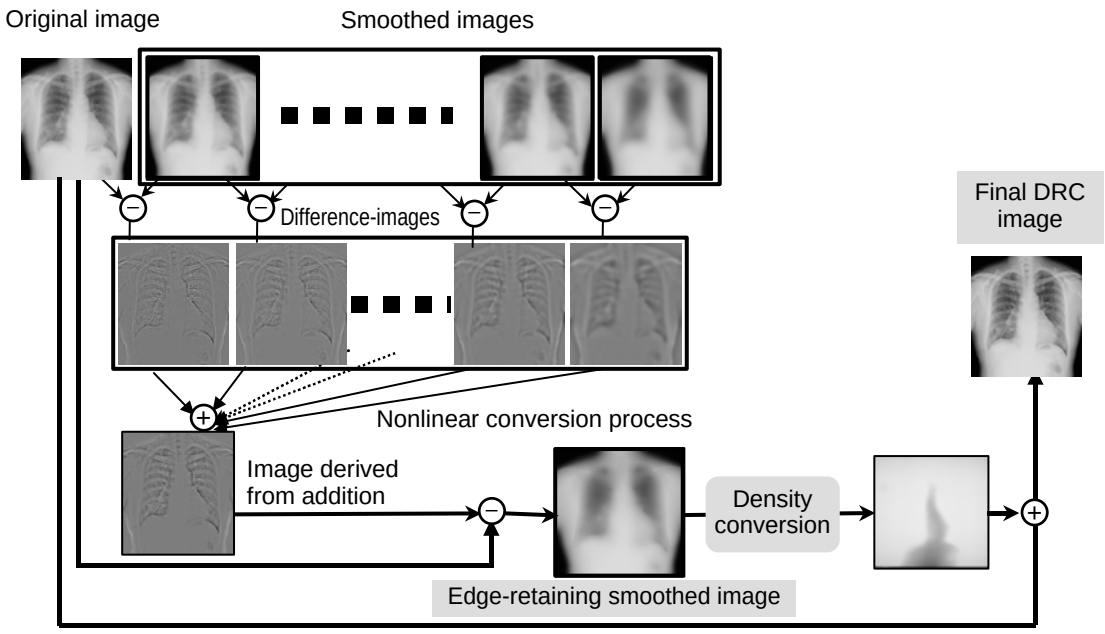

Figure 4.17 MFP DR control process block diagram

The conventional DR control process obtains smoothed images by simple averaging. As shown in Figure 4.17, the MFP performs complicated processing operations to generate smoothed images. The processing steps performed after smoothing are exactly the same as the conventional ones. The images smoothed by the MFP's DR control process retain edges; when the contrast is high, the high-frequency response is retained.

Figure 4.19 shows a smoothed image obtained from a high edge retention level. (Figure 4.21 shows its response function.) In this image, the high-contrast region is not as blurred as in the image (Figure 4.20) smoothed by the conventional DR control process. The image smoothed at a high edge retention level contains high-frequency components. With this edge-retention smoothing technique, trabecula and other edges exhibiting small density variations can be smoothed while retaining skin boundary, bone, and other edges that exhibit great density variations.

Figure 4.18 is used to explain why such a complicated process is performed.

In the conventional DR control process, low-contrast signals and high-contrast edge signals are both smoothed, resulting in a smoothed image that does not retain edges (B).

When high-density control is exercised, the high-density portions of edges may be left uncontrolled, turning them into black lines (D).

Images having unsmoothed high-contrast edges (referred to as edge-retaining smoothed images) are used for the MFP’s DR control function that smoothes low-contrast signals, which enables adequate DR control range control near edges to depict invisible areas in a relatively natural manner (G).

On the basis of the edge-retaining smoothed image characteristic determined by the MFP's DRC balance type (MDB), the optimum DR control process is implemented by the multi-DRC enhancing type (MDT) and MFP's degree of multi-DRC enhancement (MDE).

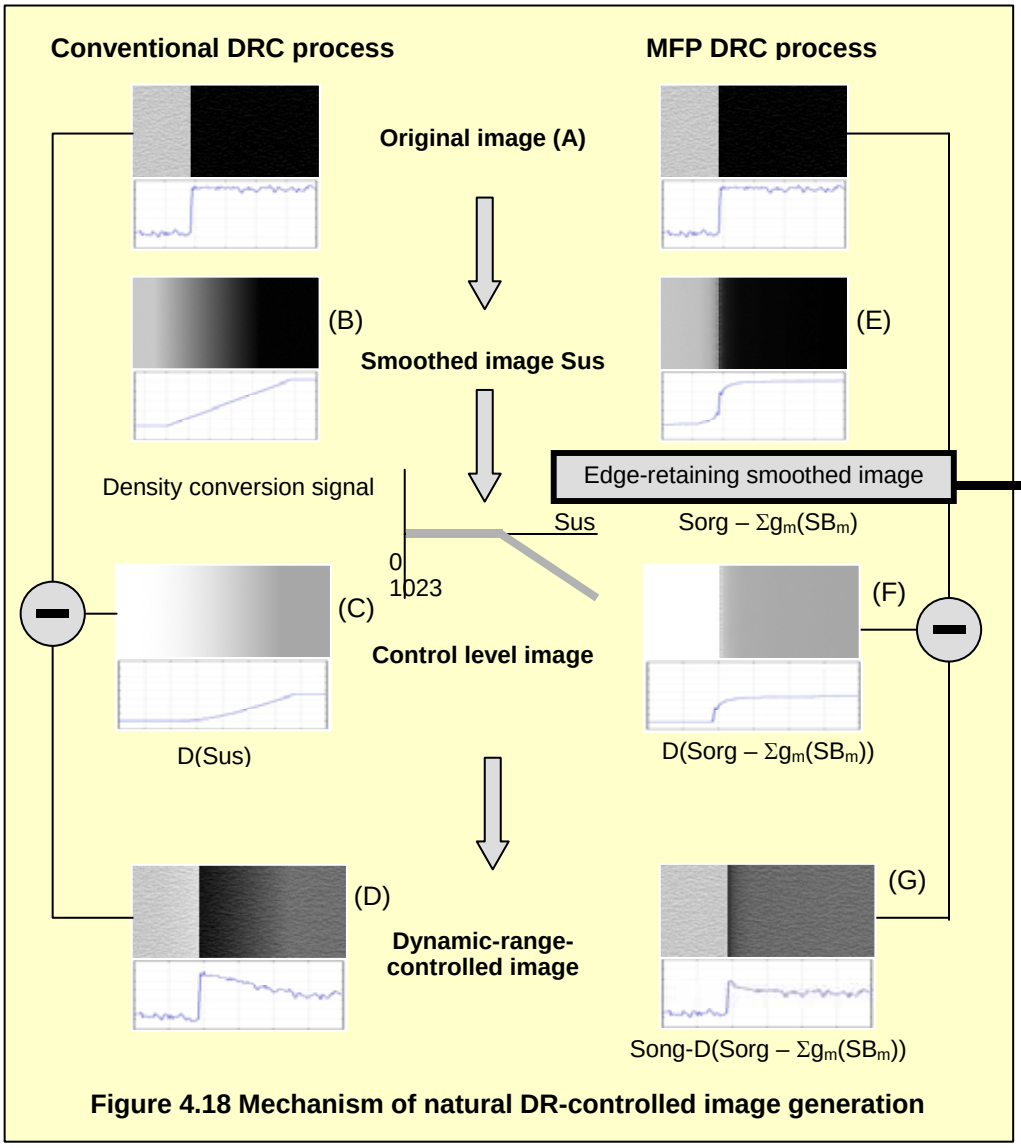

Figure 4.18 Mechanism of natural DR-controlled image generation

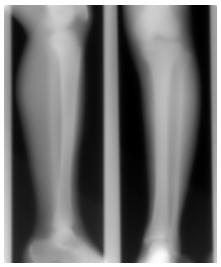

Figure 4.19 Smoothed image retaining distinct edges

Figure 4.20 Conventional smoothed image

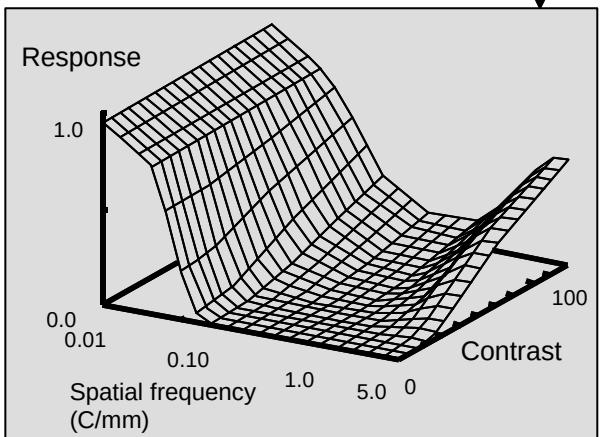

Figure 4.21 Response of smoothed image retaining distinct edges

4.5.5 Parameter overview

The MFP includes the following six types of parameters : Three types that control the frequency enhancement and the other three types that control the DRC.

Parameters that control frequency enhancement:

- Multi-frequency balance type (MRB)
- Multi-frequency enhancing type (MRT)
- Degree of multi-frequency enhancement (MRE)

Parameters that control the DRC:

- Multi-DRC balance type (MDB)
- Multi-DRC enhancing type (MDT)
- Degree of multi-DRC enhancement (MDE)

Multi-frequency balance type (MRB)

This type of parameter represents frequency characteristics of enhanced images.

However, due to contrast-dependent nonlinear function conversion, the actual frequency characteristics of the enhanced image will have characteristics as shown in Figure 4.23. To make it easier to understand differences according to balance types, Figure 4.22 illustrates frequency characteristics, when the degree of enhancement, MRE, = 1.0 in lower-contrast areas where the suppression is not applied.

Six balance types, from A to F, are available. Type A mainly enhances lower frequencies and type F, higher frequencies.

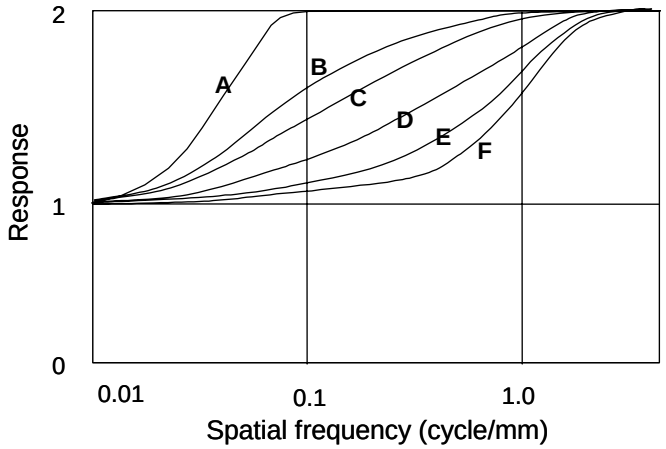

Figure 4.22 Frequency enhancement characteristics when the degree of enhancement, MRE, = 1.0 in lower-frequency areas

Multi-frequency enhancing type (MRT)

The MRT is a parameter of the definition same as that of the RT of conventional frequency processing.

Degree of multi-frequency enhancement (MRE)

The MRE has the same parameter as that of the RE of the conventional frequency processing and represents the degree of enhancement. Value ranges from 0.0 to 9.9 and 10 to 16.

Multi-DRC balance type (MDB)

This parameter represents frequency characteristics of smoothed images. However, due to contrast-dependent nonlinear function conversion, the actual frequency characteristics will be as shown in Figure 4.22. To make it easier to understand differences according to balance types, Figure 4.23 illustrates only frequency characterstics of a smoothed image observed both in lower-contrast areas and higher-contrast areas, respectively.

Seven balance types, from A to G, are available. With types A to D, frequency characteristics of a smoothed image gradually move to the high-frequency side. For types E to G, based on type A, edge saving levels have been determined larger gradually than with type A (type A is used normally).

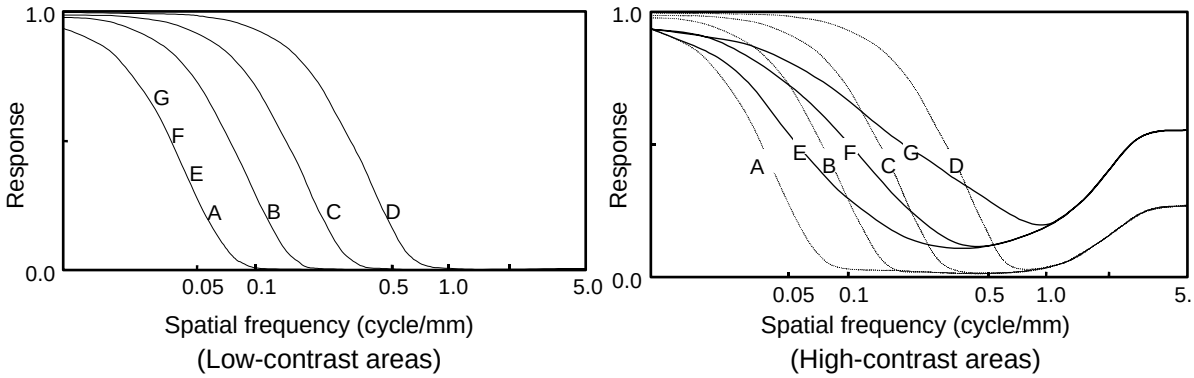

Figure 4.23 Response of a smoothed image

Multi-DRC enhancing type (MDT)

The MDT parameter has the same definition as that of the DRT of the conventional DRC processing, defining density areas to be compressed. In addition to previously used parameters A to H, the MFP adopted types I to R that control both high-density and low-density areas.

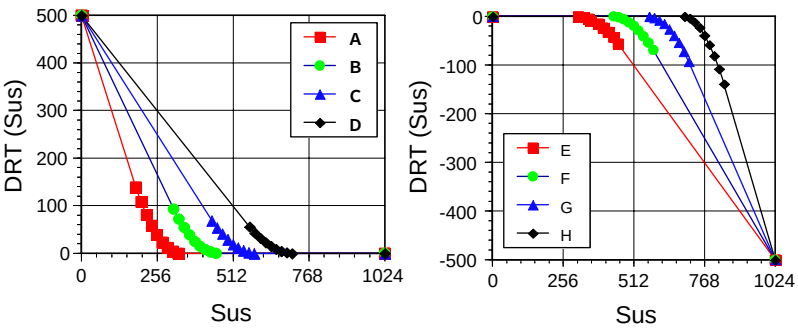

	A	B	C	D
E	I			
F	J	M		
G	K	N	P	
H	L	O	Q	R

Relationship between parameters I to R and A to H that control both low-density and high-density areas.

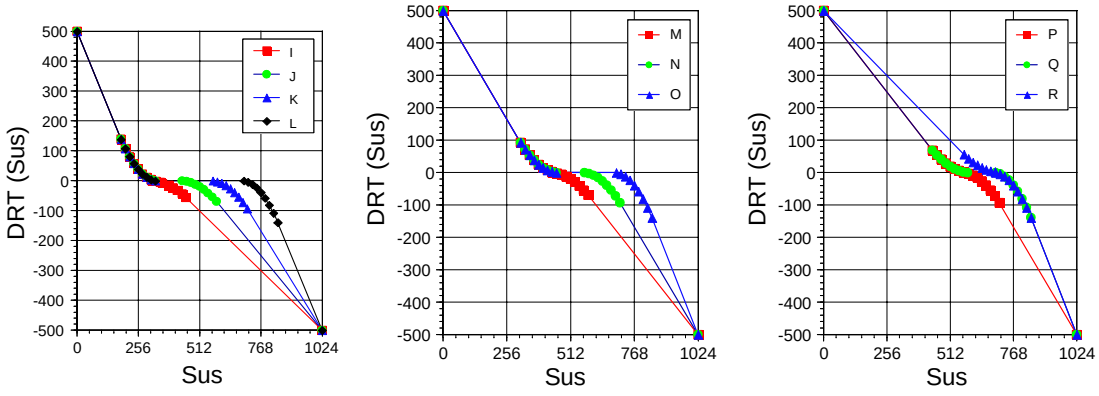

Degree of multi-DRC enhancement (MDE)

The MDE is the parameter of the same definition as that of the DRE of conventional DRC processing, taking responsibility for controlling degree of density correction. Value ranges from 0.0 to 1.0.

4.5.6 Image processing flow

The MFP can be expressed by the expression below:

$$Sproc = Sorg + \beta(Sorg) \times \sum_{m=0} f_m(SB_m) + D\left(Sorg - \sum_{M=0} g_m(SB_m)\right)$$

Frequency enhancing function — DRC function

Where,

Sorg : Original image

Sproc : Processing image

$\beta(\ )$: Density-dependent enhancing function

$D(\ )$: DRC filter function

$f_m(\ )$: Frequency enhancing nonlinear function

$g_m(\ )$: DRC nonlinear function

SB_m : Subtracted image ($SB_m = Sus_m - Sus_{m+1}$: bandpass signals)

Sus_m : Smoothed image of different special frequency characteristics (where, Sus_0 = Sorg : original image)

M : Number of smoothed images to be used

On the other hand, the previously used standard processing is accomplished in two phases and can be expressed by the expression below:

DRC processing : Sorg + D (Sus')

Spatial frequency processing : Sorg + β (Sorg) $\times$ (Sorg – Sus)

Where,

Sorg : Original image

Sproc : Processing image

$\beta(\ )$: Density-dependent enhancing function

$D(\ )$: DRC filter function

Sus : Smoothed image for frequency processing

Sus' : Smoothed image for DRC processing

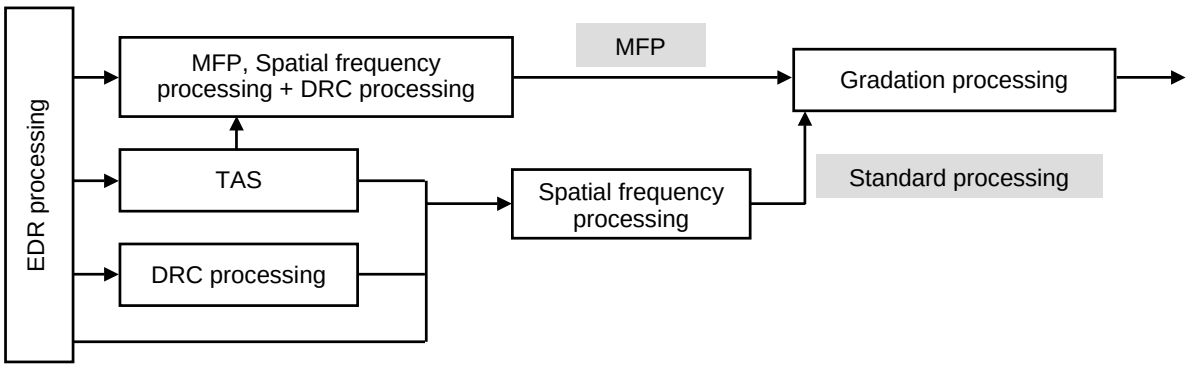

Figure 4.24 Image processing flow

4.5.7 Typical effects of the MFP

Lumbar spine, lateral

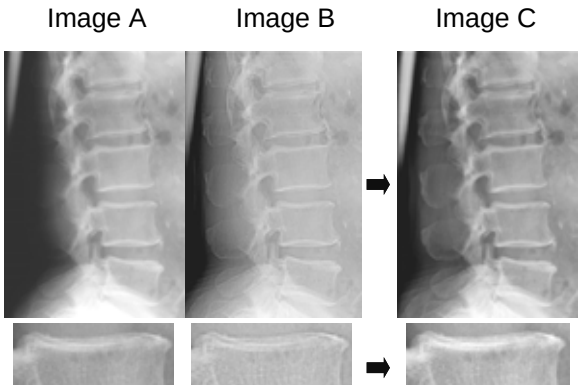

Image A : Conventional process, left image
Image based on gray-scale shadows. Radiograph similar to that derived from the conventional S/F system.

Image B : Conventional process, right image
Image having a large visible area with dot, line, and other shadows enhanced. Although the contrast is low, a wide range is observable.

Image C : MFP
Gray-scale shadows and shape shadows are subjected to well-balanced enhancement within a single image. Contrast is satisfactory and the visible area enlarged. Trabeculae are well depicted.

Dense breast

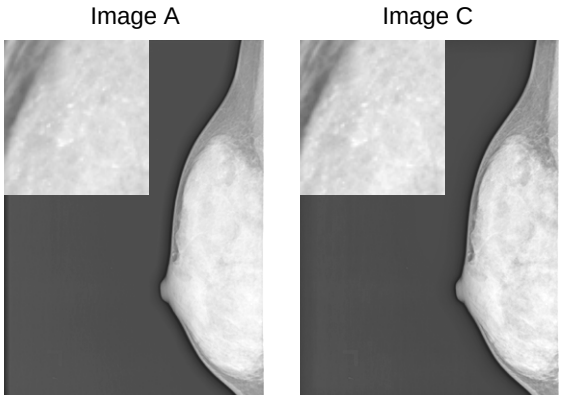

Image A : Conventional process
Image with an enhanced intermediate-frequency region. The contrast is relatively low. Calcifications are not satisfactorily depicted.

Image C : MFP
Because the low- to high-frequency regions are subjected to well-balanced enhancement, the mammary gland distribution is depicted stereoscopically in differing shades. In addition, the size distribution of fine calcifications is stereoscopically depicted.

Thigh

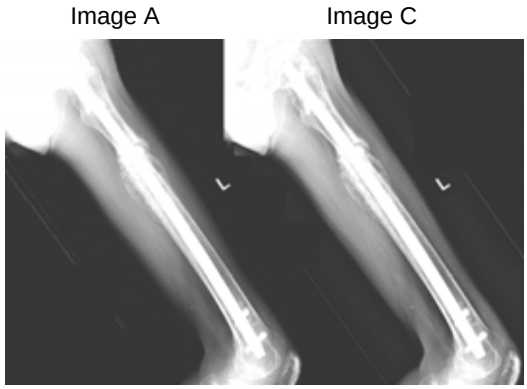

Image A : Conventional process
As is the case with the S/F system, portions involving a great X-ray absorption difference cannot easily be depicted.

Image C : MFP
The range from the knee joint to femoral head is depicted despite a great difference in the X-ray absorption.

Metal-containing radiograph

Image A : Conventional process
Black lines (artifacts) are slightly visible around the metal fastener.

Image C : MFP
The area around the metal fastener is depicted naturally. This radiograph is free from artifacts that interfere with diagnostics.

4.6 Energy Subtraction

In the energy subtraction process, two images obtained at different exposure tube voltages are subjected to proper subtraction so as to generate a soft-tissue-only radiograph or bone-only radiograph. The basic principles are indicated in Figure 4.25.

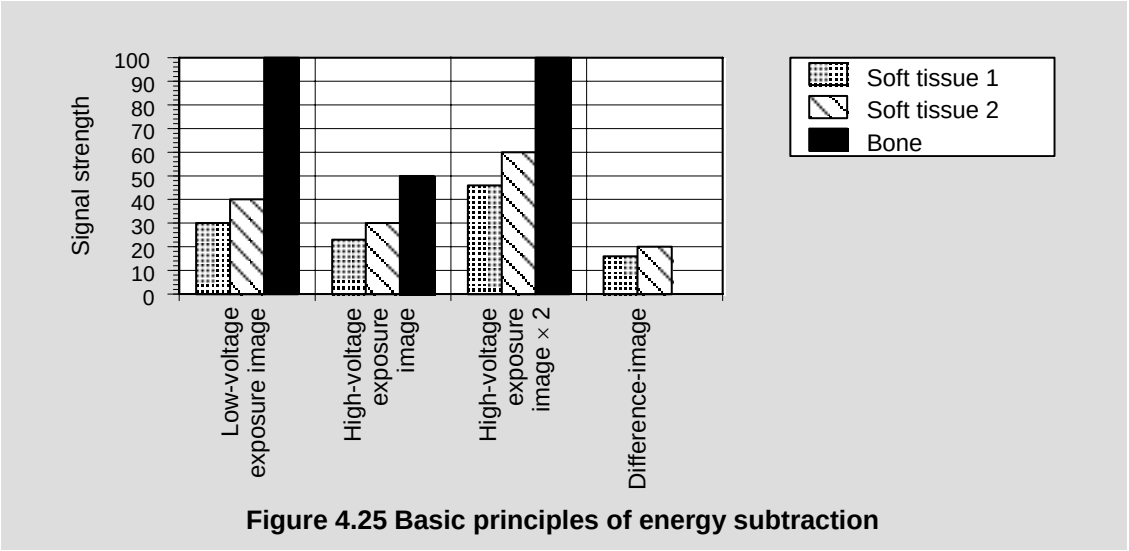

Figure 4.25 Basic principles of energy subtraction

The FCR system's energy subtraction radiography offers two methods: the two-shot method and one-shot method. The two-shot method uses two different X-ray energy radiation values. Although it uses only one shot of X-ray radiation, the one-shot method achieves X-ray energy separation by placing a metal filter between two IPs. When the one-shot method is used, the low-energy image is recorded on the IP positioned in front of the metal filter (as viewed from the X-ray source). The high-energy image is recorded on the remaining rear IP. The one-shot method is an excellent and easy-to-use radiographic technique that generates no motion-induced artifacts. However, it does not always exhibit satisfactory graininess when a normal X-ray dose is used for exposure. To deal with this problem, a repetitive processing algorithm (Figure 4.25) is used to alternately obtain soft tissue images (images from which bone portions are erased) and bone images (images from which soft tissue portions are erased). This algorithm is detailed below.

(1) Weighted averaging for most effective graininess improvement

In the process of subtraction-image graininess improvement, an original image that serves as the reference is required. A low-energy image can be used as the original image. However, since the graininess of the original image becomes the upper limit for subtraction-image graininess improvement, a weighted-average image having optimum graininess is used as the original image A (X,Y).

(2) Generating a bone image from a soft tissue image

The weighted-average image consists of bone and soft tissue signal components. The soft tissue extracted image (S1) consists of a soft tissue component only. Therefore, the following equation is obtained:

$B1(X, Y) = A(X, Y) - S1(X, Y)$ B1(X, Y) : Bone image

However, the graininess of the conventional soft tissue image is degraded because the subtraction process enhances noise more than signals. Therefore, noise is superposed over the bone image determined by the above equation. When observed from a different point of view, it implies that there is a high correlation between soft tissue image noise and soft-tissue-erased image noise. In other words, the bone image graininess can be improved by reducing the soft tissue image noise.

$B2(X, Y) = A(X, Y) - Fs1(S1(X, Y))$ Fs1 : Smoothing filter

Since the soft tissue signal component contains a limited amount of high-frequency components, the noise component is prevalent among the high-frequency components of the soft tissue image. To reduce noise, a low-pass filtering process is performed to average several pixel masks. It is important to remember that the bone signal is erased by the soft tissue image. Regardless of the type of filtering process performed on the soft tissue image, the bone signal component in the bone image will not deteriorate, although the soft tissue signal component may. The soft tissue signal component deteriorated by filtering is superposed over the bone image as an artifact.

(3) Generating a soft tissue image from a bone image

As is the case with process (2), a soft tissue image can be generated from a weighted average image and bone image.

$S1(X, Y) = A(X, Y) - Fb1(B1(X, Y))$ Fb1: Smoothing filter

This process differs from process (2) in that the former cannot use a simple low-pass filter as the smoothing filter. The role of the smoothing filter is to separate the noise from the bone signal component in the bone image and selectively reduce only the noise. The bone signal component has high-frequency components at bone edges. Areas other than bone edges consist virtually of only low-frequency components. On the other hand, the noise does not have distinct edges. Taking this characteristic into consideration, an edge-retaining smoothing filter is employed that cuts off intermediate-frequency components without degrading the edges.

(4) Repetitive processing

As stated in (2) and (3) above, either the soft tissue image or bone image can be used to improve the graininess of the other. However, if the performance of the smoothing filter is not adequate, they are superposed over each other as artifacts. Therefore, a subtraction-image can be obtained with graininess and artifact improvements both effected if processing operations are repeatedly performed while slightly varying the filter parameters.

Figures 4.27(a) and 4.27(b) show two plain images, whereas Figure 4.27(c) shows a soft tissue image (bone-erased image) that is generated by the algorithm described here

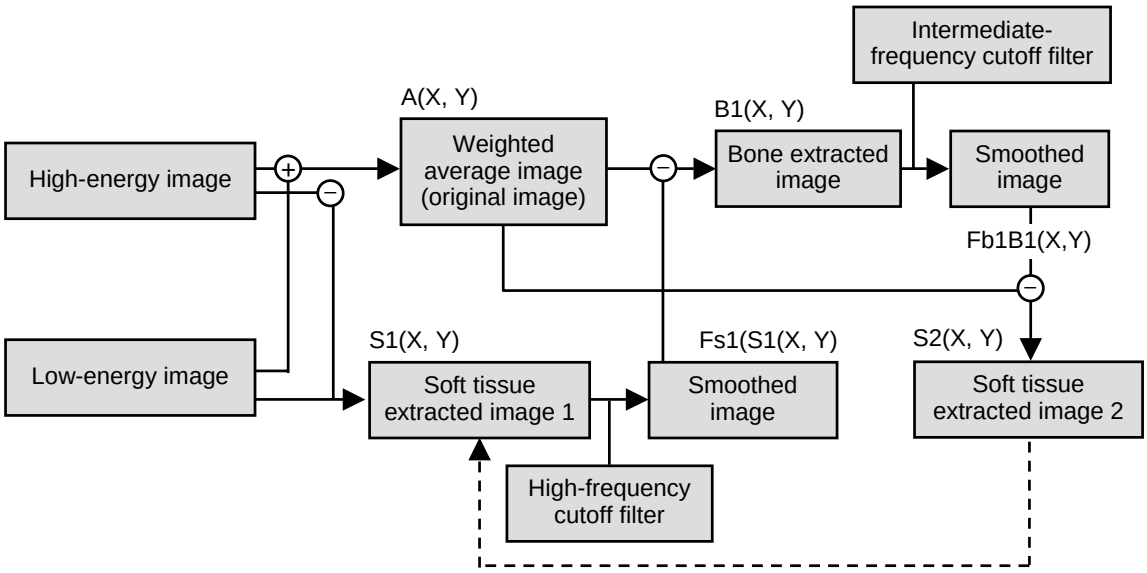

Figure 4.26 Energy subtraction algorithm for graininess improvement

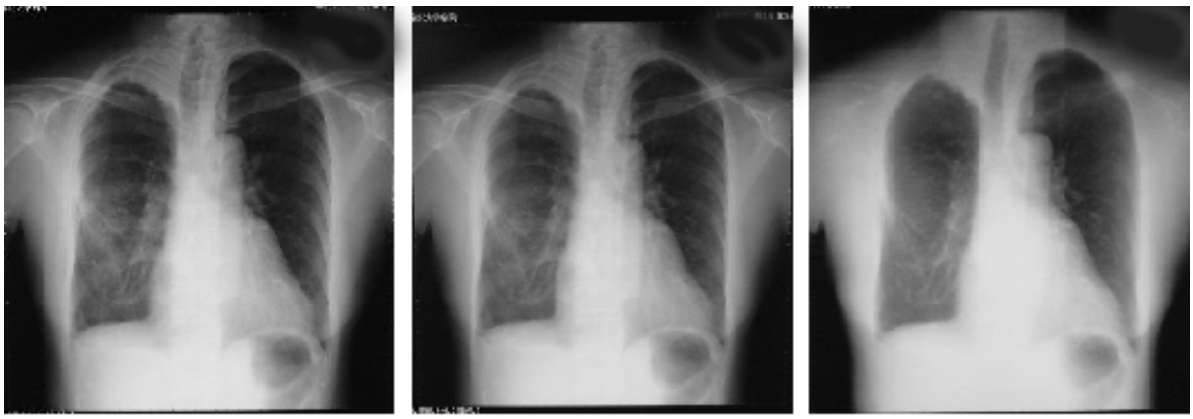

High-voltage exposure image (a) Low-voltage exposure image (b) Soft tissue image (c)

Figure 4.27

Chapter 5 Image Display

5.1 FCR Image Display Formats

5.1.1 Two-image output

In the FCR system, the image signal derived from a single exposure can be used to generate two differently processed images on a sheet of film. The image generated on the left side is called the left image, whereas the image generated on the right side is called the right image (Figure 5.1).

The two-image output format is capable of offering more diagnostic information than the conventional S/F system.

Figure 5.1 Two-image display format

Definition of the left image

The left image is based on gray-scale shadows and similar to those generated by the conventional S/F system.

Since the gray-scale based diagnostic method has already been established by the conventional S/F system, the left image is generated so that diagnoses can be made in a conventional manner. Although only one gradation characteristic can be provided by one S/F system, the FCR system furnishes every menu with an optimized gradation characteristic that suits the diagnostic purpose.

Definition of the right image

The right image has a large visibility region. While depicting various objects ranging from bones to soft tissues, it also has enhanced edges that increase the visibility of dot and line shadows. It is generated by making effective use of the IP's wide latitude and by performing an appropriate process to depict areas that are not easily imaged (e.g., chest mediastinum). Due to an increased degree of frequency enhancement, however, the metal and other areas that have density differentials may be bordered in black, with the outline of a calcification possibly rendered irregular. These problems are corrected by the use of the MFP.

5.1.2 One-image output

The one-image output format is also available in situations where the radiograph size needs to be maximized for ease of radiograph interpretation.

Definition of one-image output

The one-image output format is provided to offer a large radiograph based on images generated by the familiar conventional S/F system (left images generated in the two-image output format). This format is useful when a single large radiograph needs to be interpreted instead of observing the right and left images in the two-image output format. Application of the DR control process to the one-image output format results in the display of a single image with the merits of the two-image output format.

5.1.3 Image size

The FCR system uses 26 × 36 cm or 14" × 17" size film. The reduction ratio and sampling pixel size both vary with the size for one-image output or two-image output format images generated on 26 × 36 cm size film. In the HQ (high image quality) mode, the image size is automatically determined according to the IP used for the 26 × 36 cm or 14" × 17" size.

The table below shows the relationship between IP sizes and output image reduction ratios.

Output format	Two-image output		One-image output		One-image output	
FCR model	Standard/HQ model		Standard model		HQ model	
IP size	Reduction ratio	Film size	Reduction ratio	Film size	Reduction ratio	Film size
14" × 17" 14" × 14"	50%	26 × 36 cm	67%	26 × 36 cm	100%	14" × 17"
10" × 12"	67%	26 × 36 cm	100%	26 × 36 cm	100%	26 × 36 cm
8" × 10"	87%	26 × 36 cm	100%	26 × 36 cm	100%	26 × 36 cm

5.2 Image Enlargement/Reduction Process and Interpolation (Primarily for CT and MRI)

Image enlargement/reduction is generally performed when input data is displayed. To make a 2 × enlargement of input data consisting of 512 × 512 pixels, the input data needs to be converted to data consisting of 1024 × 1024 pixels. Interpolation data for such a conversion is created as shown below:

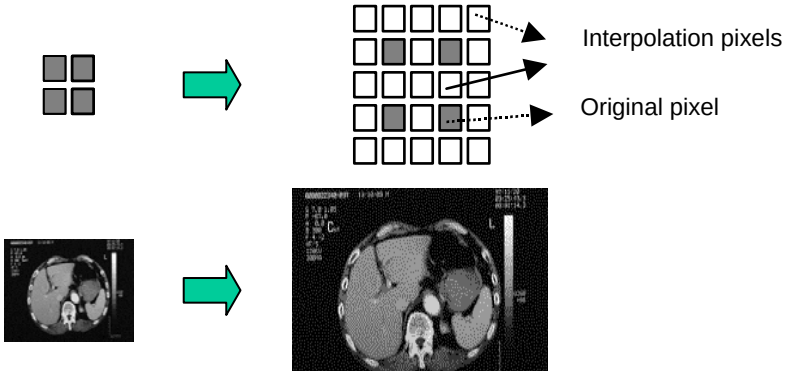

The following figures demonstrate that a soft image with a minimum of noise or a sharp, crisp image can be generated depending on how interpolation is implemented. It is important to adjust the interpolation method in accordance with the target radiograph type and the diagnostic purpose.

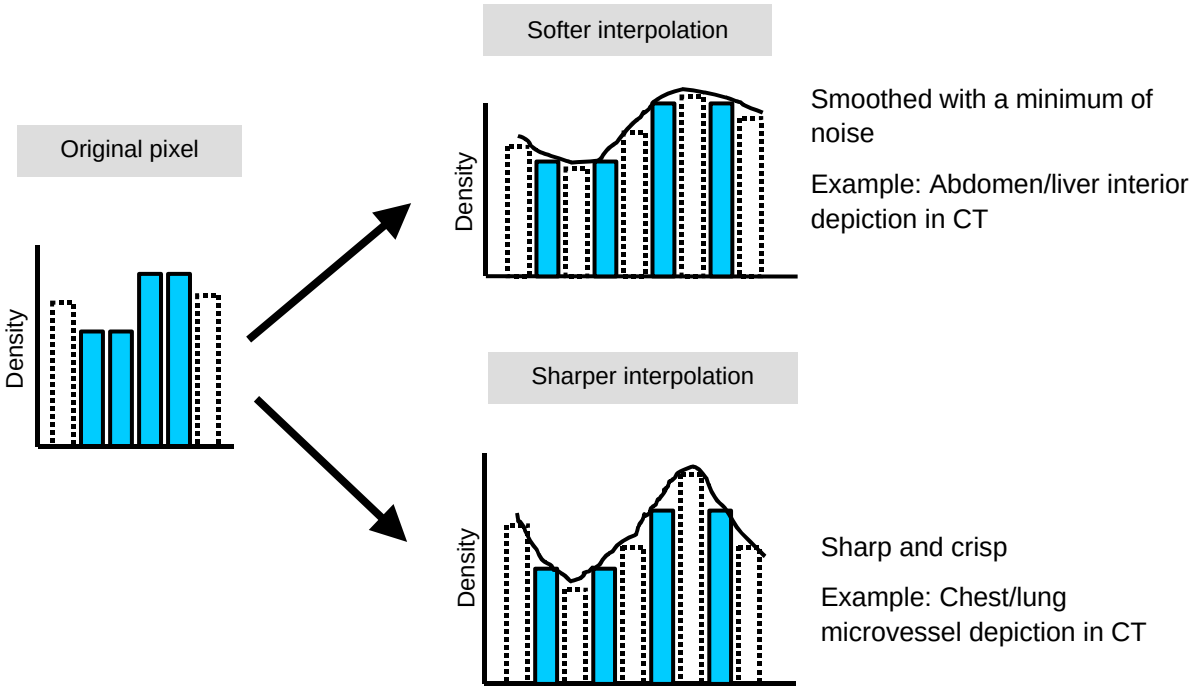

Various interpolation algorithms are available for interpolation data creation. Figure 5.2 shows the method of creating common one-dimensional interpolation data.

Nearest neighbor interpolation : The neighboring data is used without change.

Linear interpolation : Neighboring data are joined with a line. Interpolation data is created along the line.

Polynomial interpolation : Interpolation based on the Lagrange curve or spline curve.

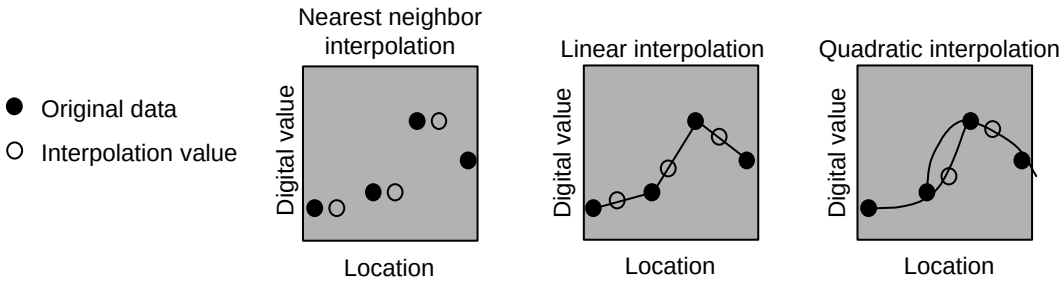

Figure 5.2 Various interpolation methods (one-dimensional data)

There are two types of polynomial interpolation: interpolation based on the Lagrange curve and interpolation based on the spline curve.

1 Interpolation based on the Lagrange curve

The data N determines a (N – 1)-th order curve. The curve always passes the original data. The data on uniquely determined, unsmooth curves (having a discontinuous slope) are used as interpolation data.

2 Interpolation based on the spline curve

It is necessary that the (N – 1)-th order spline curve pass the N original data and have a continuous (smooth) slope (differential value).

The examples in Figure 5.3 represent quadratic Lagrange interpolation, tertiary spline interpolation, and tertiary B spline curve for text data consisting of two pixels (the curve must be a continuous high-order differential curve but need not pass the original data points).

This figure indicates that tertiary spline interpolation retains continuity and offers sharper images when compared to quadratic Lagrange interpolation.

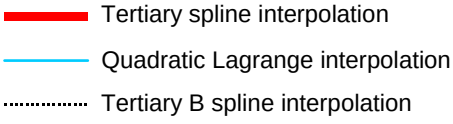

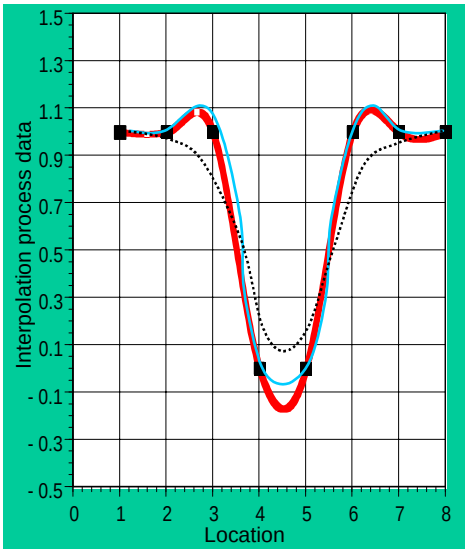

Figure 5.3 Interpolation for 2-pixel text

Linear interpolation and modified linear interpolation are adopted for FCR image enlargement/reduction algorithms, because of the moire effect of the stationary grid and image unsharpness caused by interpolation algorithms.

5.3 A-VRS (Advanced Variable Response Spline)

The A-VRS process is an interpolation process for diagnostic modalities incorporated in the Fuji Imager. This process offers the following features:

(1) Sharpness adjustments can be made as desired over a wide range. Noise and sharpness are well-balanced.

(2) The text region and diagnostic image region are distinguished from each other and subjected respectively to optimum interpolation. The resulting text is sharply defined regardless of the type of image interpolation used.

(3) Smooth images are reproduced without being roughened or jagged.

5.3.1 Image area interpolation process

As shown in Figure 5.4, the combination of tertiary spline interpolation (for obtaining the sharpest image) and tertiary B spline interpolation (tertiary spline interpolation implemented without having to pass the original data) is used to achieve image area interpolation. The combination ratio can be varied by the parameter α. When this method is used, the sharpness can be adjusted as desired over a wide range. Figure 5.5 shows chest CT images obtained at differing α settings.

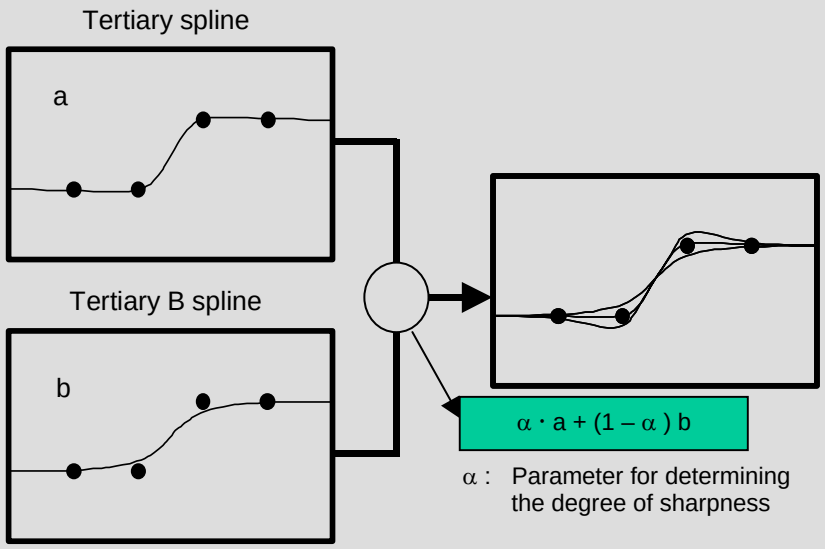

Figure 5.4 Process performed by the combination of two spline interpolation techniques

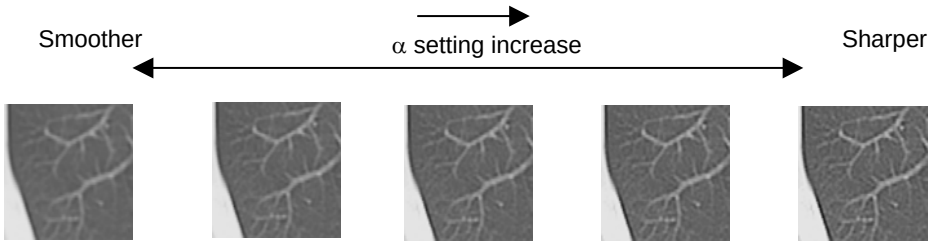

Figure 5.5 Chest CT images obtained at differing α

5.3.2 Text area interpolation process

The text information and image portions within the entire image area are first distinguished from each other. This is accomplished by checking the difference between the maximum and minimum values of four pixels surrounding the target pixel. When the difference is greater than a predetermined threshold value, it is concluded that the target pixel represents text.

The area determined to be text area has significant density variations. The density gradient vector is calculated making use of this fact. Interpolation is effected in such a manner that boundary edges remain sharp without causing jaggies in diagonal lines. Figure 5.6 shows how the A-VRS interpolation process for text areas and image areas differs from the conventional interpolation process. It reveals that the A-VRS process reproduces sharply defined text with no jaggies regardless of the applied image interpolation mode.

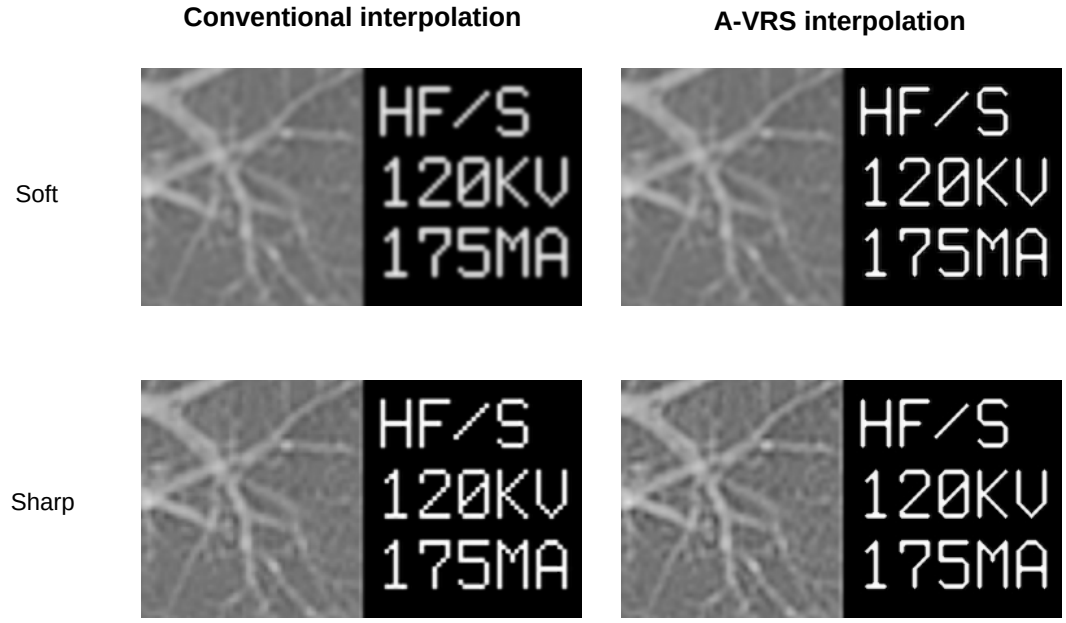

Figure 5.6 Comparison between text/image A-VRS process and conventional process

Figure 5.7 shows the comparison of MRI images derived from the conventional process and A-VRT process. When the imaging parameters are properly adjusted, images without jaggies can be reproduced. The A-VRS process can minimize the roughness of abdomen/liver CT images and suppress the conspicuousness of pixels generated by low-field MRI devices.

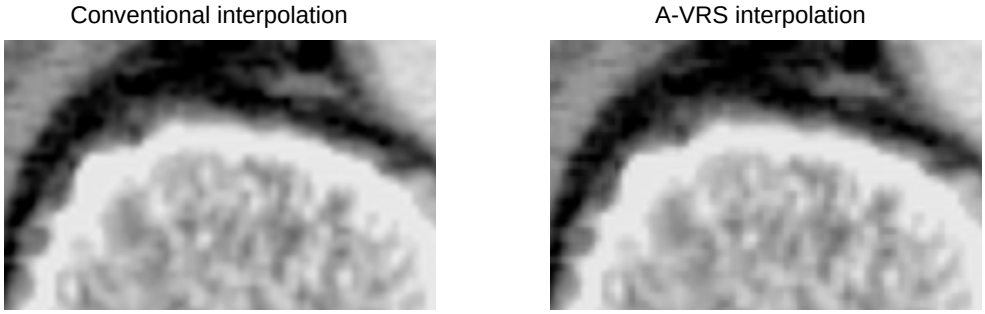

Figure 5.7

5.4 Dry Printer

There is an extremely high market demand for a dry process. This is mainly because the dry process is less bothersome (there is no need to manage developer/fixer solutions), keeps the working environment clean (no water is needed, no odor is generated, and the generation of noise is minimized), is economical (costs are limited to film and electricity), is environment-friendly (no waste solution, water, or material is generated), and can be installed anywhere.

The history of dry printing is a long one, and begins with the introduction of fax machines. However, only a few years have passed since the introduction of dry medical imaging and there are many difficult issues yet to be resolved, such as the necessity for detailed depiction of large amounts of image data. In comparison, the wet process is a highly mature process that has been in use for a period of about 100 years. Although a practical dry system has recently been completed, it is still in the process of further improvements.

The most serious bottleneck of the dry system is attributable to its dryness. More specifically, unreacted substances and substances requiring no reaction do not leave the film system. It is therefore questionable whether the image recorded on the film will remain intact for a long period of time. The resolution of this issue will lead to a successful dry system.

Currently available practical dry systems are introduced below:

1 Direct thermal printing method
2 Dry thermal development/laser exposure method
3 Image transfer sublimation method
4 Carbon separation method

This section describes methods 1 and 2 only.

5.4.1 Direct thermal printing method

Figure 5.8 shows the principles. The film mainly consists of a color developing material and a microcapsuled color forming material. When heated, the microcapsule loosens so that the color developing material can seep in. A color forming reaction then occurs to achieve color formation. When cooled, the microcapsule prevents entry of external material, bringing the color formation reaction to a stop.

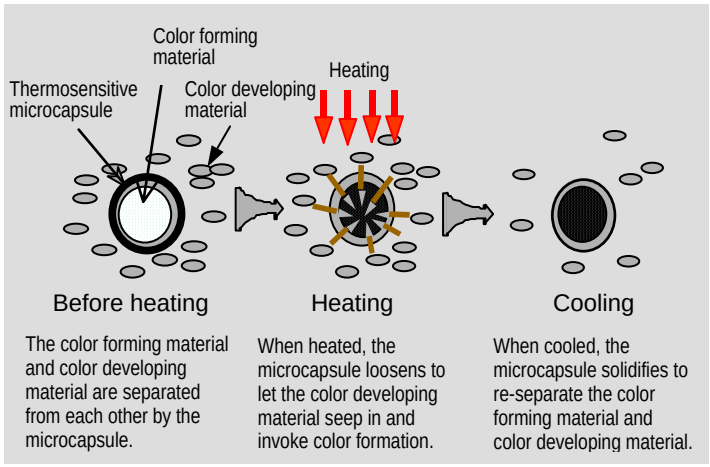
Color forming material
Thermosensitive microcapsule
Color developing material
Heating
Before heating
Heating
Cooling
The color forming material and color developing material are separated from each other by the microcapsule.
When heated, the microcapsule loosens to let the color developing material seep in and invoke color formation.
When cooled, the microcapsule solidifies to re-separate the color forming material and color developing material.

Figure 5.8 Direct thermal printing method

5.4.2 Dry thermal development/laser exposure method

Figure 5.9 shows the principles. The principles are the same as those of the wet system except that visualized silver is formed upon heating to form the image. Since no fixing process is performed, unreacted substances remain in the system. However, as fine crystals, they are transparent.

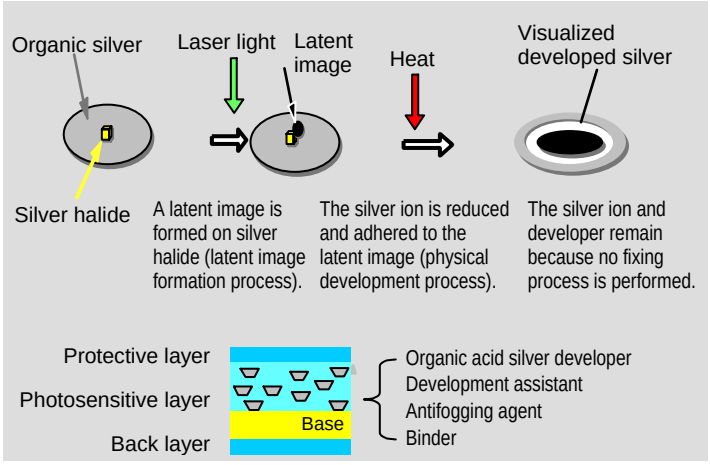

Figure 5.9 Dry thermal development/laser exposure method

5.5 CRT Display

5.5.1 Relationship between the image displayed on the CRT and the image of the film on a light box

In general radiography, a film image is used for diagnoses. The image displayed on the CRT should be similar to such a film image.

Common CRT display systems are mostly designed so that virtually linear brightness is imparted to high-brightness regions of input data (QL) (Figure 5.10).

For images viewed with a light box, logarithmically linear brightness is given in relation to the X-ray dose. That is, the film characteristic is usually expressed with the logarithm of the X-ray dose plotted along the X-axis and the density plotted along the Y-axis.

When such an expression is applied to digital data, the quantization is logarithmically linear in relation to the X-ray dose and the final processed image data is given linearly in relation to the density (see Section 3.2 in Chapter 3).

When film prepared in this manner is observed in a light box, the relationship between brightness and QL (data entered in the imager) is as shown in Figure 5.11(a) at a certain light box brightness level.

Even if the light box darkens, only downward translation occurs to the extent that the vertical axis logarithmically expresses the brightness, as indicated in Figure 5.11(b). Although the image becomes darker, slightly lowering the viewability, the basic tone remains unchanged, imparting no significant effects on radiographic interpretation.

The CRT display system should therefore be capable of giving the same expression as a film image viewed in a light box. A CRT's brightness deteriorates with time, so to provide constant expression, the CRT must incorporate a scheme similar to that of film. That is, the CRT must be linear in relation to logarithmic brightness when expressing the signal. Conversion using a special conversion table (LUT: look-up table) is required.

Figure 5.12 shows how the correspondence between input values and brightness varies depending on whether LUT conversion for film approximation is performed or not (monitor's maximum brightness: 126 nit). The figure indicates that the image obtained without LUT conversion is whitish and low in contrast.

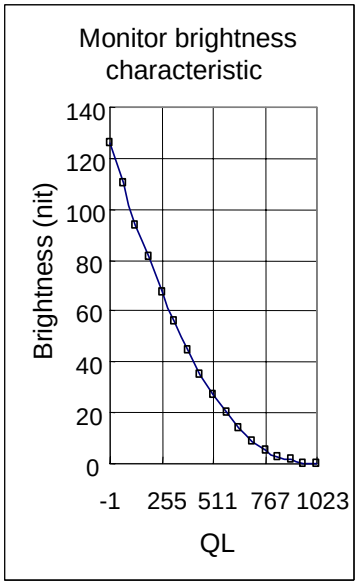

Figure 5.10
Monitor brightness characteristic

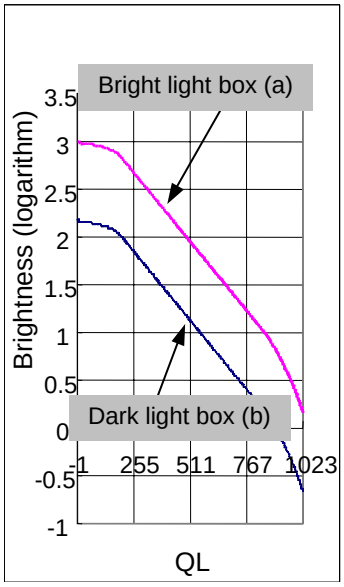

Figure 5.11
FCR image brightness as viewed on light box

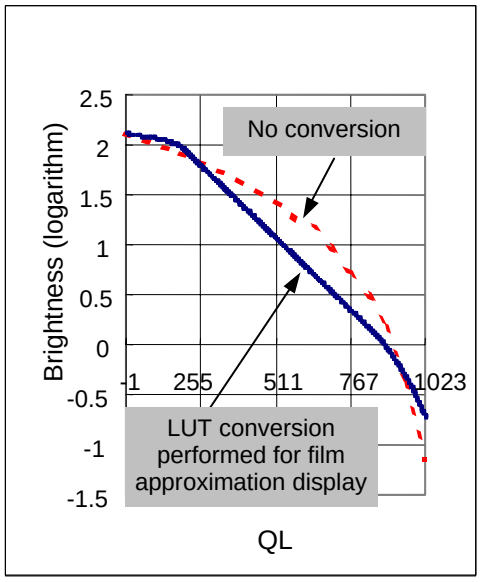

Figure 5.12
Changes in brightness characteristic of FCR image display on CRT depending on whether LUT conversion is performed

5.5.2 CRT diagnostic capabilities

As described below, CRT diagnosis can be regarded as the final form of digital image use.

1 Target images can be quickly obtained.

Previous radiographs can be quickly retrieved when necessary for comparison with currently obtained radiographs. Further, current radiographs can be quickly interpreted on the CRT screen. Printing of radiographs does, however, take a certain amount of time.

2 Economical.

Considerable economical savings are obtained because film and processing solutions need not be used. To meet the demand for medical cost reduction, there is a clear-cut trend to increase the use of filmless radiography.

Since the rise of the CRT diagnosis trend, various study groups have compared CRT diagnosis and film diagnosis. This section describes the results of studies conducted in 1991 by the Sakuma Group and in 1994 by the Ishigaki Group. Both concluded that CRT diagnosis did not significantly differ from film diagnosis in terms of diagnostic capabilities and adequacy for diagnostic purposes.

1. Study results of the Sakuma Group (1991)

J.Digital Imaging 8 (1.Suppl 1):25-30,(1995)

Conditions

Workstation : Toshiba TDIS-FILE (1024 x 1280, 8-bit), Fuji HIC (1024 x 1280, 10-bit)

Images : Normal images, interstitial diseases, aerothorax, bullae, pneumonia, and nodular opacity

Method

Twenty radiologists and five chest physicians at twelve institutions participated. A total of 90 cases (including 19 cases in which nonreversible 1/10-compressed images were used) were examined during a period of four days. Film output images and CRT images were subjected to ROC analysis to examine the diagnostic capability. For CRT diagnosis, gradation and enlargement processes were performed as desired.

Results

No significant difference in diagnostic capability was found between film images and CRT images except by one physician.

In film diagnoses and CRT diagnoses, no significant difference was found between newly obtained images and images archived for a long period of time.

In ROC analyses of various observations, no significant difference was found between CRT images and film images.

When analyses were made in relation to individual compression ratios and observations, significant differences were found between CRT and film images at a rate of 5% or 1%; however, no significant difference was found in most cases.

When compressed images were subjectively evaluated, the majority of 1/10-compressed images were statistically found inadequate for clinical examination. However, they did not exhibit any clear difference when they were subjected to ROC analyses.

2. Study results of Ishigaki Group (1994)

Radiology 201:51-60,1996

Conditions

Workstation: Fuji HIC (20-inch, 1586 × 1152, 8-bit)

Images: 87 cases (including 24 cases in which the same radiographs were used for reproducibility verification) from five institutions containing lung interstitial shadows and pale consolidations

Regarding the abnormal cases, the difficult-to-diagnose, ordinary, and easy-to-diagnose case counts were the same.

Physicians: 18 chest radiologists and 2 internists at 19 institutions

CRT diagnostic method

In addition to normally displayed images, doubled images equivalent to film images were used. These images were subjected to film-like processing, low-frequency enhancement, and high-frequency enhancement for a total of six different types, and were used for diagnostic purposes.

Results

Diagnoses made by 20 physicians exhibited satisfactory reproducibility.

No significant differences were found in the average ROC curves of film images, CRT images, and CR film images.

No significant differences were found in the difficult-to-interpret radiographs.

5.6 Relationship between Stationary Grid and Moire

5.6.1 Interference-induced moire patterns

A lead grid is generally used for radiography. X-rays scattered by the subject lower the image contrast. The greater the X-ray energy, the higher the scattered radiation intensity. Further, scattered radiation greatly depends on the subject thickness. The grid is used to reduce scattered radiation.

In digital imaging, the grid may cause moire patterns to be generated.

Film output images have virtually no problems with moire. However, if the stationary grid is positioned in parallel with the printer scanning line, the resulting interference may generate moire patterns. Figure 6.1 shows an example in which a 5 cycle/mm signal and 4 cycle/mm signal are positioned in parallel with each other. In this instance, you are likely to perceive a low-frequency signal moire pattern having a wavelength of 1 mm (1 cycle/mm).

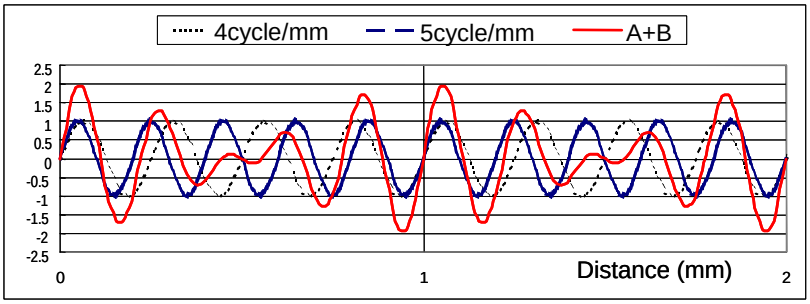

Figure 6.1 Interference caused by superposition of differing frequency components

5.6.2 Relationship between sampling interval and moire

Moire patterns may hinder image observation on a monitor when you observe a reduced version of an image consisting of large pixels.

For example, consider a radiograph obtained with a 40 line/cm stationary grid. Since the signal of the grid is cyclical, it is regarded as being approximate to the sine wave signal shown in Figure 6.2. Because CRT images are usually displayed using 1000 lines in the 17-inch screen area, 1000 to 500 lines are used in a distance of about 30 cm, which is the life-size equivalent. This means that the sampling interval is between 0.3 mm and 0.6 mm (= 30 cm/1000 to 500 lines). Figure 6.2 shows an example in which repeated images of a 40 line/cm grid are sampled at 0.3 mm intervals. The broken line shown in Figure 6.2 represents the sampled grid image appearing on the CRT screen. When the cycle is increased, the difficult-to-discern fine grid image starts to appear as a readily-discernible, low-frequency component (wavelength: 1.5 mm; frequency: 0.667 cycle/mm) moire pattern. Figure 6.3 shows an example in which sampling is performed at 0.6 mm intervals. In this example, a low-frequency moire pattern having a wavelength of 3 mm (0.333 cycle/mm) appears.

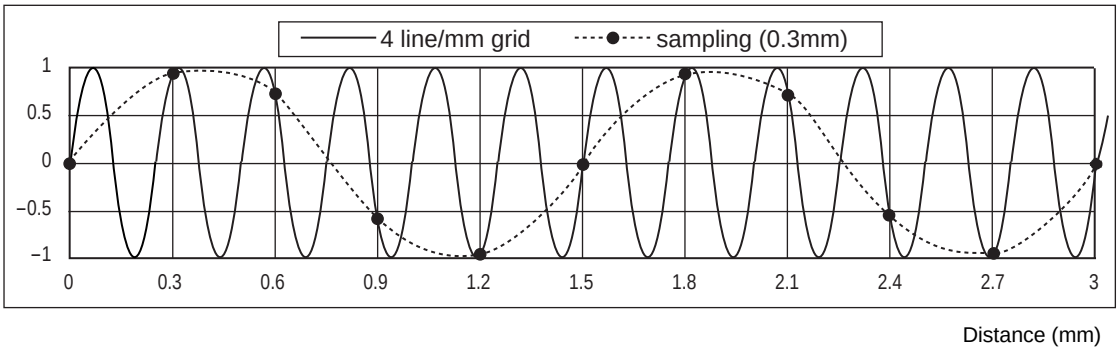

Figure 6.2 40 line/cm grid sampling at 0.3 mm intervals

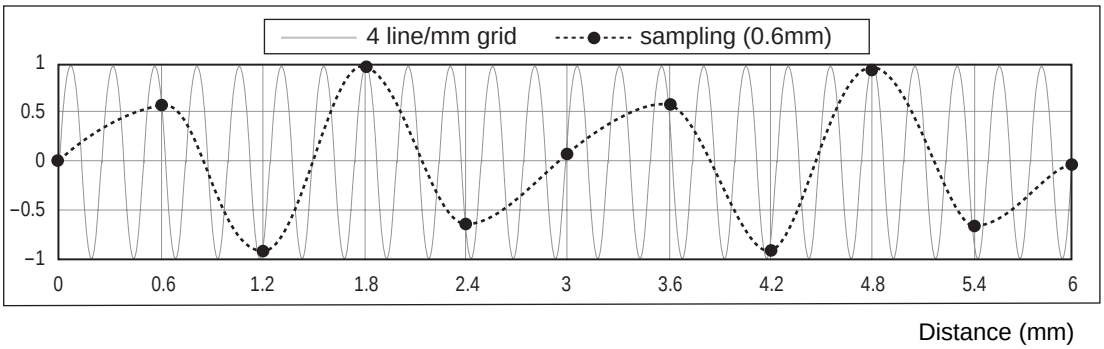

Figure 6.3 40 line/cm grid sampling at 0.6 mm intervals

As explained above, the moire pattern perceived during CRT screen observation depends on the display conditions. For example, the sampling interval is decreased to display an enlarged image, resulting in a faint or unperceived moire pattern. However, when displaying a reduced image, the sampling interval is increased, resulting in greater probability of a visible moire pattern.

If there is a signal smaller than the sampling interval, it is looped back in accordance with the Nyquist frequency that is two times the sampling interval, and superposed over the low-frequency side. This is called aliasing, as defined in relation to sampling.

Regarding low-frequency region superposition in 0.3 mm interval sampling, the Nyquist frequency (1 / 0.3 × 2 mm) is 1.667 cycles/mm and the superposition signal frequency is 0.6667 cycle/mm. In 0.6 mm interval sampling, the Nyquist frequency (1 / 0.6 × 2 mm) is 0.833 cycle/mm and the superposition signal (first order) is 0.333 cycle/mm.

NOTE

When an ideal detector is used, its frequency response is determined by the sampling interval so that Equation (1) is obtained.

$$MTF(\nu) = \mathrm{Sin}(\pi a\nu) / \pi a\nu \quad \text{..... Equation (1)}$$

where a is the sampling interval.

When the sampling interval is 0.3 mm, Equation (1) indicates the MTF shown in Figure 6.4. When the sampling interval is 0.6 mm, Equation (1) indicates the MTF shown in Figure 6.5. The Nyquist frequency is the first frequency that prevails when the response is 0. If there is a signal containing components with higher frequencies than the Nyquist frequency, some signal components are looped back and superposed. Such frequencies are indicated by the arrow marks.

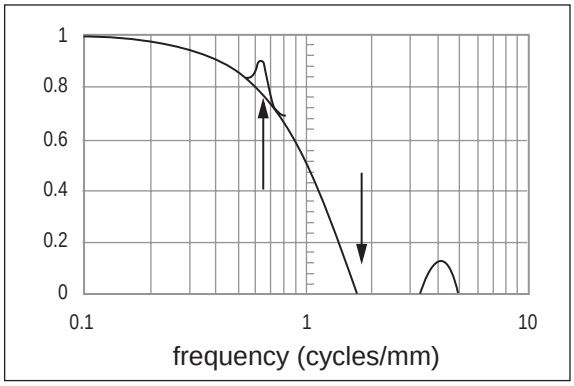

Figure 6.4 Sampling interval equals 0.3 mm

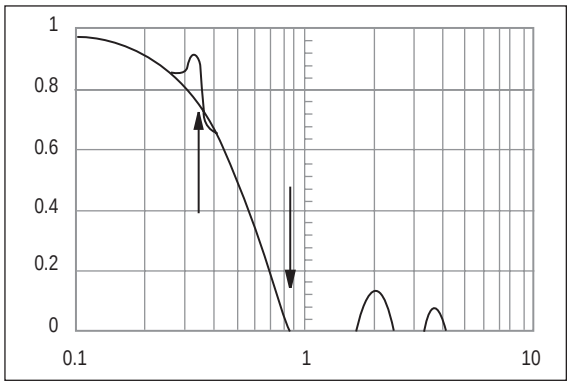

Figure 6.5 Sampling interval equals 0.6 mm

5.6.3 Moire elimination/reduction method

Moire reduction can be achieved by a filtering process that removes components having specific frequencies at which moire pattern generation occurs. For example, the signal of a 40 line/cm grid has a frequency of 4 cycles/mm (the FCR sampling interval is 0.1 mm in the HQ mode resulting in a Nyquist frequency of 5 cycles/mm as indicated in Figure 6.6). Moire reduction can therefore be accomplished by passing the signal through the filter shown in Figure 6.7.

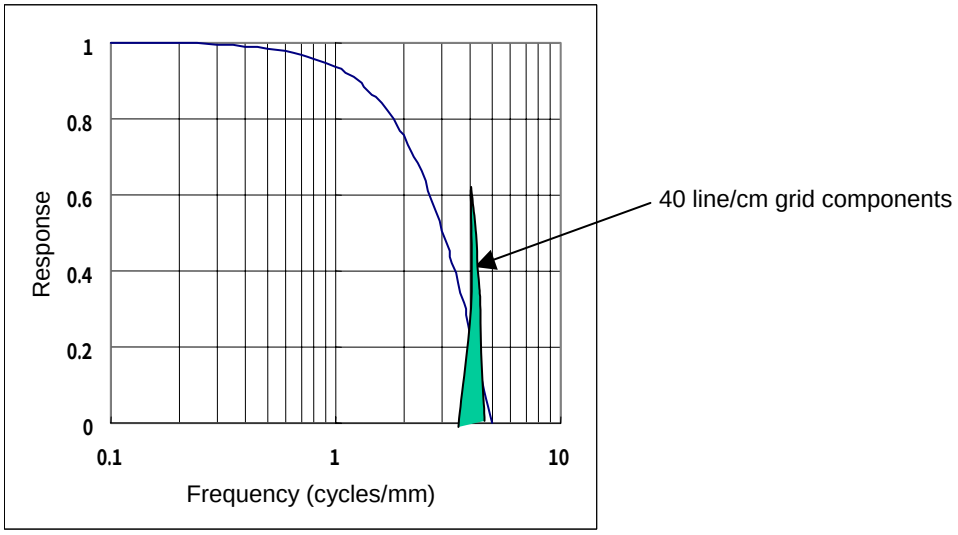

Figure 6.6 Relationship between ideal characteristics and grid components in FCR HQ mode (0.1 mm sampling)

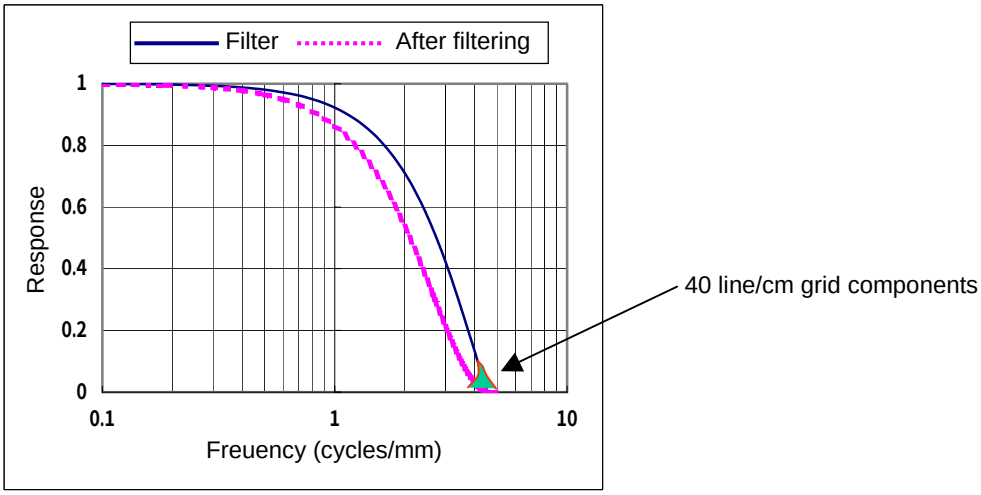

Figure 6.7 Example of moire signal reduction by filtering

Chapter 6 Image Electronic Archiving and Communication

6.1 Image Compression

Image data compression technologies determine the image quality, archiving cost (as influenced by compression ratio), transmission time, and other important factors in filing and network communication. In addition to filing operations, image transmission over networks and image diagnosis and viewing (CRT diagnosis) operations at network terminals are in wide use. Consequently, the image quality level and high-speed image transfer (reproduction) are considered important at terminals.

With this as a background, this chapter reviews conventionally used compression technologies and introduces image data compression technologies suitable for medical imaging network systems.

6.1.1 Trends in image data compression technologies

Table 6 shows the classification of image data compression technologies used in the medical image filing systems and network systems of various manufacturers. DCT (Discrete Cosine Transform) (see the next page) is now frequently used partly due to the influence of JPEG. Note, however, that DCT is not equivalent to JPEG. Its performance varies with the employed compression algorithm. Next-generation technology called "JPEG 2000", which is based on Wavelet coding, is in the process of standardization.

Table 6 Classification of image data compression technologies

Category	Technique	Features
Predictive coding	Differential predictive coding	General lossless compression method for subjecting prediction error information to Huffman coding.
	Interpolation coding	Natural images can be obtained although their sharpness is reduced by spatial resolution deterioration. This method is employed by Fujifilm's image filing equipment (ODF/HIC).
Transform coding	DCT (Discrete Cosine Transform)	Each block is subjected to DCT. Image information is resolved into frequency components and then compressed. Block distortion may occur depending on the compression ratio.
	DCT (JPEG)	International standard method. The image quality features are the same as above.
	Full-frame DCT	Although this method incurs no block distortion, it has an inferior compression ratio compared to block DCT.
Other	Block coding	Coding is effected while handing the image as blocks of similar portions. Distortion is likely to occur.
	Vector quantization	Image blocks are expressed as vectors and quantized. Loss of pixels is likely to occur.

6.1.2 Lossless JPEG

The term "lossless compression" means that the original image can be thoroughly recovered after decompression of the compressed image.

Suppose that there is an array of 10 pieces of data having the value 8. In this situation, the data can be represented by enumerating all the 10 pieces of data having the value 8. However, the data volume can be reduced by recording the fact that there are 10 pieces of data having the value 8. In this instance, the original data can be completely recovered if certain rules are established.

Image data is contiguous. When it is replaced by the differences from neighbors, the data value distribution is narrowed to facilitate compression.

Lossless JPEG calculation example

Original data: 8-bit
Amount of information:
8 bits × 16 = 128 bits

122	123	122	123	123
121	122	120	122	122
122	124	121	124	122
123	123	122	120	120

Difference-data

1	-1	1	0
1	-2	2	0
2	-3	3	-2
0	-1	-2	0

Huffman coding
Compressed to 42 bits (33% of the original data size)

Difference	Frequency	Huffman code		Frequency x bits
0	4	00	2	8
1	3	01	2	6
-2	3	100	3	9
-1	2	101	3	6
-2	2	110	3	6
-3	1	111	3	3

As shown at right, lossless JPEG converts data and gives short codes to frequently used data (Huffman coding) to achieve image compression. In the example shown at right, a compression ratio of 33% is attained.

6.1.3 Lossy JPEG compression

The JPEG lossy, or irreversible compression process is performed under the following scheme:

Block formation	Blocks of 8×8 pixels are formed (in order to reduce the calculation time required for conversion).
↓	
DCT	Two-dimensional cosine conversion is effected to determine the real conversion coefficients.
↓	
Quantization	The coefficients are rounded to reduce the amount of data. The alternative is to cut off high-frequency components.
↓	
Huffman coding	Variable-length codes are given to the quantized coefficients.

1. Two-dimensional DCT (discrete cosine transform)

$$F(uv) = 4c(u)\,c(v)/N^2 \sum \sum f(ij)\cos(2i+1)\,u\pi/2N \times \cos(2j+1)\,v\pi/2N$$

$$c(u), c(v) = 1/\sqrt{2}\ (\,u, v = 0\,), 1\,(u, v = 1 \ldots N-1\,), 0\ (\text{otherwise})$$

F(uv) : converted coefficient

F(ij) : original image data

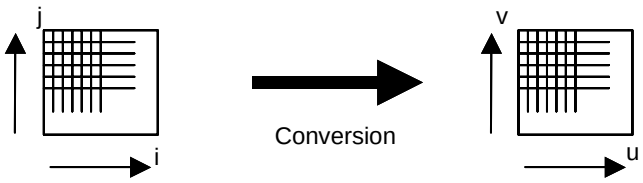

DCT itself does not effect image compression. However, DCT converts the coefficients so that they can readily be compressed regardless of the image.

(1) The lower the component frequency, the greater the coefficient value.

(2) The conversion coefficient value distribution of all AC components is a plus distribution that peaks at 0.

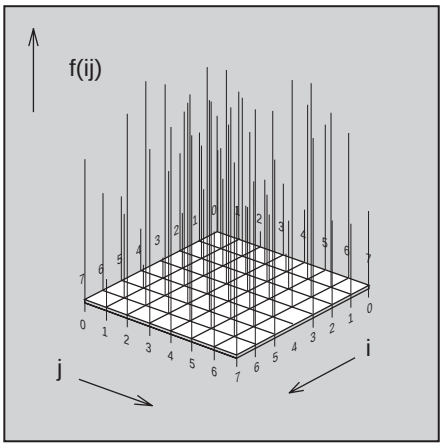

Image spatial distribution

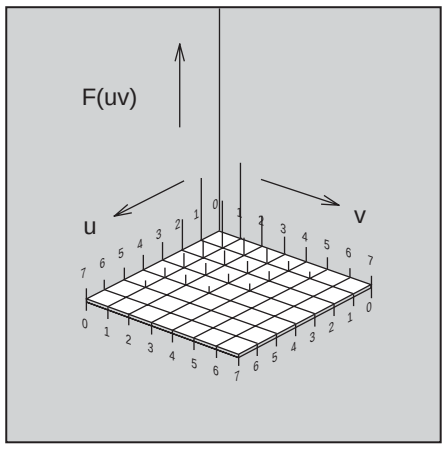

DCT coefficient amplitude distribution

2. Quantization and coding

1 A certain quantization matrix Q(uv) is defined for F(uv), which is converted. This matrix is such that the higher the frequency, the greater the given number (the number to be given increases as the frequency location within the matrix moves toward the lower right corner of the matrix).

2 Rounding process (drop the fractional portion of the number) in matrix D will make high-frequency components zero. A large amount of information will then disappear for the data to be compressed. This process is irreversible (lossy compression). The image compression ratio and image quality depend on quantization table Q(uv) and the degree of rounding proess.

3 DC components D(OO) and AC components D(uv) are separately processed. Individual block numbers for D(OO) closely correlate to their neighbors so that compression is effected by difference process Huffman coding.

4 AC components are arranged in a zigzag manner and compressed by Huffman coding.

Quantization table example

Q(uv)

3	5	7	9	11	13	15	17
5	7	9	11	13	15	17	19
7	9	11	13	15	17	19	21
9	11	13	15	17	18	20	22
11	13	15	17	19	21	23	25
13	15	17	19	21	23	25	27
15	17	19	21	23	25	27	29
17	19	21	23	25	27	29	31

D(uv)

151	10	-9	4	-1	0	0	0
-5	-1	-3	0	-1	0	0	0
5	2	0	1	1	0	0	0
3	0	0	1	0	0	0	0
-2	1	0	0	0	0	0	0
1	0	0	0	0	0	0	0
0	0	0	0	0	0	0	0
0	0	0	0	0	0	0	0

Images derived from JPEG lossy compression

JPEG provides block DCT coding while handling 8 × 8 pixels as one block. The higher the compression ratio, the lower the decompressed image quality.

High-frequency components are gradually lost, rendering the image monotonous.

Artifacts called block distortion and mosquito noise begin to appear at block boundaries and in blocks having sharp edges.

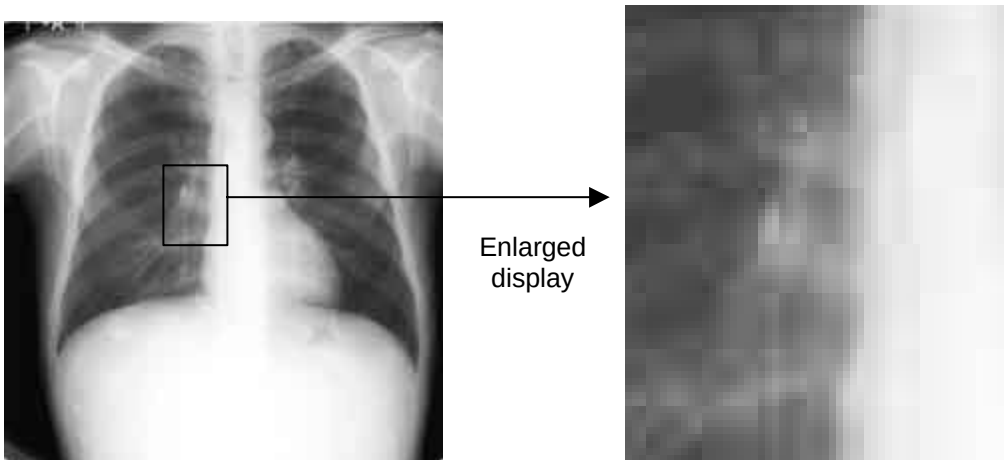

Figure Example of a block distortion

6.1.4 Image compression by Wavelet transform coding

6.1.4.1 Wavelet transform

The Wavelet transform consists of filtering processing and a sampling process. More specifically, a low-pass filter and high-pass filter shown in Figure 6.8 are each used to create an image by reducing the amount of data by half.

For a two-dimensional image, the Wavelet transform process is performed first in the horizontal direction and then in the vertical direction. This results in an image divided into four subband data with the number of horizontal pixels and vertical pixels reduced by half in relation to the original image.

The resulting four data are designated LL, LH, HL, and HH. The LL data consists of low-frequency components in both the horizontal and vertical directions. The LH data consists of low-frequency components in the horizontal direction and high-frequency components in the vertical direction. The HL data consists of high-frequency components in the horizontal direction and low-frequency components in the vertical direction. The HH data consists of high-frequency components in both the horizontal and vertical directions.

The low-frequency components (LL) are repeatedly subjected to hierarchical filtering and down-sampling processes and broken down into frequency components differing in resolution (Figure 6.9). Figure 6.10 shows three hierarchical levels of chest CR image data that are resolved by the Wavelet transform. The resolved data is equal to the original image in the total number of pixels.

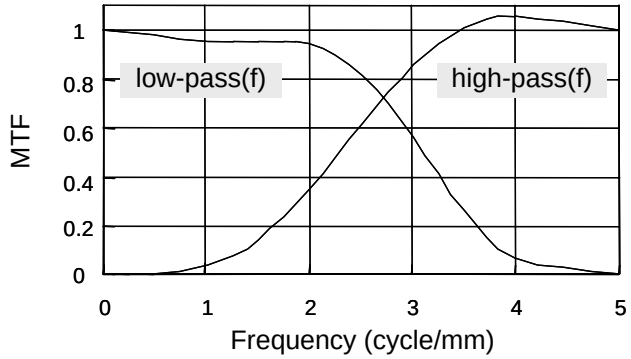

Figure 6.8 Example of filter characteristics used for Wavelet transform

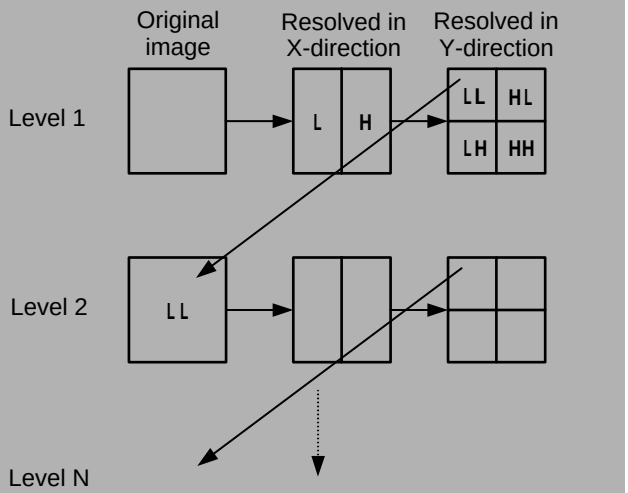

Figure 6.9 Break down into multiple resolutions by two-dimensional wavelet transform

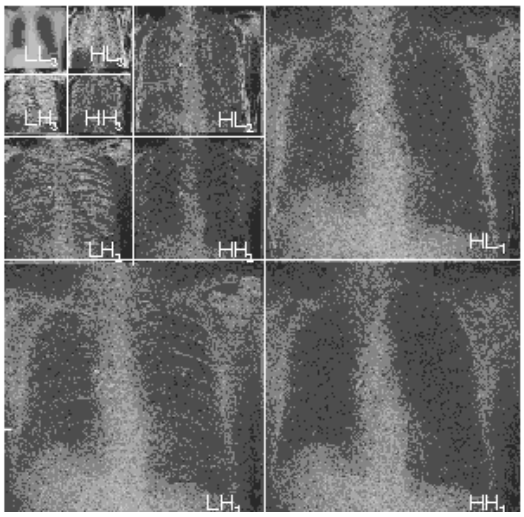

Figure 6.10 Level 3 Wavelet-transformed images

6.1.4.2 Image compression by Wavelet transform coding

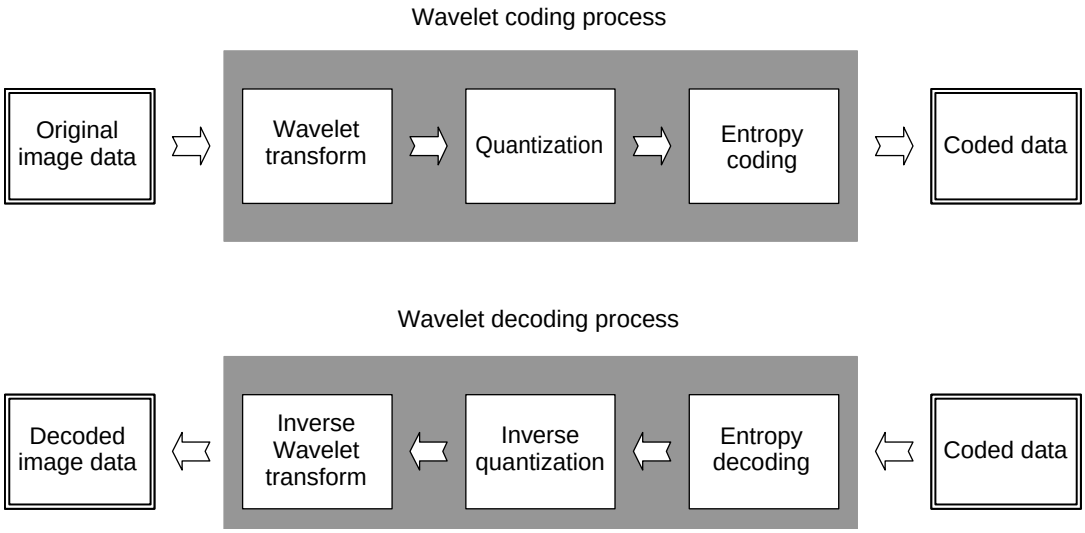

Quantization

In Wavelet transform coding, the image compression and image decompression processes are performed as indicated in the above block diagram. Images broken down into various Wavelet-transformed resolutions are quantized. The quantization sequence determines the image compression ratio and image quality.

Quantization can be performed in various ways and can be effected uniformly. However, the relationship between the image quality and compression ratio can be improved by determining the degree of quantization variously for all resolutions.

Entropy coding

In entropy coding, the quantized converted data is compressed without degrading the image quality (lossless compression). The aforementioned Huffman coding method is a typical technique for entropy coding.

Performance of images obtained by decompressing images that are compressed by Wavelet transform coding

In JPEG lossy compression, there is a tendency for block distortion to occur when the compression ratio is increased. However, no block distortion occurs in Wavelet transform coding because it entails no block processing. Wavelet transform coding surpasses JPEG in performance particularly when it uses a high compression ratio.

6.1.4.3 Application to networks

Wavelet-transformed coded data is rearranged in order from the lowest to the highest resolution component, and then stored as a file on a server or the like. All the coded data can be used to reproduce high resolution image data that has the same number of pixels as the original image. It is also possible to reproduce an image from part of the resolution information. This achieves quicker image reproduction because the time required for reading from a hard disk or other media, transmission over networks, and decoding is shorter than required for the use of all the coded data.

6.1.5 Compression algorithms for OD-F614/OD-F624

The following four different compression methods are employed by the OD-F units, which use a unique FCR protocol for electronic archiving.

The 1/2 lossless compression method can reproduce completely the original image. The 1/5, 1/12, and 1/20 lossy compression methods subject the original image to quantization and averaging processes and cannot reproduce completely the original image. The numerical prefixes to these compression method names indicate the approximate compression ratio.

For normal archiving, the 1/20 compression method is frequently used. It is useful for browsing through images.

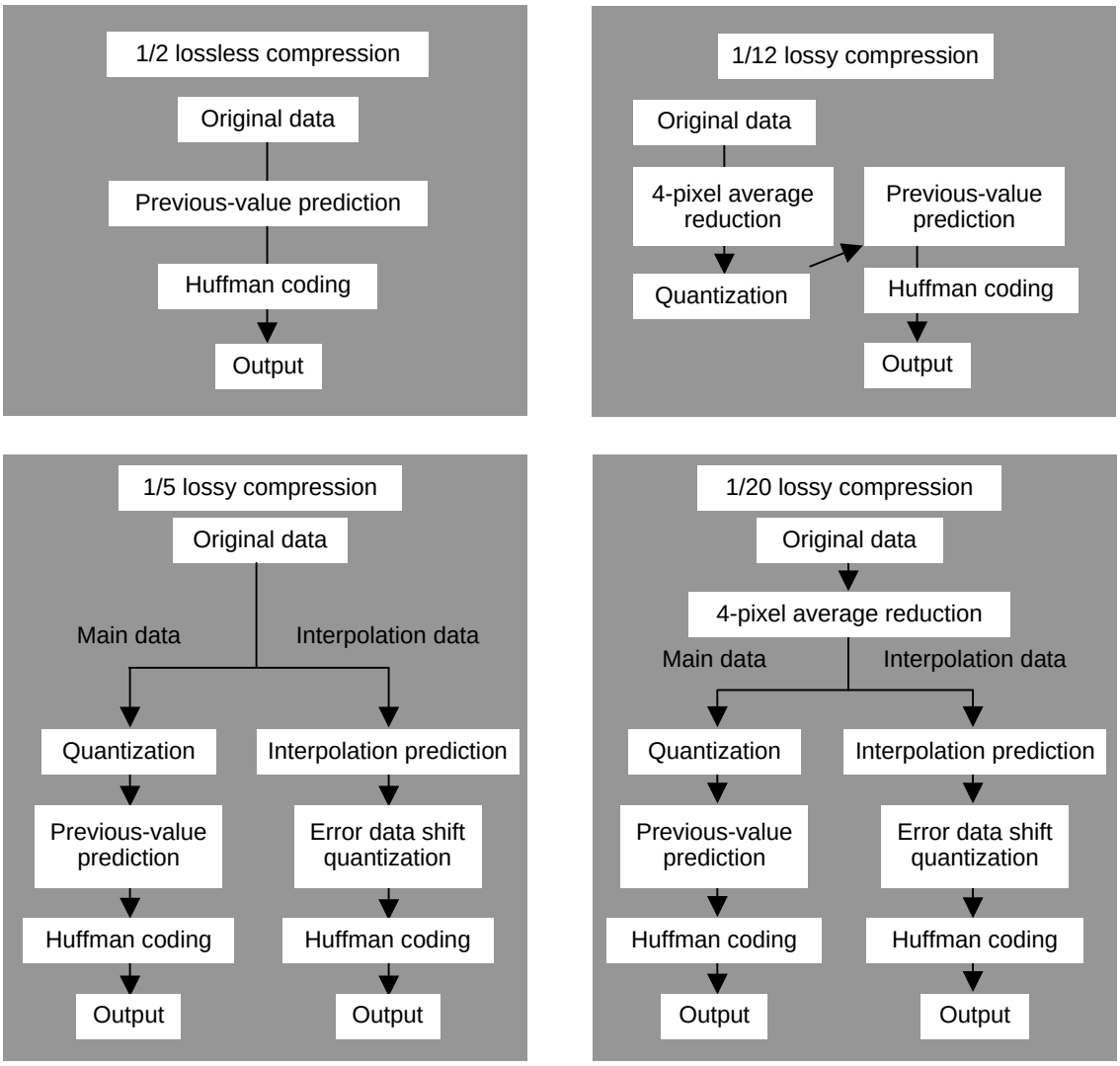

X11	A11	X12
B11	C11	B12
X21	A21	X21

A11 = (X11 + X12) / 2

B11 = (X11 + X21) / 2

C11 = (X11 + X12 + X21 + X22) / 4

Main data

Interpolation data

Appendix 1 Digital Image Evaluation Methods

In the screen/film system, its sensitivity, graininess, and sharpness are inevitably determined when certain conditions are given, that is, when the film and screen (system 1) brands are decided. By changing the film and screen brands (system 2), systems 1 and 2 can be compared to determine which is the better image formation system. In such an examination, the two systems can be evaluated only by comparing them in terms of sensitivity, graininess, and sharpness. For example, the evaluation results may indicate that system 1 is superior to system 2 in sensitivity but inferior to system 2 in graininess and sharpness. Sensitivity is also closely related to radiation exposure and limited by the exposure system (for example, when a high X-ray dosage is not properly reproduced or the image quality is reduced by body motion when the exposure time is increased). Because the required system sensitivity is determined by such factors, the image quality is determined in a manner beyond our control. In the end, it is difficult to come to a decisive conclusion as to which system is better.

If the comparison of systems similar in sensitivity indicates that one system is superior to the other in sharpness but inferior in graininess, the obtained numerical values fail to help answer the question of which system is better. In such a situation, visual evaluation results may better be able to determine which system is better. A visual evaluation is performed by checking whether the ROI (region of interest) is readily discernible. In this instance, the visual evaluation results frequently vary with the ROI. For example, the ROI may be a fine calcification or a low-contrast tumor. The visibility of a calcification frequently depends on sharpness, whereas the visibility of a tumor frequently depends on graininess.

Various methods based on image formation theory are available for assessing overall image quality mathematically and physically. Typical examples are DQE (Detective Quantum Efficiency) and NEQ (Noise-Equivalent Quanta).

The NEQ is defined by the output image alone. Its signal to noise ratio is expressed using the spatial frequency and X-ray dose as variables. The signal is proportional to $\gamma\,(Q)\cdot \mathrm{MTF}\,(\nu, Q)$, and the noise is $(\mathrm{WS}\,(\nu, Q))^{1/2}$. Thus, the following equation is obtained:

$$\mathrm{NEQ}(\nu,Q) \propto \gamma\,(Q)^2 \bullet \mathrm{MTF}(\nu,Q)^2 / \mathrm{WS}(\nu,Q)$$

where ν is the spatial frequency, Q is the X-ray quantum number, γ is the contrast, WS is the Wiener spectrum (a measure of graininess), and MTF is the modulation transfer function (a measure of sharpness).

Expressed as a percentage (%), the DQE is a factor that indicates the efficiency with which image data is transmitted to the image detection system and eventually displayed as an image. In other words, it is the duplicate ratio between input signal-to-noise ratio (S/N) and final image signal-to-noise ratio.

$$\mathrm{DQE}\,(\nu,Q) = (S/N)^2\,\mathrm{out} \,/\, (S/N)^2\,\mathrm{in}$$

When an ideal image sensor is used, the DQE is 100%. (When common sensors are used, the DQE is as low as 10% or so. The higher the frequency, the lower the DQE.) The DQE is an index that permits you to make an overall evaluation of sensitivity and image quality.

Since the input $(S/N)^2\mathrm{in}$ is proportional to the input X-ray quantum number Q, the equation $\mathrm{DQE}\,(\nu,Q) = \mathrm{NEQ}\,(\nu,Q)/Q$ is obtained.

The value Q is inversely proportional to sensitivity. Thus, the DQE is indicated below:

$$\mathrm{DQE}(\nu) \propto \mathrm{Sensitivity} \times \mathrm{NEQ}(\nu) \propto \mathrm{Sensitivity} \times \gamma\,(Q)^2 \bullet \mathrm{MTF}(\nu,Q)^2 / \mathrm{WS}(\nu,Q)$$

Consequently, the DQE can be determined by measuring the MTF(ν,Q), WS(ν,Q), sensitivity, and γ.

How should the FCR image quality be evaluated?

Unlike the screen/film system, the digital imaging system allows you to vary the sensitivity, MTF, WS, and γ as desired. Even if you vary the exposure amount as desired, the FCR system provides appropriate density and contrast and allows you to adjust the sensitivity setting. Further, recorded image data can be subjected to the desired image processes, which enable you to vary the MTF, WS, and γ as desired. Conventional evaluations based on contrast, RMS, and MTF would therefore be meaningless. In addition, the FCR sensitivity, contrast, MTF, and WS cannot be determined indiscriminately.

Ultimately, the quality of digital images and, in particular, differing digital formation systems, should be evaluated according to the DQE (NEQ for a predetermined exposure amount). The DQE can be determined by measuring the MTF, WS, γ, and Q. It is not easy to measure these values accurately. For the MTF, in particular, there are various measurement methods. The simplest method is to shoot a rectangular chart and measure the resultant output film with a microphotometer. However, you then have to go the trouble of making corrections because the γ value is not linear with respect to density. In addition, Coltman rectangular/sine wave conversion is needed.

If print losses can be ignored, which is usually the case, you can directly analyze digital data without having to measure the filmed image with a microphotometer. To make such analyses, however, you need a data exchange interface and analysis application software.

Needless to say, image quality (DQE) is important for FCR imaging. Note, however, that the FCR system can perform various processes to effect image conversion before generating images. Image processes can be selectively performed to greatly enhance the image viewability with virtually no basic changes to the image quality. This means that the visual evaluation results will not always coincide with the absolute physical evaluation results. In that sense, the importance of visual evaluation is considerably high in digital image evaluation. The most practical method of digital image quality evaluation is to use a burger-phantom, an example of which is shown in the figure on next page. The burger-phantom contains plastic circular cylinders or circular cylindrical holes, whose diameter and height are gradually varied. It is used to visually determine the discernible diameters and heights of cylinders or cylindrical holes. Discernibleness can be digitized by indicating the numbers assigned to discernible cylinder/cylindrical hole sizes.

More specifically, the FCR recording conditions should be set up so as to provide an appropriate uniform density of approximately 1.2 (the SEMI AUTO mode should normally be used). The phantom should be radiographed under conditions similar to those of the actual exposure system in terms of display parameters, exposure voltage, exposure distance, and grid, and by passing the human body through the scatterer to be simulated. On either side of the exposure amount for the actual exposure mAs value, the exposure amount should be increased and decreased over several steps to make several exposures and determine discernibleness with reference to the radiation dose.

The burger-phantom permits you to check image noise, sharpness, and γ objectively and comprehensively. In addition, it is a simple, helpful tool because it digitizes your evaluation results.

A more practical method is to make ROC analysis. It allows you to statistically evaluate the system under comparison and formulate your judgment from a clinical viewpoint. A detailed description of ROC analysis is not discussed here. ROC analysis requires a considerable amount of time and labor.

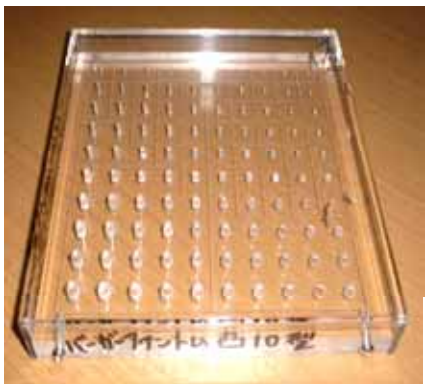

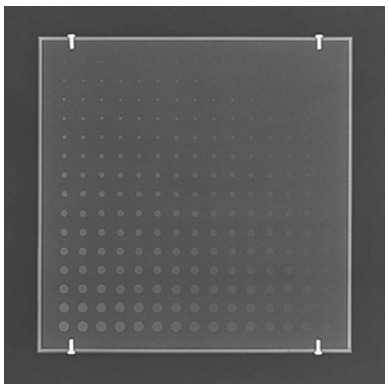

Convex burger-phantom example

Reference

Digital Radiography Image Evaluation, Edited by Hiroshi Fujita, Japanese Society of Radiological Technology

Appendix 2 Fourier Transform (Real Space-to-Frequency Space Conversion)

1. Introduction

The Fourier transform converts a real space (density relative to position in the case of an image) to a frequency space (components relative to frequency). That is, the Fourier transform resolves a certain periodic waveform into a trigonometric function wave consisting of differing frequencies contained in the periodic waveform.

The Fourier transform is a useful method for simplifying problems in many fields. For example, the Fourier transform of a linear system output is given by the product of the system's transmission function and input Fourier transform. In particular, when an image is handled, the Fourier transform is performed to reduce its high-frequency components (which are not important visual components) to zero. The inverse Fourier transform is then performed to restore such components to a real space with the purpose of decreasing the amount of image data and effecting image conversion (image compression) to obtain an image that is not visually different from the original. Further, the components in a specific frequency band are enlarged and then restored to a real space to enhance the image (the image enhancement process).

Historically speaking, the Fourier expansion of a periodic function was developed first. The Fourier transform was later developed to provide a means of converting a function to a frequency space.

The Fourier transform is not performed for the unsharp masking process of FCR image processing, Instead, a real-space filtering process is used. The extended multi-objective frequency process is based on the use of multiple unsharp masks and performed with several types of bandpass filters. This process is similar to the Fourier transform technique in that the frequency response can be varied as desired, and the time required for processing reduced.

Supplementary explanation

1 Frequency (spatial frequency)

When the change cycle of a signal (e.g., sound wave) that periodically varies with the distance or time is t, the value 1/t denotes the frequency. That is, the frequency indicates the number of changes per unit time (or distance). When the signal change per second is equivalent to one period, the frequency is 1 cycle/second. When the signal change per millimeter is equivalent to one period, the frequency is 1 cycle/mm.

2 Trigonometric function and period

COS function $f(x) = \cos 2\pi n x$

When the value n increases, its period shortens. It represents a fine signal.

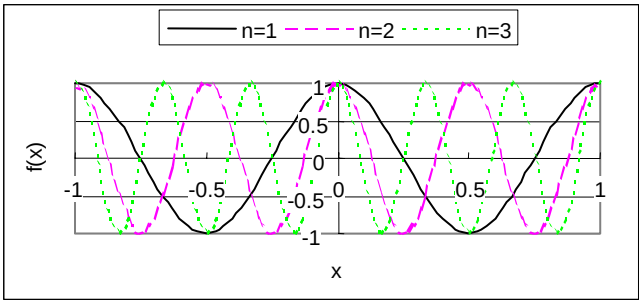

Reference

Digital Signal Processing for Applications, Keiji Hiramatsu, et al.; Triceps Publishing
Fast Fourier Transform, Translated by Hiroshi Miyagawa, et al.; SciTech Press
Digital Picture Processing, Translated under the supervision of Makoto Nagao; Kindai Kagaku Sha Co., Ltd.

2. Fourier expansion

The periodic function of the period T can be expanded as the sum of trigonometric functions as indicated in Equation (1).

$$f(X) = a_0 + \sum a_n \cos 2\pi nx / T + \sum b_n \sin 2\pi nx / T$$
$$a_0 = 1/T \int_{-T/2}^{T/2} f(x)\,dx$$
$$a_n = 2/T \int_{-T/2}^{T/2} f(x) \cos 2\pi nx/T\,dx$$
$$b_n = 2/T \int_{-T/2}^{T/2} f(x) \sin 2\pi nx/T\,dx \qquad n = 1 \ldots \infty$$

..... Equation (1)

A periodic function is expressed as the sum of trigonometric functions having differing frequencies. Its coefficient a_0 is a DC component and a_n and b_n are its frequency amplitudes. These are called Fourier coefficients.

Fourier expansion is to define the amplitude and phase (expressed with sin and cos) of trigonometric functions having discontinuous frequencies and to use their sum to achieve expansion.

3. Fourier expansion example

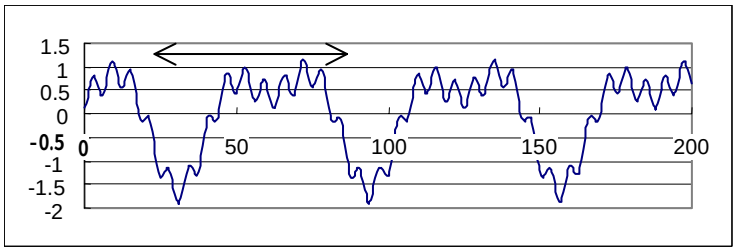

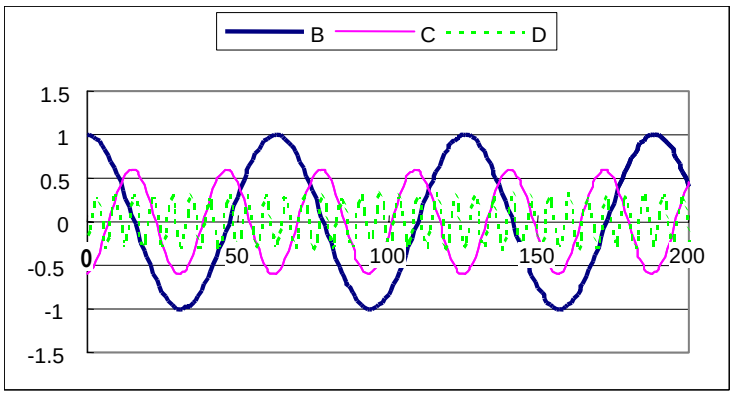

Example 1

The Fourier expansion indicated in the left-hand side figure is B + C +D.

$$A = \cos 2\pi x + 0.6 \cos 4\pi x + 0.3 \cos 20\pi x$$

Example 2 Expression with rectangular wave sin function $f(x) = 4/\pi \sum \left[1/(2n-1)\sin\{1/(2n-1)\ x\}\right]$

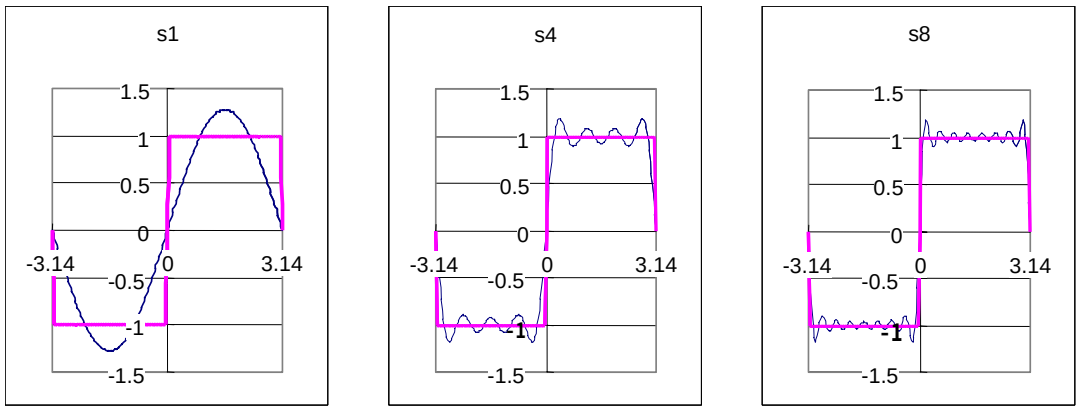

The trigonometric functions in Equations (1) can also be expressed with the exponential functions in Equation (2). (Demonstration of this equation is omitted here (*).)

$$f(x) = \sum F_n\, e^{j2\pi nx/T}$$
$$F_n = 1/T \int_{-T/2}^{T/2} f(X)\, e^{-j2\pi nx/T}\, dx \quad -\infty < X < \infty, \quad n = 1, \ldots$$

.....Equation (2)

$$(*)\ e^{2\pi jx} = \cos(2\pi x) + j\sin(2\pi x)$$
$$e^{-2\pi jx} = \cos(2\pi x) - j\sin(2\pi x)$$

(*) To be deduced from the following relationship.

4. Deriving the Fourier transform from the Fourier expansion

Let us consider the Fourier expansion of a rectangular wave signal having the period T and width 1. The equations on the left-hand side can be expanded to the Fourier series in the equation on the right-hand side.

$$f(x) = \sum g(x - nT)$$

$$g(x) = 1\,(-1/2 < x < 1/2)\,, \text{else } 0$$

$$\rightarrow \quad f(x) = \sum F_n\, e^{j2\pi nx/T}\,, F_n = \sin(\pi n/T)/(\pi n/T)$$

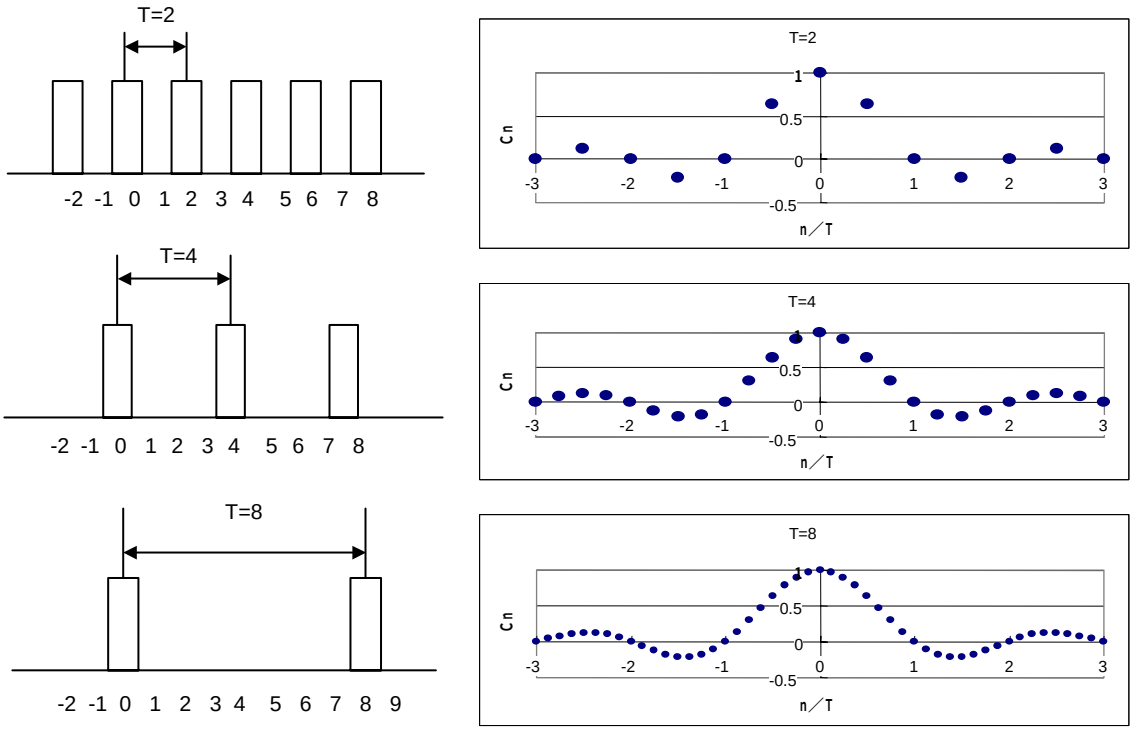

Rectangle having the width 1 (not a periodic function)

When $f(x) = 1 \quad |x| \leq 1/2,\ f(x) = 0 : |x| > 1/2$ is considered, its Fourier coefficient Fn can be extended by making the period T infinite. In this instance, the Fourier coefficient Fn can be regarded as a continuous function as estimated from the T change. When n/T is u, F(u) = sin(πu)/(πu).

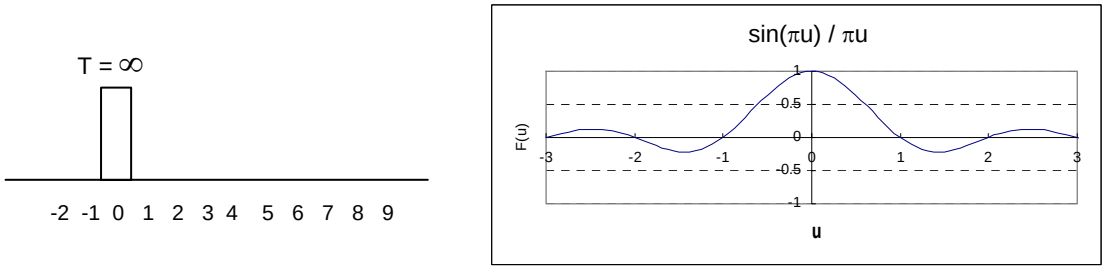

If the Fourier expansion is generalized when T = ∞ , F_n can be replaced by F(u); n/T by u (frequency); and ∑ by an integral. The result is indicated below:

$$f(x) = \sum F_n e^{j2\pi nx/T} \quad \rightarrow \quad f(x) = \int_{-\infty}^{\infty} F(u)e^{j2\pi ux}dx$$

$$F_n = 1/T\int_{-T/2}^{T/2} f(x)e^{-j2\pi nx/T}\,dx \quad \rightarrow \quad F(u) = \int_{-\infty}^{\infty} f(x)e^{-j2\pi ux}dx$$

The equations on the right-hand side are the Fourier transform or inverse Fourier transform that is obtained by generalizing the Fourier expansion.

Consequently, the Fourier transform and inverse Fourier transform are expressed by Equation (3).

Fourier transform (real space-to-frequency space conversion)

$$f(x) \quad \rightarrow \quad F(u) = \int_{-\infty}^{\infty} f(x)e^{-j2\pi ux}\,dx$$

Inverse Fourier transform (frequency space-to-real space conversion)

$$F(u) \quad \rightarrow \quad f(x) = \int_{-\infty}^{\infty} F(u)e^{2j\pi ux}du$$

.....Equation (3)

5. Special function Fourier transform

Real space **Frequency space**

1 $f(x) = a$

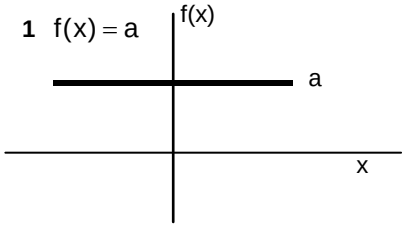

$F(u) = a\delta(u)$

$\delta(u)$ $u = 0:1$, $x \neq 0:0$

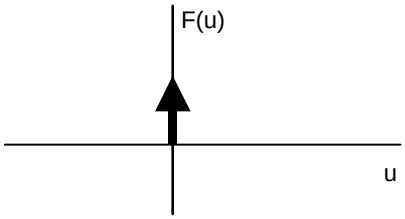

2 $f(x) = a\delta(x)$

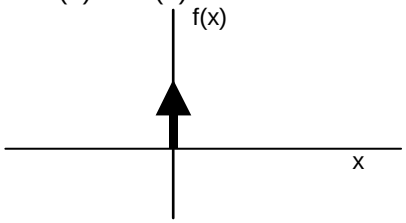

$F(u) = a$

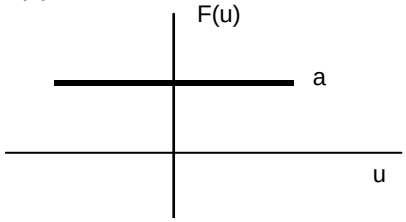

3 $f(x) = \sum \delta(x - nT)$ Comb function $n = -\infty \sim \infty$ $F(u) = 1/T \sum \delta(u - n/T)$

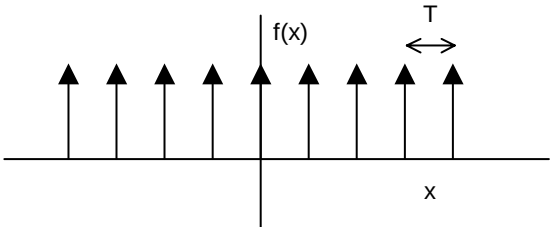

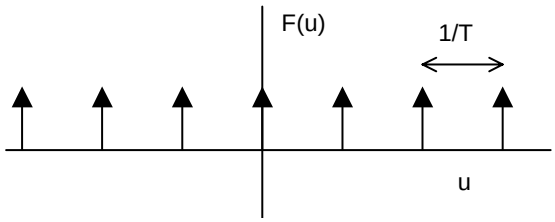

4 $\cos 2\pi u_0 x$ $F(u) = 1/2\,(\delta(u - u_0) - \delta(u + u_0))$

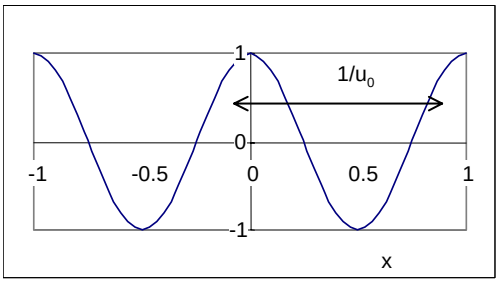

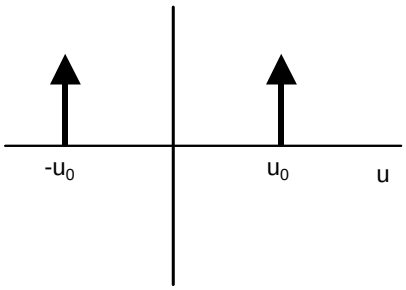

5 $\sin 2\pi u_0 x$ $F(u) = -j/2\,(\delta(u - u_0) - \delta(u + u_0))$

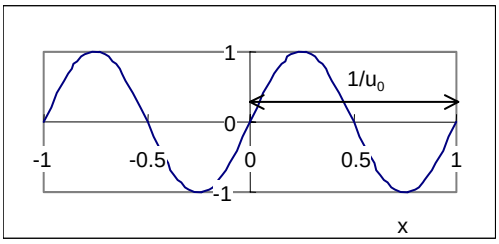

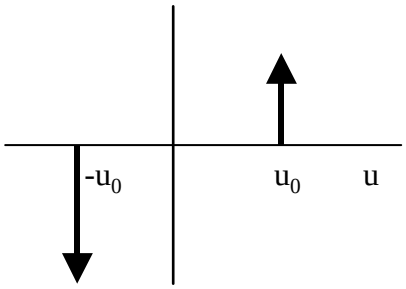

6 Rectangle

$f(x) = 1 \quad (x \leqq |\tau/2|), = 0 \quad (x > |\tau/2|)$ $F(u) = \tau \sin(\pi\tau u) / (\pi\tau u)$

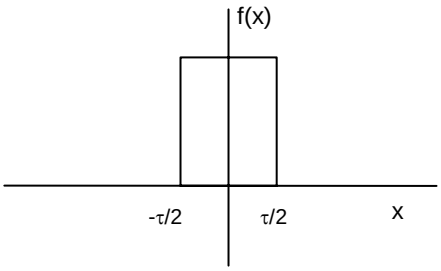

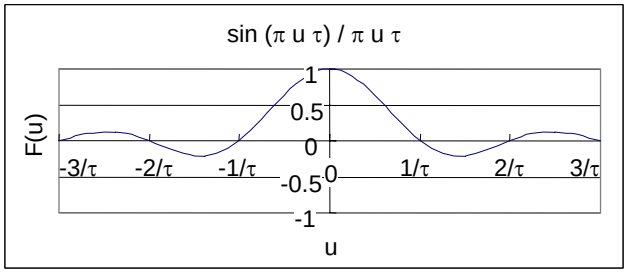

6. Relationship between original function and Fourier transformed function

Let the original function be f(x) and its Fourier transformed function be F(u).

6.1 Symmetry properties

The Fourier transform of F(x) is f(-u).

6.2 Linearity

The Fourier transform of $\sum a_n f_n(x)$ is $\sum a_n F_u(u)$.

6.3 Downscaling capability

The Fourier transform of f(ax) is $1/|a|F(u/a)$.

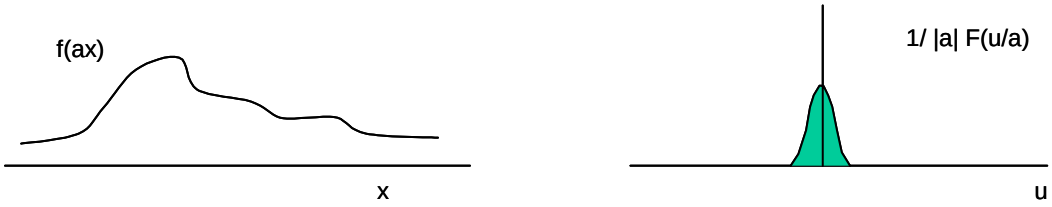

6.4 Migration

The Fourier transform of $f(x-x_0)$ is $F(u)e^{-2j\pi/x0}$.

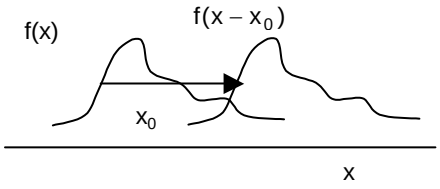

The function spectrum remains unchanged.
Only the phase changes.

6.5 Function product

The Fourier transform of the product of two functions is the convolution of Fourier functions.

$$f_1(x) \times f_2(x) \rightarrow F(u) = \int F_1(t)\, F_2(u-t)\, dt = F_1(u) * F_2(u) \quad \text{.....Equation (4)}$$

The convolution (convolution integral) of the two functions is defined by Equation (5). It is obtained by looping back the function $f_2(x)$, changing it by t, multiplying it by the function $f_1(x)$, and integrating it with respect to t.

$$f_1(x) * f_2(x) = \int f_1(t)\, f_2(x-t)\, dt \quad \text{.....Equation (5)}$$

7. Fourier transform of a sampled function

Equation (6) indicates that a certain function f(x) is sampled at intervals of T. It means that the original function is multiplied by a comb function.

$$f_s(x) = f(x) \times \sum \delta(x - nT) \quad \text{.....Equation (6)}$$

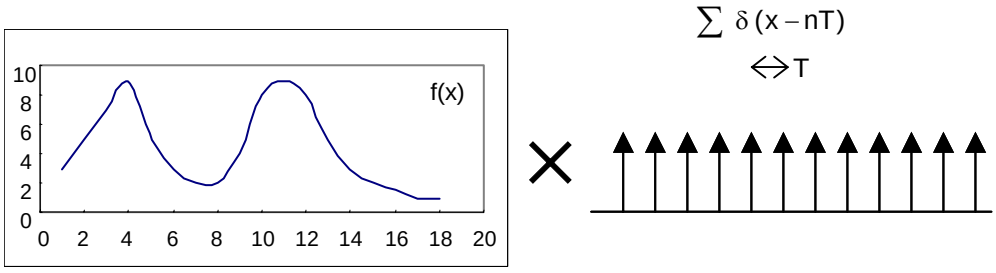

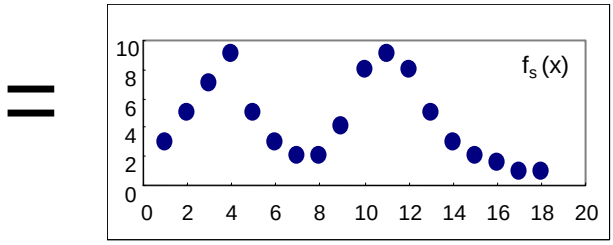

The Fourier transform of the comb function $\sum \delta(x - nT)$ is $1/T \sum \delta(u - n/T)$. When the Fourier transform of F(x) is F(u), the Fourier transform Fs(u) of the sampled data stream fs(x) is the convolution of the two Fourier-transformed functions $F(u) * 1/T \sum \delta(u - n/T)$. Thus, Equation (7) results.

$$Fs(u) = 1/T \sum F(u - n/T) \qquad n = -\infty \sim \infty \quad \text{.....Equation (7)}$$

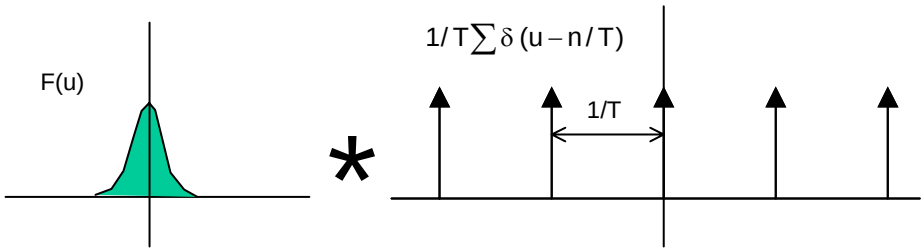

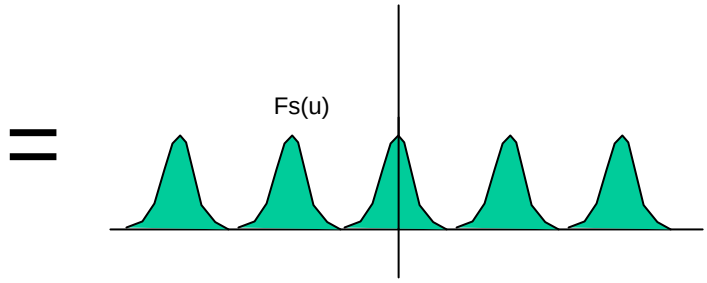

Equation (7) shows the Fourier transforms F(u) of the continuous function f(x) before sampling that are arrayed at intervals of 1/T within a frequency space.

8. Sampling theorem and Nyquist frequency

In Equation (7), Fs(u) is the Fourier transform of the sampled digital signal fs(x).

If the reciprocal of the sampling interval is smaller than two times the maximum frequency u_m of the Fourier transform F(u) of the original data (analog signal), the F(u) values are arrayed at intervals of 1/T without overlapping. When one F(u) value is selected and subjected to inverse Fourier transform in this instance, the original continuous function (analog signal) prevailing before sampling is obtained.

The above means that the sampled image can be accurately restored to the original image if the reciprocal of the sampling interval is smaller than two times the maximum frequency (u_m) of F(u). This is called the sampling theorem.

On the other hand, if the sampling interval is increased so that 1/T is smaller than two times the maximum frequency u_m, F(u) overlapping occurs. In such an instance, the high-frequency components loop back when an attempt is made to restore the sampled image to the original image. The resulting loopback distortion is then superposed over the data to the detriment of restoration accuracy. This phenomenon is called "aliasing".

The Nyquist frequency is the frequency that is the reciprocal of two times the sampling interval T.

$$1/(2T) = u_N$$ u_N : Nyquist frequency

Conditions for sampling theorem establishment

$$u_m < u_N = 1/(2T)$$ 1/T : Sampling density (pixels/mm)

.....Equation (8)

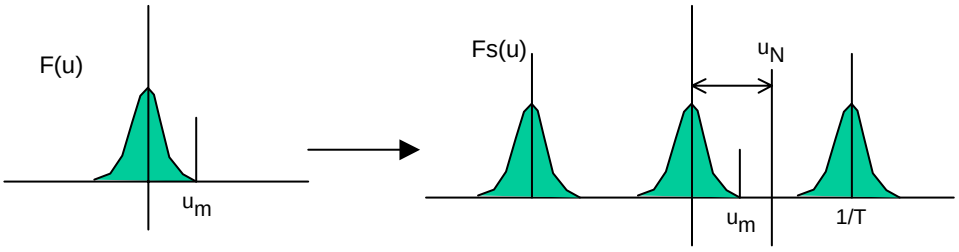

When the sampling interval is short so that F(u) overlapping does not occur, $u_m < u_N$.

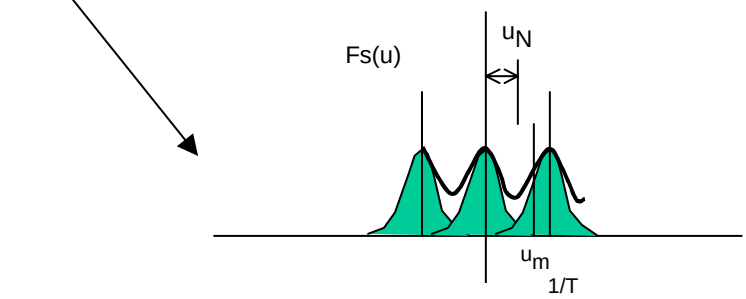

When the sampling interval is long so that F(u) overlapping occurs, $u_m > u_N$.

To suppress aliasing, high-frequency components should be reduced by passing the analog signal through a high-frequency cutoff filter. Typically, aliasing occurs when an image is displayed on CRT screen with a limited number of scanning lines (coarse sampling is performed). In such an instance, the stationary grid appears as a moiré pattern.

9. Discrete Fourier transform (DFT)

The Fourier transform of digital data differs from the Fourier transform of a continuous function because the former uses discontinuous, finite, discrete data as the original data.

In this transform process, the coefficients corresponding to N frequencies are given to N measured data.

When Equation (3) for the Fourier transform of the continuous function (analog signal) f(x) is converted into the equation of the discrete signal $f_s(x)$, the following is obtained:

$$F_s(u) = \int_{-\infty}^{\infty} f_s(x)\, e^{-j2\pi ux} dx \quad \text{.....Equation (3)}$$

When consideration is given only to situations where x = n/N and x = nT with the sampling period T regarded as being 1, $f_s(x)$ is f(n). Further, when the value u is substituted by the value k because the frequencies are to be expressed as discontinuous values, the integral becomes the sum and Equation (3) turns into Equation (9).

$$F(k) = 1/N \sum_n f(n)\, e^{-j2\pi kn/N} \quad \text{.....Equation (9)}$$

$$n = 0, 1, 2, 3, 4\ldots\ldots, N-1 \qquad k - 0, 1, 2, 3, 4\ldots\ldots, N-1$$

Now, let us consider N one-dimensional digit strings {f(n)}. The Fourier transform of the digit strings, that is, the discrete Fourier transform (DFT) {F(k)} is expressed by Equation (10) when a phase factor is introduced for increased brevity. The digit strings are enclosed in braces ({ }).

$$\begin{aligned} &\{f(n)\} = \{f(0), f(1), f(2), f(3), \ldots\ldots f(N-1)\} \\ &\{F(k)\} = 1/N \sum_n \{f(n)\}\, W^{nk} \\ &k = 0, 1, 2, 3, 4\ldots\ldots, N-1, \qquad n = 0, 1, 2, 3, 4\ldots\ldots, N-1 \end{aligned} \quad \text{..... Equation (10)}$$

where W is the phase factor and expressed as indicated below:

$$W = e^{(-j2\pi/N)} = \cos(2\pi/N) + j\sin(2\pi/N)$$

Equation (10) is an N × N matrix equation. Thus, Equation (11) is obtained.

$$\begin{bmatrix} F_0 \\ F_1 \\ F_2 \\ \vdots \\ F_{n-1} \end{bmatrix} = 1/N \begin{vmatrix} w^0 & w^0 & \ldots\ldots\ldots & \\ w^o & w^0 & \ldots\ldots\ldots & w^{N-1} \\ \vdots & & & \\ \vdots & & & \\ w^0 & w^{N-1} & \ldots\ldots\ldots & w^{N-1\times N-1} \end{vmatrix} \begin{bmatrix} f_0 \\ f_1 \\ f_2 \\ \vdots \\ f_{n-1} \end{bmatrix} \quad \text{.....Equation (11)}$$

10. Fast Fourier transform (FFT)

When the DFT is actually performed with a computer, a more efficient calculation method called "FFT" is used. If, for instance, N = 8 for the DFT, calculations are performed in accordance with Equation (12).

$$\{f(n)\} = \{f(0), f(1), f(2), f(3), \ldots\ldots f(7)\}$$

$$F(k) = 1/N \quad \sum_{n} \{f(n)\} W^{nk}$$

$$\begin{bmatrix} F_0 \\ F_1 \\ F_2 \\ \vdots \\ F_6 \\ F_7 \end{bmatrix} = 1/8 \begin{vmatrix} w^0 & w^0 & \ldots\ldots & w^0 \\ w^0 & w^1 & \ldots\ldots & w^7 \\ w^0 & w^2 & \ldots\ldots & w^6 \\ \vdots & & & \vdots \\ w^0 & w^6 & w^5 \ \ldots & w^2 \\ w^0 & w^7 & w^6 \ \ldots & w^1 \end{vmatrix} \begin{bmatrix} f_0 \\ f_1 \\ f_2 \\ \vdots \\ f_6 \\ f_7 \end{bmatrix} \quad \ldots\ldots\ldots\ldots \text{Equation (12)}$$

$$\begin{bmatrix} F_0 \\ F_2 \\ F_4 \\ F_6 \\ F_1 \\ F_3 \\ F_5 \\ F_7 \end{bmatrix} = 1/8 \begin{vmatrix} w^0 w^0 w^0 w^0 w^0 w^0 w^0 w^0 \\ w^0 w^2 w^4 w^6 w^0 w^2 w^4 w^6 \\ w^0 w^4 w^0 w^4 w^0 w^4 w^0 w^4 \\ w^0 w^6 w^4 w^4 w^0 w^6 w^4 w^2 \\ w^0 w^1 w^2 w^3 w^4 w^5 w^6 w^7 \\ w^0 w^3 w^6 w^1 w^4 w^7 w^2 w^5 \\ w^0 w^5 w^2 w^7 w^4 w^1 w^6 w^3 \\ w^0 w^7 w^6 w^5 w^4 w^3 w^2 w^1 \end{vmatrix} \begin{bmatrix} f_0 \\ f_1 \\ f_2 \\ f_3 \\ f_4 \\ f_5 \\ f_6 \\ f_7 \end{bmatrix} \quad \ldots\ldots\ldots\ldots \text{Equation (13)}$$

Use of phase factor periodicity and symmetry

Equation (12) is obtained by using the properties of the phase factor W^{nk} for increased brevity. The phase factor is periodic and symmetrical. When, for instance, the value nk increases and N = 8 in every case (e.g., $W^8 = W^0$, $W^9 = W^1$, $W^{10} = W^2$, ...), the phase factor is equal to the values W^0 to W^8. Calculations can therefore be simplified due to the use similar equations. Further, when N = 8, symmetry is exhibited (e.g., $W^0 = -W^4$ and $W^1 = -W^5$). When the odd-numbered positions and even-numbered positions of the matrix equation are interchanged by making use of such properties, Equation (13) is obtained.

In general, when you simply perform calculations, you have to perform calculations 64 times (= 8 × 8). However, when you make use of the phase factor's periodicity and symmetry, you can accomplish the same purpose by performing two 4 × 4 matrix calculations. In the end, you have to perform (8/2) × (8/2) × 2 calculations, which means that the required number of calculations is reduced to half. In other words, you have to perform calculations 32 times only.

When there are N data and N is a value obtained by raising the value 2 to a power, $N = 2_n$ data is generally divided into two, the resulting two divisions are each calculated, and the calculation results are used as data to perform calculations n times in succession in order to reduce the required number of calculations.

If calculations are performed without using any special scheme, the required number of calculations is N^2. For the FFT, however, the required number of calculations is $(N/2)Log_2N$. If, for instance, N = 10 bits, the required number of calculations is decreased from approximately 1 million to 5,000, a factor of 1/200.

This technique was announced as early as 1965 by Cooley and Tukey. The DFT was rendered practicable by the development of this technique.

FUJI PHOTO FILM CO., LTD.

26-30, NISHIAZABU 2-CHOME, MINATO-KU, TOKYO 106-8620, JAPAN

Fuji Photo Film Co., Ltd. No. 000-223-00 2002.02 Printed in Japan